CHARACTERISATION AND DEVELOPMENT OF NEW BIO-FILLER USING *MIMUSOPS ELENGI* SEED SHELL POWDER FOR POLYPROPYLENE COMPOSITES

TAN WUAN CHIEN

MASTER OF ENGINEERING SCIENCE

FACULTY OF ENGINEERING AND GREEN TECHNOLOGY
UNIVERSITI TUNKU ABDUL RAHMAN
JULY 2020

CHARACTERISATION AND DEVELOPMENT OF NEW BIO-FILLER USING *MIMUSOPS ELENGI* SEED SHELL POWDER FOR POLYPROPYLENE COMPOSITES

By

TAN WUAN CHIEN

A dissertation submitted to the Faculty of Engineering and Green Technology,

Universiti Tunku Abdul Rahman,

in partial fulfillment of the requirements for the degree of

Master of Engineering Science

July 2020

ABSTRACT

CHARACTERISATION AND DEVELOPMENT OF NEW BIO-FILLER USING *MIMUSOPS ELENGI* SEED SHELL POWDER FOR POLYPROPYLENE COMPOSITES

In recent year, high dependency on petroleum based plastics, deterioration of the environment due to the pollution caused by the unmanageable plastics waste disposal has emerged the interest in sustainable development of biocomposites. Plant fibers are abundantly available, biodegradable, light weight with high specific properties. The present research study is an effort to combine the advantages offered by the renewable resources for the production of the biocomposites. The greatest challenges is the weak compatibility between the natural fiber and matrix resulted in the weak mechanical properties of the composites. Alkaline treatment is one of the well-known approach to overcome this problem.

Biocomposites were prepared from *Mimusop elengi* seed shell powder (MESSP) and polypropylene (PP) blend by using Brabender internal mixer at 180 ℃ and rotor speed of 60 rpm for a mixing time of 8 minutes. The MESSP loading was varied from 0 - 40 wt. % and it was found that the saturation point was achieved at 20 wt. % MESSP. Composite development is not feasible above 20 wt.% MESSP due to poor wetting by PP. Characterisation of MESSP were conducted to study the potential of MESSP as the filler for PP composites. Physico-mechanical properties, processing-ability, thermal stability, bio-degradability and water absorption properties of PP/MESSP composites were

studied. Processing-ability and thermal stability of the composites were comparable to the neat PP showing insignificant effect on the composites up to 20 wt. % MESSP. Tensile modulus and impact strength were enhanced with increasing MESSP loading. However, reduction of tensile strength and elongation at break was obtained with increasing MESSP loading attributed to the poor interfacial adhesion between PP and MESSP as confirmed by the scanning electron microscopic (SEM) morphological analysis. Positive results were observed with the increased weight loss in the soil burial test indicating significant extend of bio-degradability of the composites with increasing MESSP loading. Chemical modification of MESSP with alkali treatment was performed to improve the polymer-matrix compatibility. Fourier transform infrared (FTIR) and SEM analysis proved that treatment with 5 w/v % sodium hydroxide (NaOH) solution produced a better modification on the chemical compositions and structural characteristics of MESSP as compared to 6 w/v %, 7 w/v % and 8 w/v % of NaOH solution. Treated MESSP filled PP (PP/TMESSP) composites had an affirmative effect on the mechanical properties and water absorption resistance. It was found that an increase of 30 % in tensile strength and 28% in impact strength at the optimum 15 wt. % of PP/TMESSP composites as compared to that of untreated MESSP filled PP (PP/MESSP) composites. Water absorption resistance and the crystallinity of PP/TMESSP composites were also improved. Better interfacial adhesion between PP and TMESSP were observed as compared to PP and MESSP through SEM images. However, thermogravimetric analysis showed that the maximum decomposition temperature of PP/TMESSP composites was lower as compared to PP/MESSP

composites due to removal of thermally stable lignin layers of MESSP upon alkali treatment.

ACKNOWLEDGEMENTS

I would like to thanks everyone with the kind support and help to make this thesis becomes a reality. Foremost, I would like to express my gratitude to Universiti Tunku Abdul Rahman with the grant number of (IPSR/RMC/UTARRF/2017-C2/M01) for providing financial aid for me to pursue my Master's degrees. I really appreciate my research supervisor, Dr. Mathialagan a/l Muniyadi for his guidance and enormous patience throughout the development of the research. I would like to express my gratitude to my co-supervisor, Dr Ooi Zhong Xian for sharing his knowledge and technical know-how.

Furthermore, I would like to extend my gratitude to my family and friends who gave me support and encouragement throughout the research study. Lastly, I sincerely want to thank to the lab officers including Ms. Lim Cheng Yen, Puan Zila Binti Mohd Tahir, Mr. Yong Tzyy Jeng, Mr Tamilvanan a/l Muniandi, Puan Zila Binti Mohd Tahir and Encik Zulfadli Bin Mat Zin for their considerable help in this research.

APPROVAL SHEET

This dissertation entitled "**CHARACTERISATION AND DEVELOPMENT OF NEW BIO-FILLER USING *MIMUSOPS ELENGI* SEED SHELL POWDER FOR POLYPROPYLENE COMPOSITES**" was prepared by TAN WUAN CHIEN and submitted as partial fulfillment of the requirements for the degree of Master of Engineering Science at Universiti Tunku Abdul Rahman.

Approved by:

(DR. MATHIALAGAN A/L MUNIYADI) Date: 25 July 2020

Supervisor

Department of Petrochemical Engineering

Faculty of Engineering and Green Technology

Universiti Tunku Abdul Rahman

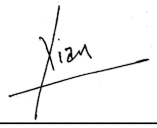

(DR. OOI ZHONG XIAN) Date: 25 July 2020

Co-supervisor

Department of Chemical Science

Faculty of Science

Universiti Tunku Abdul Rahman

FACULTY OF ENGINEERING AND GREEN TECHNOLOGY

UNIVERSITI TUNKU ABDUL RAHMAN

Date: 22 July 2020

SUBMISSION OF DISSERTATION

It is hereby certified that **Tan Wuan Chien** (ID No: **18AGM06172**) has completed this dissertation entitled "CHARACTERISATION AND DEVELOPMENT OF NEW BIO-FILLER USING *MIMUSOPS ELENGI* SEED SHELL POWDER FOR POLYPROPYLENE COMPOSITES" under the supervision of Dr. Mathialagan a/l Muniyadi (Supervisor) from the Department of Petrochemical Engineering, Faculty of Engineering and Green Technology, and Dr. Ooi Zhong Xian (Co-Supervisor) from the Department of Chemical Science, Faculty of Science.

I understand that University will upload softcopy of my dissertation in pdf format into UTAR Institutional Repository, which may be made accessible to UTAR community and public.

Yours truly,

(Tan Wuan Chien)

DECLARATION

I, TAN WUAN CHIEN hereby declare that the dissertation is based on my original work except for quotations and citations which have been duly acknowledged. I also declare that it has not been previously or concurrently submitted for any other degree at UTAR or other institutions.

(TAN WUAN CHIEN)

Date: 22 July 2020

TABLE OF CONTENTS

LIST OF TABLES

LIST OF FIGURES

LIST OF SYMBOLS AND ABBREVIATIONS

Symbols/Abbreviations	
%	Percentage
%T	Percentage of transmittance
W_p	Weight fraction of PP matrix in the composite
X_c^m	Degree of crystallinity
ΔH_{100}	Melting enthalpy of 100% crystalline PP
ΔH_m	Melting enthalpy of composite
°C	Degree celcius
°C /min	Degree celsius per minutes
µm	Micrometre
Al	Aluminum
$Al(OH)_3$	Aluminum hydroxide
Al_2O_3	Aluminum oxide
APS	Aminopropyltriethoxysilane
ASTM	American Society for Testing and Materials
ATR-FTIR	Attenuated total reflectance-fourier transform infrared
$BaSO_4$	Barium sulphate
B_f	Weight of the sample after soil burial test
B_i	Initial weight of the samples before soil burial test
Ca	Calcium
$CaCO_3$	Calcium carbonate
CAGR	Compound annual growth rate

CaO	Calcium oxide
CAS	Chemical abstract service
$CaSO_4$	Calcium sulphate
Cl	Chlorine
cm	Centimetre
cm^3	Cubic centimetre
DSC	Differential scanning calorimetric
DTG	Derivative thermogravimetric
ED-XRF	Energy dispersive x-ray fluorescence
F	Fluorine
Fe	Iron
Fe_2O_3	Ferric oxide
FTIR	Fourier transform infrared
g	Gram
g/ cm^3	Gram per cubic centimetre
g/min	Gram per minutes
g/mol	Gram per mole
GJ	Gigajoule
HDPE	High density polyethylene
J	Joule
J/g	Joule/gram
J/m	Joule per metre
K	Potassium
K_2O	Potassium oxide
LCD	Liquid crystal display

LDPE	Low density polyethylene
m^2/g	Weight fraction of PP matrix in the composite
MA	Maleic anhydride
MAPP	Maleic anhydride grafted polypropylene
MESSP	*Mimusop elengi* seed shell powder
Mg	Magnesium
Mg	Milligram
$Mg(OH)_2$	Magnesium hydroxide
MgO	Magnesium oxide
Min	Minutes
Ml	millilitre
Mm	millimetre
MPa	Megapascal
MRPS	3-mercaptopropyltrimethoxysilane
mw/mg	Milliwatt/milligram
N	Newton
Na	Sodium
Na_2O	Disodium oxide
NaOH	Sodium hydroxide
NFPC	Natural fiber reinforced polymer composites
Nm	nanometre
Nm	Nanometre
OH	Hydroxyl group
P	Phosphorus
P_2O_5	Phosphorus pentoxide

PALF	Pineapple leaf fiber
PC	Polycarbonate
PE	Polyethylene
PEEK	Polyether-ether ketone
PET	Polyethylene terephthalate
PP	Polypropylene
PP/MESSP	MESSP filled PP composites
PP/TMESSP	Treated MESSP filled PP composites
PS	Polystyrene
PSA	Particles size analysis
PVC	Polyvinyl chloride
Rb	Rubidium
Rb_2O	Rubidium Oxide
Rpm	Revolution per minutes
S	Sulfur
Sb_2O_3	Antimony trioxide
SEM	Scanning electron microscope
Si	Silicon
SiH_4	Silane
SiO_2	Silicon dioxide
SO_3	Sulfur trioxide
T_c	Crystallisation temperature
TGA	Thermogravimetric analysis
Ti	Titanium
TiO_2	Titanium dioxide

T_m	Melting Temperature
T_{max}	Maximum degradation temperature
TMESSP	Treated MESSP
Ton	Tonne
T_{onset} 10 %	Temperature at 10% weight loss
US$	US dollar
VTMO	Vinyl trimethoxy silane
W_{Ash}	Weight of the crucible and the ash
W_{cr}	Weight of the crucible with the dried residue
W_f	Weight of the sample after water absorption test
W_i	Initial weight of the sample before water absorption test
wt. %	Weight percentage
XRD	X-Ray Diffraction
ZnO	Zinc oxide

CHAPTER 1

INTRODUCTION

1.1 Overview

Over decades, utilization of petroleum based synthetic plastic become an indispensable part in our daily lives for numerous applications ranging from household packaging and appliances, automotive, agriculture purpose and in building construction. High demand and supply of synthetic plastics increases the disposal of plastic products to the environment after a single use application. Persistence of plastics disposed create tremendous impact to the environment, the scarcity of landfill space, emission of greenhouse gasses during incineration as well as depletion of petroleum resources (Alabi et al., 2019). Awareness on the sustainable development has grown due to unavoidable and unmanageable consumption and disposal of plastics to environment which spurred the effort on research related to natural fiber reinforced polymer composites (NFPC) (Mohammed et al., 2015).

NFPC is also known as biocomposites, can be produced with the incorporation of renewable resources sourced from plants and animals into synthetic polymer or biopolymer. Researchers have explored and investigated the development of various natural fibers such as jute, kenaf, flax, coconut shell, nutshell, coir, and bamboo as the reinforcing material or filler in the polymer

matrix from the past (Mohanty et al., 2002; Mohammed et al., 2015; Berzin et al.,2019). Besides, natural fibers has gain much attention and interest among industries and researchers due to its advantages over synthetic fibers such as renewability, bio-degradability, low density, low cost, competitive specific strength and environmental friendly (Kumar et al., 2017; Jiang et al., 2019). Despite the advantages, natural fiber also exhibited some drawback such as low wettability due to hydrophilic nature of the natural fibers resulting in high moisture absorption and low compatibility with polymer matrix which is hydrophobic. Therefore, natural filler requires pretreatment prior to addition into polymers to improve the interfacial adhesion between polymer-matrix through surface chemical modification (Chimeni et al., 2017).

Mimusops elengi Linn is a popular evergreen tree reaching a height about 9-18 m and abundantly available in among countries around India, Sri Lanka, Thailand, Malaysia, Indonesia, Philippines and New Guinea (Lim, 2012). *Mimusops elengi* is also known as Spanish cherry or Bakul which is plentiful available and grow naturally without the need for cultivation. Different parts of the plant have been widely studied in medication field; however, *Mimusops elengi* seeds are currently disposed into landfill and underutilized (Muniyadi et al., 2018). From the past research and applications, there were only few findings related to the *Mimusops elengi* seed applications in medical field. There are only two research has been reported in the past on the development of *Mimusops elengi* seed shell powder (MESSP) filled polymer composites (Muniyadi et al., 2018; Tan et al., 2019). The characteristics of

MESSP were not reported in depth to justify the suitability as filler for thermoplastic materials.

Therefore, the main aim of this research focused on the feasibility study, the property correlation of MESSP as the biofiller in PP composites through the melt mixing method (PP/MESSP) and the properties improvement of the composites (PP/TMESSP) through the alkaline treatment of MESSP. MESSP was produced from the seed shells of the ripe *Mimusops elengi* and used as filler in the production of biocomposites. Characterisation of MESSP and treated MESSP (TMESSP) were carried out to determine their physical and chemical functionality. Besides, the effect of NaOH treatment of MESSP on the physio-mechanical properties, processability, thermal stability, mechanical properties and water absorption of the composites were studied and compared with the PP/MESSP composites.

1.2 Problem Statement

Petroleum based plastic materials are seems to be ubiquitous in our daily life and a world without plastic is unimaginable today. Plastic have outgrown and is often preferred over other materials such as metals and ceramics due to its versatile properties which can be tailored, low cost, easily formable and remarkable bio-inertness (Geyer et al., 2017). Plastic were started to be produced commercially in 1950s at around 2 million ton and increased nearly 200-fold to reach the present global annual production of 380 million ton by the year 2015 with a compound annual growth rate (CAGR) of 8.4 % (Geyer et al., 2017; Ritchie and Roser, 2018). Ritchie and Roser (2018) reported the rapid growth of the global plastic waste which has exceeded the annual primary plastic production. The widespread use of plastics and tremendous amount of plastic wastes disposed to the environment especially into landfill and ocean become a growing global concern. High resistance of synthetic plastic towards degradation end up accumulated in our environment rather than decomposed. In fact, a plastic bag takes up to 1,000 thousand years to degrade (Hogan and Steinbach, 2019). There were around 4.8 to 12.7 million ton of plastics have been discharged into the ocean annually. This causes a negative impact to aquatic life when the plastic wastes were mistaken as food by the marine animal and ingested. In worse case, the plastic waste also stuck up on the different parts of its body which further endangers their survival. A plastic that has been consumed by the aquatic life such as fishes and crustaceous then being transfer up to the food chain and eventually end up in humans in the form of micro

plastics which causes an astonishing risk to human health (Lebreton and Andrady, 2019).

In conjunction with avoiding more plastics from being dumped and accumulating in the landfill and ocean, recycling emerged as a solution to encounter the environmental issues (Hogan and Steinbach, 2019). However, the plastic recycling rate are extremely low, as reported by Geyer et al. (2017), there was only 9% from a total of 6300 million tons of plastic waste being recycled, whereas 12% was incinerated, and there are large percentage up to 79% of wastes were streamed into landfill. Global plastic consumption is continually increases while recycling of plastic lags when the plastics are designed for single-use disposable applications has increase the municipal plastic waste (Lebreton and Andrady, 2019).

Recycling is not a preferable way to manage plastic wastes due to non-cost-effective recovery as the collecting, segregation, cleaning and processing of the recycled plastic involved a complex and tedious work and labor intensive. Moreover, the lack of advanced processing technology and the low demand for recycled plastic is one of the shortcomings of plastic waste recycling (Palmer, 2013). The slow growth in recycling rates has shifted the plastic wastes to be incinerated or openly burned. The release of toxic and greenhouse gases also resulting in harmful effect to human health (Hogan and Steinbach, 2019).

In response to these problems, research in the field of polymer composites from natural sources strives to partially replace the synthetic

polymer in developing greener and environmentally friendly polymer composites (Mohammad et al., 2018). However, the main challenge in the incorporation of natural filler into polymer matrix is the incompatibility between the hydrophilic natural fibers and the hydrophobic polymer matrix. The different nature of filler-matrix system causes poor interfacial adhesion and interaction, resulting in weak stress transfer and consequent low mechanical performance of the composites. Thus, an additional chemical pretreatment process is essential and involves the surface modification of filler or matrix which can help to improve the compatibility and increase the interfacial adhesion and interaction between the filler and matrix for better desired properties of the composites (Fiore et al., 2015; Shesan et al., 2019).

1.3 Objectives

The ultimate aim of this research is to study the feasibility of MESSP as bio-filler in PP matrix. The following specific research objectives were targeted:

i. To produce and characterise MESSP from the *Mimusops elengi* fruits.
ii. To develop MESSP filled PP composite through melt blending method at different filler loading by using Brabender internal mixer.
iii. To evaluate the effect of MESSP loading on the processing, physico-mechanical properties, thermal stability, water absorption resistance and bio-degradability of the composites.

iv. To study the effect of alkaline treatment of MESSP on the characteristics and properties of the PP composites.

1.4 Thesis Outline

The thesis is divided into five chapters as following:

Chapter 1 presents the introduction of the research and discussed the background of study, problem statement, research objective and the structure outline of the thesis.

Chapter 2 covered a comprehensive literature review outlining the thermoplastic, properties and application of PP, fiber reinforced polymer composites followed by the introduction of bio-composite to combat the environmental problems. This chapter also review on the current status of the natural fillers studied, in particular MESSP: its origin, characteristic and its application are reported. A review on the development of bio-composite with emphasis on bio-based thermoplastic polymer are presented.

Chapter 3 provides the details of the material sources, PP/MESSP composite fabrication process, characterisation and testing procedures of MESSP, TMESSP and the composites.

Chapter 4 details the physical and chemical properties of MESSP and TMESSP. This chapter also covers the detailed discussion of the processing, thermal stability, mechanical properties, morphological, water uptake and the bio-degradability of the bio-composites. A parallel comparison is reported to study the effect of the alkaline treatment of MESSP on the performance of the PP composites.

Chapter 5 covers the conclusions based on the findings from the study with recommendation for future.

CHAPTER 2

LITERATURE REVIEW

2.1 Thermoplastic

2.1.1 Introduction

Plastics are one of the most popularly used materials nowadays which are derived from petrochemical resources, joined by monomers through polymerization to form a long chain of molecules known as polymer (Shah et al., 2008). Plastic is a term derived from Greek “plastikos”, describing the polymeric material that is capable to be melted for shaping or molding. There are two categories of plastic, which is thermoplastic and thermoset (Joel, 1995). Thermoplastics are the materials can be melted when heated, shaped and harden when cooled. Thermoplastic can be reprocessed by the application of heat which is known as reversible polymerization. In contrast, thermoset cannot be re-melted or reformed again upon heat curing. Thermoset are cured by chemical reaction when heated which forms a three dimensional network and become an insoluble material (Grigore, 2017).

Basically, thermoplastic materials can be further classified into three different groups which is crystalline, semi-crystalline and amorphous polymers depending on the chains arrangement. The molecules of crystalline

thermoplastics present a regular arrangement whereas the molecules in the amorphous thermoplastic are randomly arranged (Grigore, 2017). Thermoplastics with the unique properties were rapidly commercialized when it replaced wide range of traditional materials due to their light weight, low cost and the ease of processing (Sastri, 2010). Figure 2.1 showed the rapid growth of the production of plastic throughout the past 67 years up to year 2017.

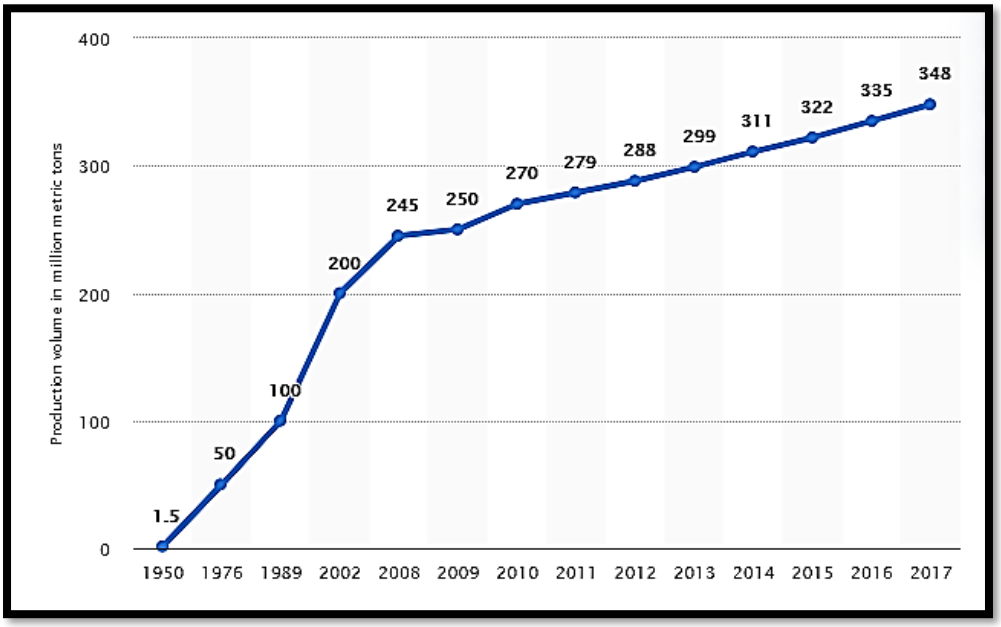

Figure 2.1: Global Plastic Production from 1950 to 2017 (in million metric tons) (Garside, 2019)

2.1.2 Variety of Thermoplastics and Applications

Thermoplastic can be classified as commodity and engineering plastics based on the application and performance level. Engineering thermoplastics are also known as high performing thermoplastic are typically higher cost as compare to commodity plastic. Table 2.1 presents the examples of commodity plastics that are widely used in our daily life.

Table 2.1: Production of the Commodity Thermoplastic and its Usage in 2015 (Stein, 2017; Beckman, 2018)

Type of Resin	Million tonnes	Example Product
Polypropylene (PP)	68	Syrup bottles, yogurt tubs
Low density polyethylene (LDPE)	64	Wrapping films, grocery bags
High density polyethylene (HDPE)	52	Milk and water bottles, detergent bottles, toys
Polyvinyl chloride (PVC)	38	Pipe, meat wrap, cooking bottles
Polyethylene terephthalate (PET)	33	Soft drink bottle, medicine containers
Polystyrene (PS)	25	Coffee cups

According to Biron (2016), thermoplastic governs at least 80% of overall plastic consumption and polyolefin such as polyethylene (PE) and PP are dominating the market of the synthetic polymer. Figure 2.2 shows that more than one-third of the plastic are used for packaging application, followed by building and construction, automotive, electrical and electronic appliances. Packaging application is the thermoplastics' largest market due to the ductility properties (Biron, 2016). Plastic can be shaped and molded into different products for wide variety of application such as packaging, household appliances, textile, construction materials and automotive parts (Stein, 2017).

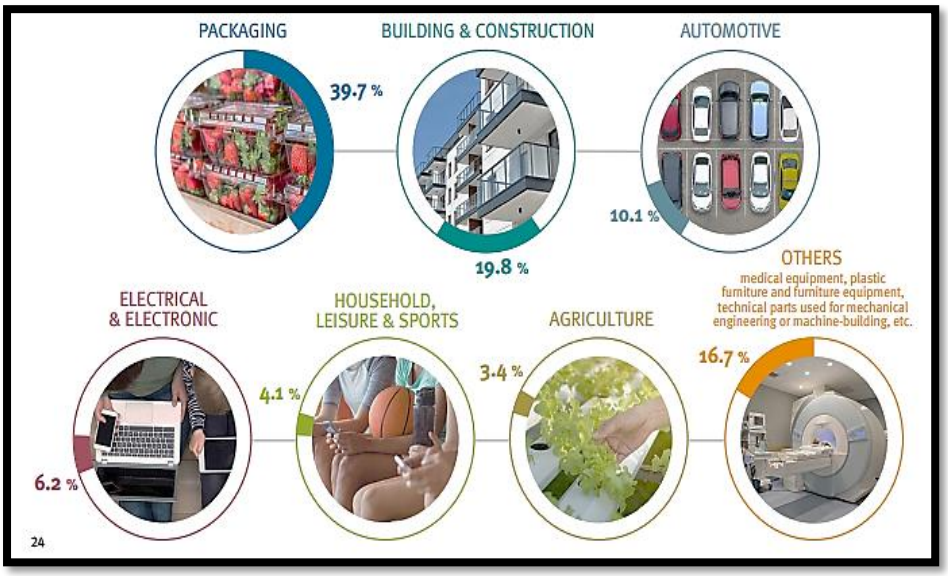

Figure 2.2: Plastic Demand in Different Sector (PlasticsEurope, 2018)

2.1.3 Processing of Thermoplastic Polymer

Different processing method and parameters can alter the plastic's properties depend on their functional uses. Thermoplastic can be stiff and hard or flexible and soft depending on the processing method (Grigore, 2017). Over decades, ease of the processing is among the factors that triggers the growth and demand of polymers. Thermoplastic material can be easily shaped and molded when heated before being cooled into hard and dimensionally stable solid plastic products. Basically, the selection of the processing method depends on the product's shape, size, the quantity and the aspect on the totality of the part surface (Stein, 1994). Due to the thermoplasticity properties, the manufacturing processes for thermoplastic are diversified included molding, extrusion, calendaring, thermoforming, welding and also boiler making. The most common conversion techniques used in the industry are extrusion, injection molding, blow molding and rotomolding (Biron, 2013).

Injection molding is the most widely used process which able to produce three-dimensional complex shape with accurate dimension and good surface finishing for mass production (Biron, 2013). Injection molding machine comprises of an injection unit and clamping unit. In injection unit, thermoplastic pellets are fed into the hopper and melted in the cylindrical chamber that contains a rotating screw. The pellets are push forward and melted into a homogeneous polymer melt by shear exerted from the rotating screw. Polymer melt is then pushed into the close mold cavity located in the clamping unit where the plastic melt flows into the shape of the mold cavity and solidifies on cooling.

When the average temperature of the polymer fall below the solidification temperature, the mold opens and ejects the product. The time taken for an injection molding cycle times is effected by the cooling time, part thickness, melting temperature and the demolding temperature (Stein et. al, 1994,; Mallick, 2010).

On the other hand, extrusion process is a continuous process used to produce profile products, cast and blown sheet, co-extrusion and blow-molded hollow parts. A wide range of products with different cross sectional dimensions can be fabricated with the use of a suitable die (Hollaway, 1993). Raw thermoplastic material usually in the form of pellet or powder is gravity fed in the hopper. The polymer is heated to the melting temperature by the mechanical work of the internal screw and the heat from the chamber. The extruder screw transports the polymer across a heated barrel to the die opening. The depth of the channel is reduced to compact the polymer before entering the shape-forming die. The homogeneously melted polymer will then be pushed through the die orifices by the force created by the screw rotation. The product exiting the die orifies is then pulled through water bath or air blower for cooling purposes before cutting into desire length or shape (Hollaway, 1993; Stein et. al, 1994).

The other type of thermoplastic processing method is the blow molding processes which can be sub-classified into extrusion blow molding, injection blow molding and stretch blow molding. Blow molding is a process of producing large scale of hollow objects such as bottle or containers (Biron,

2013). Thermoplastic in the form of pellets is heated and extruded through a die into a continuous semi-molten tube called parison. Parison is then clamped in the mold and a mandrel (steel rod) is inserted into the parison to allow highly pressurized air to enter. The internal pressure forces the parison through high pressure blowing to fit the interior of the mold. The product is cooled quickly to avoid creep and discharged through mold opening (Stein et al., 1994).

2.1.4 Processing of Reinforced Thermoplastic Composites

The processing technique used to manufacture reinforced thermoplastic composites is similar to the methods applied for the unreinforced thermoplastic polymer. Few common processing of reinforced thermoplastic composites are extrusion, injection molding with the addition of fiber, blow molding and thermoforming of fiber reinforced thermoplastic. Other than that, film stacking, in-situ polymerization, solution mixing and melt mixing methods are also reported in the literature review to incorporate fibers into thermoplastic polymer (Béland, 1990; Hollaway, 1993).

Out of all the techniques available, melt blending is probably one of the most widely and commonly used process because the process is simple, low cost, industrially favorable and environmentally friendly (Sekar et al., 2019). Bhandari et al. (2012) experimented with bamboo flour as reinforcement in PP by using melt blending technique. Koay et al. (2013) melt blended PP polymer matrix and the modified cocoa pod husk by methacrylic acid solution and

concluded the modified composite improved the mechanical and thermal properties of the composites. Most of the compounding process between the polymer matrix and filler are produced by melt blending technique as it is one of the easier and convenient. Besides, study by Ercan et al. (2015) reported that nanocomposites prepared by melt blending method gave a better structure and superior physical performance as compared to nanocomposites prepared from solution mixing method. According to Jlassi et al. (2017), melt mixing is more favorable over solution mixing for the polymerization process. Brabender internal mixer and the Banbury mixer are the most common batch type mixers. Banbury is suitable for large scale production whereas Brabender internal mixer is suitable for laboratory scale.

Brabender internal mixer is a measuring mixer that provide an immiscible polymers blend or an efficient mixing between the polymer matrixes and reinforcing filler. Majority of the fabrication for composites adopted melt blending and hot press through the compression molding technique. Polymer matrix have to go through melting to form a continuous phase before good dispersion of filler can be achieved (Han, 2007). Figure 2.3 presents the front view of the Brabender internal mixer. Figure 2.4 (a) shows the schematic diagram of the Brabender internal mixer with the blade and bowl which the matrix and filler are blended. Homogenous phase between single or multi components can be achieved with the shear created by the non-intermeshing, counter-rotating mixing blades as shown in Figure 2.4 (b); the configuration of two rotors create the shear during melting blending process. The amount of mechanical energy applied on the mixture depends on the rotor speed. In other

words, higher mechanical energy exerted with the higher rotor speed (Han, 2007). During heating, the volatiles and moisture of the mixutre will evolves. Crystalline polymer required higher processing temperature than the normal melting temperature for removing all the spherulite nuclei and facilitate the formation of the new uniform crystalline morphology (Béland, 1990). Figure 2.5 illustrates the schematic diagram of the evolution of the blending morphology during compounding (Han, 2007).

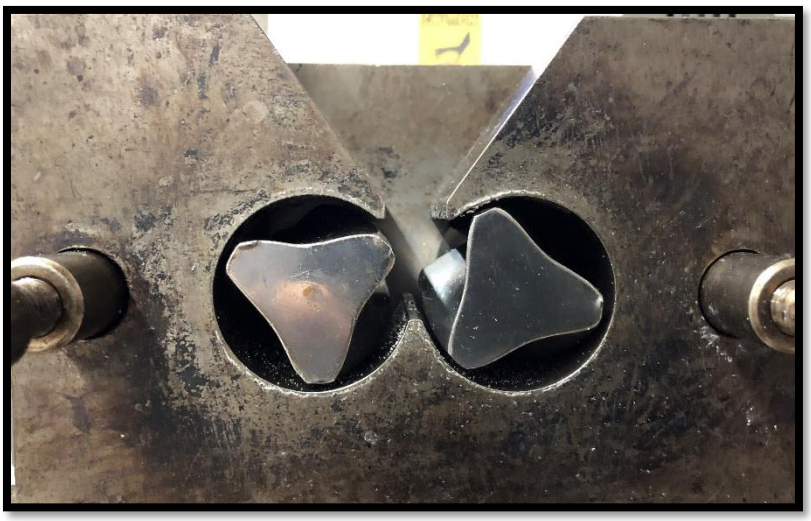

Figure 2.3: Photograph of Front View

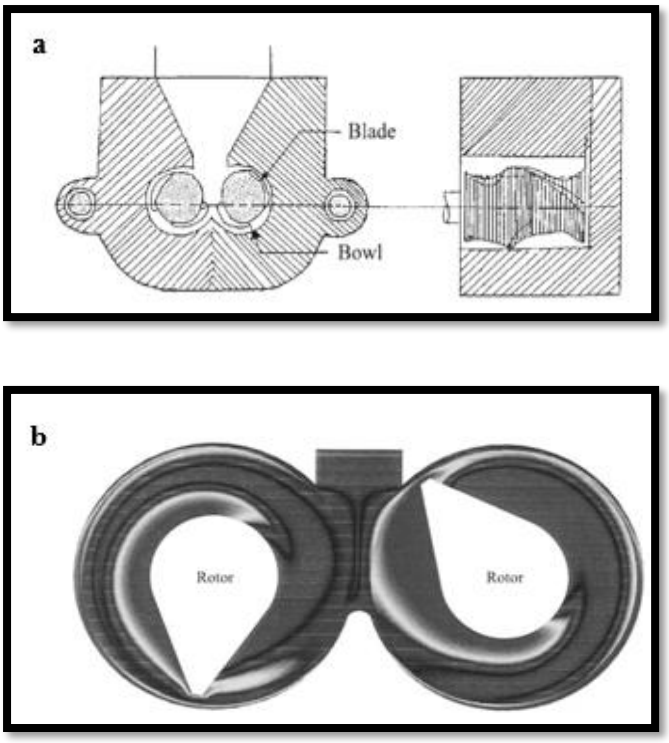

Figure 2.4: (a) Schematic Diagram of Brabender Internal Mixer with Blade and Bowl; (b) Schematic Diagram of the Flow Pattern of the Rotor (Han, 2007).

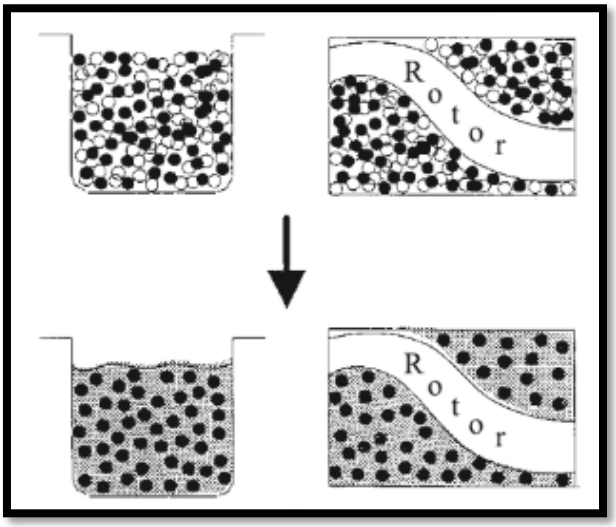

Figure 2.5: Evolution Morphology of Blending of Filler with Polymer Matrix (Han, 2007).

After melt blending, the mixed composite obtained from Brabender is pressed into composite sheets using a compression molding. Premalal et al. (2002) reported on the melt-blending of PP with rice husk powder and talc respectively, by using Brabender internal mixer, and the different filler of the polymer composites with different compositions were compared for mechanical properties. The processing temperature of the melt mixing process was 180°C with the rotation speed of 50 rpm. Shamsuri et al. (2015) conducted melt blending of PP with natural filler (kenaf fibre) and inorganic filler (dolomite) as the secondary filler using Brabender internal mixer at 180°C at 60 rpm to achieve maximum shear rate. It was reported that the kenaf filled PP bio-composites shows promising processing, thermal and mechanical properties in comparison to dolomite as secondary filler.

2.2 Polypropylene (PP)

PP was discovered in year 1955 through catalytic addition polymerization of propene as monomer. Propene olefin monomer is one of the vital building blocks next after ethylene in downstream petrochemical industry (Zaaba and Ismail, 2019). Figure 2.6 shows the asymmetrical structure of propene molecules. Propene is also known as propylene, are polymerized and combined together to form the long polymer chains. PP is a vinyl polymer with the attachment of the methyl group. The arrangement of the methyl group will affect the basic of polymeric chain structures which known as tacticity such as isotactic, syndiotactic and atactic as shown in Figure 2.7. Gas oil, naphtha, ethane and propane are the major sources of propylene (Sastri, 2014).

Manufacturing of PP through bulk process or gas phase process takes place with the presence of Ziegler-Natta catalyst which comprise of titanium (IV) chloride and triethyl aluminium (Shamiri et al., 2014). The reaction in the catalytic system produces radicals and initiate the propagation of the polymerization. Figure 2.8 illustrates the basic mechanism of the catalytic PP polymerization. Other than that, metallocene are also commonly used as the catalyst in the production of PP. The properties of PP are affected and vary depending on the process parameter, molecular weight and copolymer components (Shamiri et al., 2014).

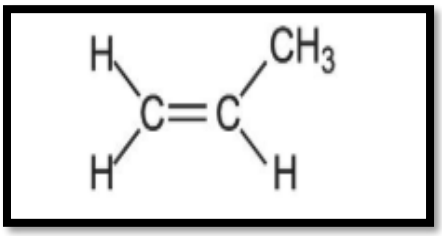

Figure 2.6: Propene Structure (Sastri, 2014)

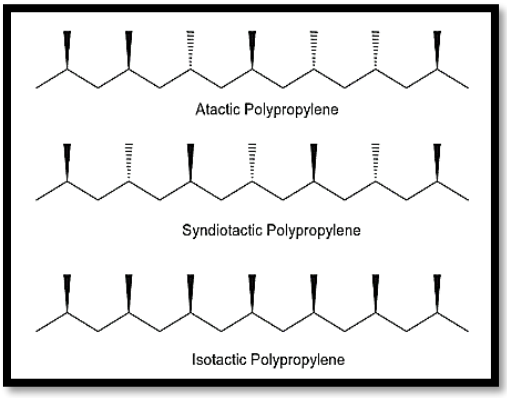

Figure 2.7: PP Structure (Sastri, 2014)

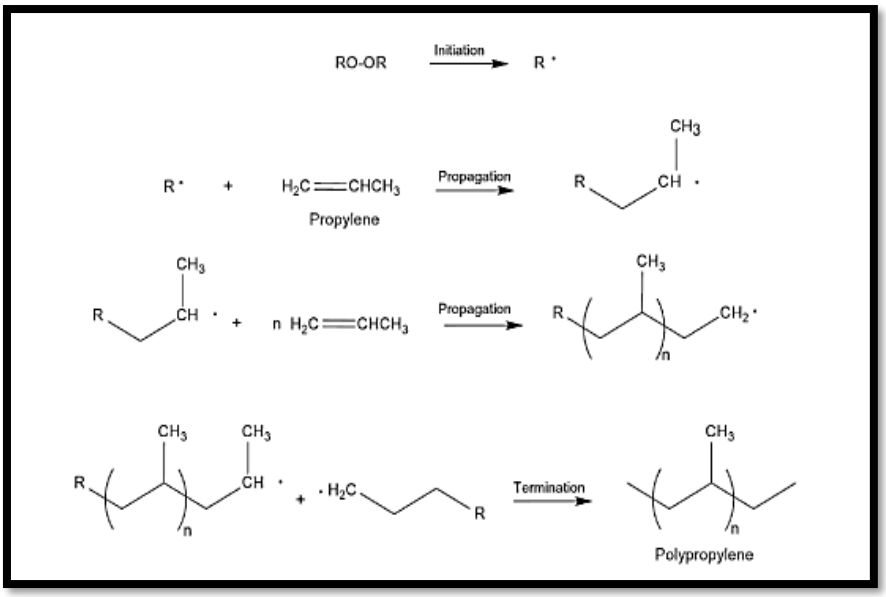

Figure 2.8: PP Polymerisation Mechanism (Sastri, 2014)

The consumption and production of PP keep rising due to its diverse properties and ease of processing method that meet the industrial requirement (Zaaba and Ismail, 2019). Figure 2.9 depicts that PP has the highest demand next after PE, accounting for approximately 19% of all thermoplastic demand worldwide. Based on the Figure 2.10, Richardson (2018) reported that the global average operating rates of PP has the healthier condition as compared to PE in term of the better profitability and capacity of utilization. The major factor driving the growth of PP over the past 20 years is the replacement of the metal, glass and other polymers with PP for various ranges of applications requiring durability and endurance. Emerging potential is foreseen to anticipate the growth in the profit of the PP market during the forecast period (Richardson, 2018).

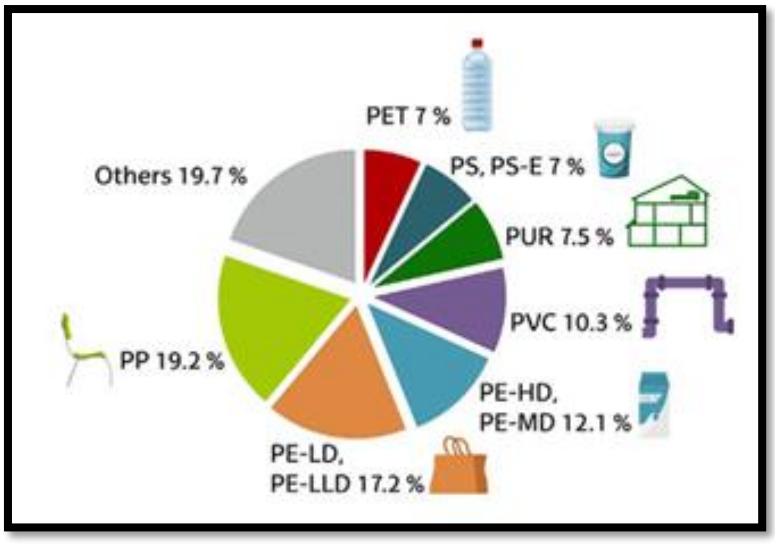

Figure 2.9: Types of Thermoplastic Demand (Lopez et al., 2017)

Figure 2.10: Global Average Operating Rates of PP and PE (Richardson, 2018)

2.2.1 Properties of PP

PP has remarkable combination of properties which lead to the diversity of application from single use disposal product to the long term durable products. PP is semi-rigid, translucent, has good heat resistance, good steam barrier properties, good impact strength and recyclability. Also, PP is considered as the lightest thermoplastic due to its low density properties. It is majorly advantageous for high chemical resistance applications due to nonpolar structure and also good mechanical properties at high temperature with the good performance-to-cost ratio (Sastri, 2014; Zaaba and Ismail, 2019). PP also has good chemical resistance towards the polar liquids such as alcohol, organic acid and esters and some aqueous solutions such as salts, alkaline and acid. Other than that, PP has a good water absorption resistance, high fatigue resistance and good electrical resistance, good dimensional stability and non-toxicity properties (Sastri, 2014).

Out of the three stereo specific configuration of PP, the most commercially used is the isotactic PP. Around 60% of PP produced are graded as homo-polymer which was the most commonly used in the industry (Maddah, 2016). PP has a variety of molecular weight distributions with the average of the molecular weight ranging from 200,000 g mol^{-1} to 600,000 g mol^{-1}. Table 2.2 shows the general properties of the isotactic homo-PP (Maddah, 2016; Zaaba and Ismail, 2019).

Table 2.2: Properties of PP (Maddah, 2016)

Property	Value
Density (g/cm^3)	0.91-0.94
Tensile strength (MPa)	22.1-34.5
Water absorption (%)	0.01
Elongation (%)	3-700
Softening point, T_g (°C)	140-150
Melting point, T_m (°C)	160-166
Thermal expansion (10-5 in./in. °C)	5.8-10

2.2.2 Application

The versatile properties of PP stimulate its growth for various end-use industries. Figure 2.11 presents the major uses of PP such as film packaging, rigid packaging, consumer products, and technical parts as well as for textiles application in year 2015 (Clement et al., 2010; Lazonby, 2016)

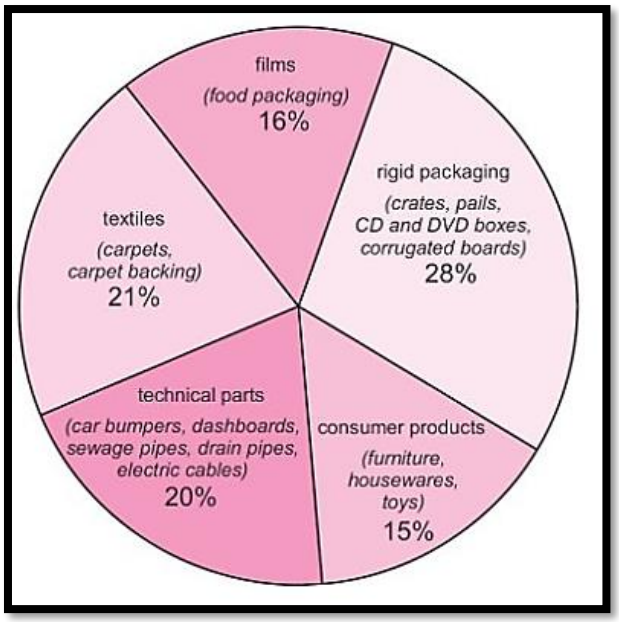

Figure 2.11: Application of PP (Clements et al., 2010; Lazonby, 2016)

Packaging industry accounts for the largest demand of PP with an average of 44% out of the total PP applications. PP can be processed into films or thin-walled container for food and rigid packaging. PP is an ideal choice for food packaging due to its low moisture transmission, high tensile strength and inexpensive for single uses and long term application **(**Clements et al., 2010**)**. High optical clarity, excellent moisture barrier property, low density and high temperature resistance of PP contributes to usefulness in healthcare and pharmaceutical industry for surgical equipment and other product such as syringes, tubing, pipettes and etc (Sastri, 2014). Moreover, PP also is used in high performance packaging for electrical and electronic products due to its good optical clarity, high strength and electrical non-conductivity properties (Du, Hou and Li, 2018).

Another significant consumption of PP is in automotive industry due to rising demand for lightweight and fuel efficient vehicles. The light weight to strength properties, easy processability, high durability and high stiffness properties make PP a more desirable material for production of the technical part for the automotive (Singh and Dutta, 2013). For instance, PP is injection molded into the interior and exterior part of automotive including battery case, door pillar, consoles, dashboards, seat assemblies and car bumpers. In addition, PP can also be injection molded for production of housewares applications such as toy, sport equipment, pipes and furniture due to its high toughness, durability and long term mechanical strength (Zaaba and Ismail, 2019). Besides, PP can be extruded into high strength fibers for textiles application such as nonwowen fabrics, carpet and clothing due to its semicrystalline nature which allows the chains to align easily to form high strength fibers.

Figure 2.12 shows the global consumption of PP by end use application is majorly account for the injection molding and fibers. The development of PP based composites has further extended the use of PP into a wide range of application through compounding of PP with other material, such as elastomers, fillers and pigments. PP also has good process ability as compared to other commercial polyolefin polymers and is suitable for filling or reinforcing with filler materials. Given this, the research for the new bio filler remain of great interest and pivotal to the plastics industry for a sustainable environment (Singh and Dutta, 2013).

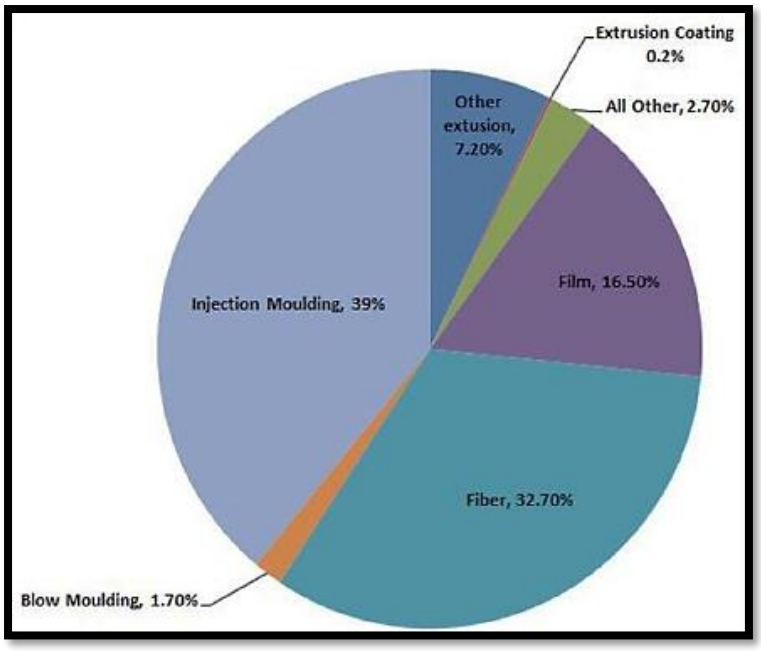

Figure 2.12: Global PP Consumption by End Use Application (Maddah, 2016).

2.3 Fillers Material

2.3.1 Introduction

Fillers are defined as the solid particulates that are added into polymers for different purposes depending on the source and nature of the material. Filler are either inorganic or organic materials with irregular shape and sizes which can be further classified according to the chemical family as shown in Table 2.3. In general, there are two types of filler include space fillers and functional fillers. Cost reduction and the ease of process ability are the main purposes of the addition of space filler; however it does not improve the mechanical performance of the polymer composite significantly (Friedrich and Breuer,

2015). The primary function of the functional fillers is to impart desired properties to the polymer composite to achieve enhanced properties. For instance, reinforcing fillers improve the mechanical properties in term of stiffness, tensile strength and elongation at break, and tear resistance of polymers (Kogel et al., 2006).

Most widely used filler materials are in particulate or fibrous forms and particulate filler are more desired for thermoplastic materials due to its good dispersion and no orientation effect on the properties as that imposed by fibers. Among the commercially available and widely used particulate fillers in thermoplastic polymers are silica, calcium carbonate, talc, kaolin, mica, etc. Glass fibers which are human made and other more environmentally friendly natural fibers of diverse categories are the most widely used fibrous fillers in thermoplastic polymers. Glass fibers are generally used to impart strength to the polymer matrix but it is costly as compared to natural fibers. Whereas higher loading of low cost natural fibers such as wood filler can be used to reduce the overall polymer composition in composites. As reported by Tolinski (2009), around one third of the polyolefin resin is replaced with wood fillers to enhance the durability of the construction materials.

Table 2.3: Chemical Families of Fillers for Plastics (Craig, 2010; Iqbal and Goyal, 2010)

Chemical family		Examples
Inorganics		
	Oxides	Glass (fibers, spheres, hollow spheres, and flakes), Magnesium oxide (MgO), Silicon dioxide (SiO_2), Antimony trioxide (Sb_2O_3), Aluminum oxide (Al_2O_3), and Zinc oxide (ZnO)
	Hydroxides	Aluminum hydroxide ($Al(OH)_3$) and Magnesium hydroxide ($Mg(OH)_2$)
	Salts	Calcium carbonate ($CaCO_3$), Barium sulphate ($BaSO_4$), Calcium sulphate ($CaSO_4$), phosphates, and hydrotalcite
	Silicates	Talc, mica, kaolin, wollastonite, montmorillonite, feldspar, and asbestos
	Metals	Boron and steel
Organics		
	Natural polymers	Cellulose fibers, wood flour and fibers, flax, cotton, sisal, and starch

2.3.2 Natural Filler

Natural fillers are derived from renewable resources that can be obtained naturally. Natural fillers can be easily degraded through microbacterial activities as compared to polymers. Thus, incorporation of natural filler or fiber as the degradable component in the synthetic plastic materials can improve the biodegradation property of the polymer composites upon disposal (Chauhan and Chauhan, 2013). The origin of natural fillers and fibers are sourced from either plants or animals as depicted in Figure 2.13. There are seven types of plant fibers namely stalk, root, seed, grass, stem, fruit and leaf that are extracted from plants whereas hairs, wool or silk are the examples of animal fibers (Azwa et al., 2013).

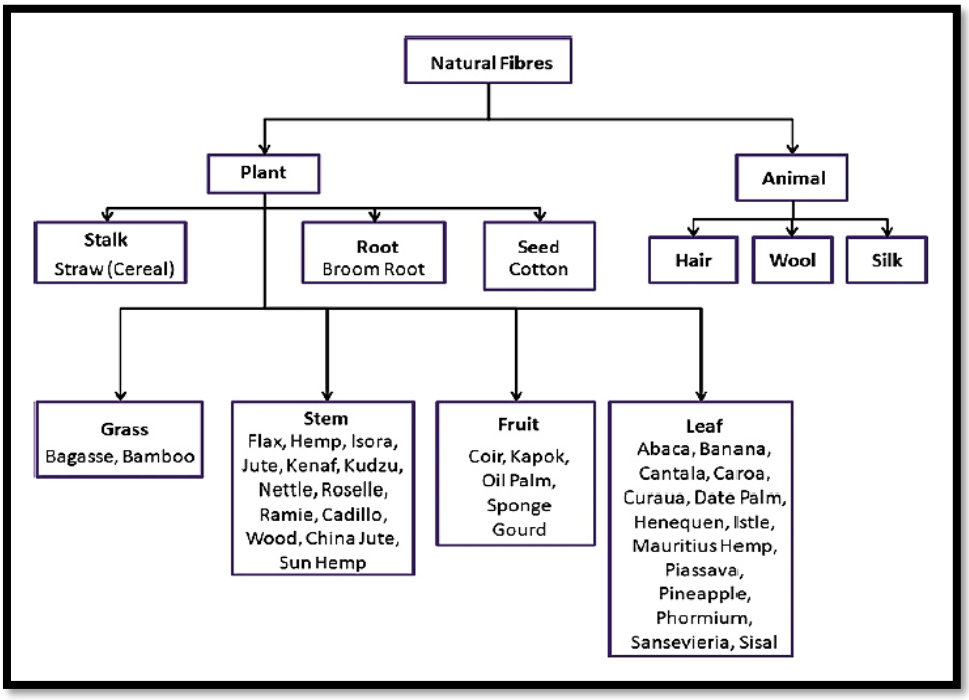

Figure 2.13: Classification of Natural Fibers (Azwa et al., 2013)

In polymer composite industries, natural filler is generally referred to plant fibers such as wood fiber and agro-based fiber that commonly used to reinforce plastics. The increasing demand for sustainable and environmentally friendly materials has gained more interest on the usage of natural fibers as compared to synthetic fibers in polymer composite development. Replacement of glass fiber and carbon fibers with natural fibers were due to the reasonable mechanical properties, low cost and low energy consumption for the production of natural fiber as compared to synthetic fibers. Table 2.4 shows the comparison of cost and energy consumption of natural and synthetic fibers (Peças et al., 2018). This comparison between natural and synthetic fiber has become the main factor contributing to the substitution of synthetic fibers with natural fibers in the polymer composites nowadays (Peças et al., 2018).

Table 2.4: Comparison of Cost and Energy Consumption of Natural and Synthetic Fibers (Peças et al., 2018)

Fibers	Cost (US$/ton)	Energy (GJ/ton)
Natural fiber	200-1000	4
Glass fiber	1200-1800	30
Carbon fiber	12500	130

2.3.3 Structure, Chemical Component and Properties of Natural Fiber

Natural fiber comprised of numerous cell walls which is made up of cellulose microfibrils and hemicelluloses-lignin matrix. The reinforcing of cellulose's microfibrils in the hemicellulose-lignin matrix in different composition forms the fiber cell wall. As shown in Figure 2.14, the layer structure of the cell wall is divided into two part which is the primary and secondary cell wall. Cellulose microfibrils in the primary cell wall are closed packed. Secondary cell wall are subdivided into three layers. Out of the three layer cell wall, the middle layer, S_2 is the thickest which controls the mechanical properties of the fiber (Thomas et al., 2011). Natural fibers has different variety of properties in term of the physical and strength properties according to their species, growth conditions, fiber extraction technique and also the inherent properties of fiber such as fiber cell geometry and chemical composition (Pasangulapati et al., 2012). In general, the complex structure of natural fibers is primarily made up of cellulose, hemicellulose and lignin. These three components are comprise of 85–90% of lignocellulosic biomass (Mohan et al., 2006).

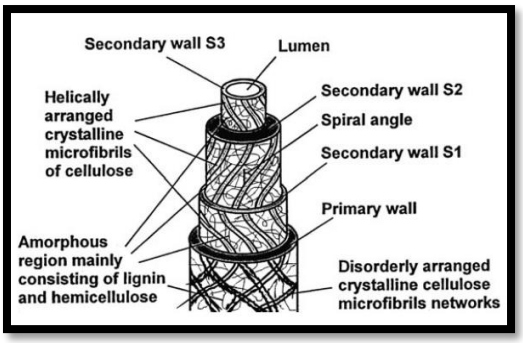

Figure 2.14: Structural of Natural Fiber (Thomas et al., 2011)

Among the three main components mentioned, cellulose is the main framework in the fiber with the least variation in the structure. Cellulose is the major structural polymer that has high crystallinity and resistant to hydrolysis. Strong crystalline structure and high degree of polymerization of the microfibrils is the factors that contribute to the strength, stiffness and the structural stability of natural fibers (Pérez et al., 2002; Machmudah et al., 2017). Also, cellulose is a linear polysaccharide whereas the hemicellulose is a branched polysaccharide. Cellulose is a homopolymer that comprise of the glucose monomer. On the other hand, hemicellulose consisting of different monomeric units of sugar including glucose, xylose, mannose, galactose and arabinose. There is no microfibrils formed in the hemicellulose. Hemicellulose polymers are directly connected to cellulose by hydrogen bonds (Ferreira et al., 2019).

As compared to cellulose, hemicellulose is more soluble and has low resistance toward chemical degradation. Lignin is the cementing material with amorphous structure. It is a highly cross-linked polymer between the phenylpropane units. Lignin has lower polarity than cellulose and higher thermally stability than hemicellulose (Mohan et al., 2006; Pasangulapati et al., 2012; Bajpai, 2018). Cellulose content, degree of polymerization and the microfibrillar angle are the three factors that affect the fiber's mechanical properties. Higher mechanical properties are contributed by higher cellulose content and degree of polymerization with a minor microfibrillar angle (Thomas et al., 2011).

2.3.4 Advantages, Disadvantage and Challenges of Natural Filler in Polymer Industry

Adoptions of natural fiber in different field of applications possess many pros and cons in term of their physical-mechanical properties, processing-ability and the effect to the environment (Pickering, et al., 2016). The growing interest of natural fiber in automotive industry was mainly urged by the implementation of legislation imposed in Europe with the objective to improve the vehicles recyclability up to 95% by weight. Low density and weight of natural fiber contributes to the lighter natural fiber composites. Low economic value of natural fiber with low density properties also possess high specific strength and stiffness serve reinforced to the structure of polymer composites (Witayakran et al., 2017).

Natural fiber with low frequency of acoustic absorption has the potential to be used in sound adsorption application. Also, natural fiber has good thermal insulation properties due to its low thermal conductivity. Moreover, natural fiber is a good electrical insulator thus the natural fiber composite is ideal to be applied in electrical and electronic application (Mamtaz et al., 2016). Processing of natural fiber has numerous favorable circumstances as compared to synthetic fiber including low abrasive damage to the processing equipment, low human health hazard during manufacturing process of the composites, no skin and eye irritation and also low emission of toxic fumes during the incineration (Tajuddin, et al., 2016). Besides, natural fibers are abundantly available from wide variety

of renewable resources which are biodegradable and eco-friendly (Faruk et al., 2013; Väisänen et al., 2016)

Production of natural fiber requires low energy consumption as the cultivation rely mainly on the solar energy whereas the extraction of the natural fiber consumes little amount of fossil fuel energy. On the other hand, production of synthetic fiber requires ten times more fossil fuel energy as compared to the natural fiber. In this manner, natural fiber poses less harm to environment as compared to synthetic fiber as less gas pollutants emitted throughout the production process (Begum and Islam, 2013). Other than that, increase demand of natural fiber opens more opportunity to the rural area by which more plantation and agricultural sector blooms up in producing natural fibers as byproducts. It also aid in accomplishing the sustainable development goals where it copes the poverty issue, and provides good health and well beings of future generation (Faruk et al., 2013).

Despite the advantages of the natural fiber as mentioned, the drawback of natural fiber creates the challenges and limits the use of natural fiber in polymer industry. Decomposition of natural fiber at high processing temperature due to low thermal stability of natural fillers as compared to polymers restricts the maximum processing temperature and the selection of polymer matrix. Natural fiber has low durability and higher moisture absorption which results in low mechanical properties and moisture absorption of the plastic products used in outdoor applications or in high humidity environments. Besides, natural fibers also possess lower durability as compared to synthetic

fibers due to ease of fungus attack in an open environment. Also, high moisture uptake by the natural fibers results in swelling which further deteriorate the strength of the composites. The disadvantages discussed are mainly due to the inherent hydrophilic properties of natural fibers that caused low compatibility to hydrophobic polymer composites. Low wetting between natural filler and polymer matrix is one of challenging phenomena which could be observed during the processing and results in poor performance of natural filler filled polymer composites (Faruk et al., 2013; Pickering, et al., 2016; Tajuddin, et al., 2016).

2.4 *Mimusops Elengi* Linn

2.4.1 Introduction

Mimusops elengi is a ubiquitous evergreen tree grows in India due to its great potential in medical application since the prehistoric days. It is belonging to the Sapotaceae family and it has common vernacular names in various languages as tabulated in Table 2.5. The bark of *Mimusops elengi* tree is black in color, thick and tough whereas, the trunks grow upright with the spreading branches. The hard and tough properties of the central wood make it an excellent timber wood. The heartwood is valuable and used as construction material for temples in India to build ornate pillars, ceilings, windows and doors. The star-shaped of Bakul tree flowers are in yellowish-white colour with pleasant smell. The ovoid shape of berry is 2.5 cm long as shown in Figure 2.15.

Table 2.5: Names of *Mimusops Elengi* Linn in Different Language (Baliga et al., 2011)

Language	Names
English	Spanish cherry, Medlar and Bullet wood
Sanskrit	Bakula, Bramarananda, Stri-mukhamadhu, Anankantha, Madhuparijara
Hindi	Maulseri, Molchari, Maulsiri, Bakula
Bengali	Bakul
Malayalam	Elengi, Ilanni, Ilenji
Tamil	Alagu, Kesaram, Magilam, Mogadam, Nakum, Magizham Magizhamboo
Malay	Tanjong
Myanmar	Kha-Yay
Thai	Pikul

Figure 2.15: Flowers and Ripe Fruits of *Mimusops Elengi* Linn (Baliga et al., 2011)

Being a neglected and underutilized fruit, the information regard to the composition and components of the fruit is very limited. However, based on the

research done by Nazarudeen (2007), the compositions of Bakul fruits were approximated in the study. Based on the fresh fruit basis, the fruit consist of approximately 79.27% moisture, 1.29 % protein and 2.76% fat. Out of the 15.2% of the total sugar, there is 8.9% of reducing sugar and 6.3% of non-reducing sugar. Fiber content in the fruit is 1.13% and the remaining is a small amounts of minerals, vitamin C, iron, sodium and potassium. In phytochemistry study, betulinic acid, β-sitosterol, lupeol and ursolic acid were found to be the main chemicals in the bark as shown in Figure 2.16 (Nazarudeen, 2007; Baliga et al., 2011).

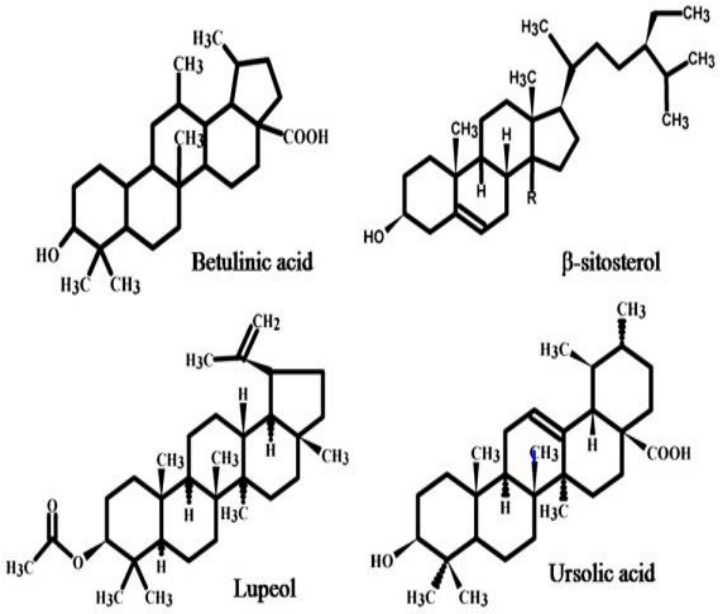

Figure 2.16: Important Phytochemicals present in Bakul (Baliga et al., 2011)

In addition, hentriacontane, carotene and lupeol are the phytochemical constituents isolated from the leaves, heartwood and roots. Besides, volatile oils are also widely extracted from the flowers to be used as oilment and fragrance (Kadam et al., 2012). The seeds are known to have pentacyclic triterpenes,

mimusopgenone and mimugenone, triterpenoid saponins (Gami et al., 2012). These phytochemical constituents extracted from different parts of the plant were useful for the biological activities (Sen et al., 1995; Lim, 2013).

2.4.2 Application

Mimusops elengi is widely used in India for many daily applications. In the early year after discovery of *Mimusops elengi*, the berries are edible and commonly consumed once ripe. Seed kernel was reported to contain about 22% oil where the oil was extracted and used in cooking (Kadam et al., 2012; Lim, 2013). However, the fruits are no longer consumed after the chemical such as alkaloid was found in the plant. The toxic alkaloid can pose a risk to human health (Gupta, 2013; Diaz, 2015). Meanwhile, the dried flowers are used as a filling in pillows due to the fragrance of the flower which last long and comforting during sleep. Besides, the flowers are used to make necklaces for decoration (Fern, 2017). Moreover, *Mimusops elengi* is well known in India due to its high value as traditional medicinal. In modern study, research related to the application of *Mimusops elengi* in biological and medical have been carried out intensively. Tannin, saponin, quercitol, d-mannitol, quercetin, alkaloids and taraxerol are found to be the active components embedded in different parts of *Mimusops elengi* which contain high medicinal value (Baliga et al., 2011). According to Kadam et al. (2012), the bark, fruit, leaves, seed and flowers extracted from the plant has pharmacological or toxicological effect (Kadam et

al., 2012). Table 2.6 summarizes the effect contributed by different parts of *Mimusops elengi* plant.

Table 2.6: Pharmacological/toxicological Effect of *Mimusops Elengi* Plant (Amir et al., 2013; Singh et al., 2014)

Parts used	Effect
Bark	Antimicrobial
	Antiviral
	Antiulcer
	Anti-inflammatory
	Antihyperlipidemic
	Antianxiety
	Diuretic
	Wound healing
	Larvicidal activity
	Anthelmintic
Leaf	Anti-inflammatory
	Antioxidant
	Antihypertensive
	Antidiabetic
	Analgesic
Stem	Antiprotozoal
Fruit	Antioxidant
Seed	Molluscicidal activity

The bark was found to have in-vitro antimicrobial effect to many types of bacterias such as *Staphylococcus aureus, Streptoccus mutans, Streptococcus salivarius, Lactobacillus acidophilus* and *Candida albicans* (Prabha et al., 2010; Amir et al., 2013). Other than antimicrobial properties, the bark was examined to have antiulcer activity against serotonin induced ulcer in albino rats (Dabadi et al., 2011). Antiurolithiatic activity was ttested in male albino Wistar rats by using the petroleum ether, chloroform, and alcohol extracts of bark. Gargling liquids are also made from the mixture of decoction of the bark with the flowers and helps in curing gum inflammation and toothache (Hebbar, 2016).

Based on the past research works, it was evaluated that the leaf extract to have in-vitro antibacterial activity especially on *Xanthomonas campestris* and *Bacillus anthracis*. Extraction process of volatile oil from the leaf was used to investigate the effect on fungal. Positive result was obtained when the oil showed the anti-fungal activity on *Keratinonyces ajelloi, Microsporum gyseum* and *Trichophyton equinum* on the agar plates. The alcoholic extracts such as ethyl acetate, ethanol and water extract of *Mimusops elengi* were evaluated in diuretic activity (Roqaiya et al., 2015). Hence, the investigation and researches had been carried out are the supporting evidence to prove that *Mimusops elengi* plant is a potential medicinal plant for now and future (Amir et al., 2013; Shivatare et al., 2013; Singh et al., 2014).

As mentioned, *Mimusops elengi* is widely available without specific plantation area required. For this research study, *Mimusop elengi* fruits was collected from the plant located at roadside of the residential area. Large scale

of *Mimusop elengi* seed could be also supplied from different sellers in the market. For instance, the price of the *Mimusop elengi* seeds was USD 5- USD 10 / kg of the seed (Alibaba.com, 2020).

2.5 Natural Fiber Reinforced Polymer Composites (NFPC)

There are different definitions of the composite reported by different researchers. Composites in simple definition are the combination of two or more compatible material to produce the cohesive structural properties of the blended material. Composites consist of two main phases namely matrix and fillers. For the constituent of the composites, matrix is the continuous phase whereas the filler or fiber is the discontinuous phase. The utilization of NFPC becoming more prevalent due to the increase in environmental conscious among the public during the past few decade. In the view of that, NFPC are getting huge interest from researchers in the various fields including production, fabrication and applications of NFPC in term of their sustainability and economically (Chandramohan and Marimuthu, 2011).

2.5.1 Types of Natural Fiber Reinforced Polymer Composites

NFPC is known as bio-composites derived from the polymer matrix reinforced with renewable, organic and biological resources. NFPC can be categorised according to the nature and the origin of the constituent either fully

renewable composites or partially renewable composites. Fully renewable composites namely green composites implies that both matrix and the filler are derived from bio-renewable resources. In the partially renewable composites such as NFPC, the matrix is made of polymer derived from petroleum resources whereas the filler is made of natural resources (Peças et al., 2018; Gowda et al., 2018). Figure 2.17 shows the classification of the NFPC. The most commonly used petroleum based matrix is thermoplastic and thermoset. Table 2.7 presents the example of the polymers used as the matrix in the composites respectively.

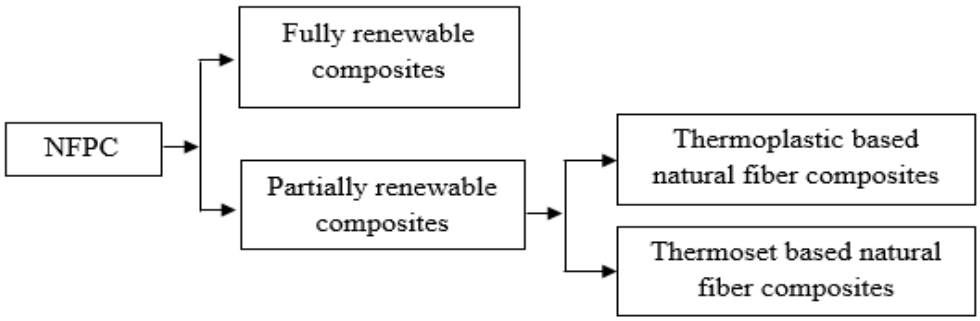

Figure 2.17: Classification of NFPC (Gowda et al., 2018; Peças et al., 2018)

Table 2.7: Types of Polymer Matrix for NFPC (Gowda et al., 2018)

Thermoplastic	Thermosets
PP	Polyester
PE	Phenolic
Polycarbonate (PC)	Epoxy
PVC	Polymide
PS	Polyurethane
Polyether-ether ketone (PEEK)	

2.5.2 Properties and Performance of Natural Fiber Reinforced Polymer Composites

The properties and the performance of NFPC are mainly affected by few factors such as matrix properties, compatibility of matrix and filler as well as the fiber-matrix ratio and/or composition. Besides, appropriate fabrication method and processing parameters are essential to achieve the desired performance of NFPC (Mohammed et al., 2015). The main properties of NFPC that keen the interest of the researcher are the light weight properties, environmental friendly, ease of processing and also economically. Hence, extensive researches have been conducted on the development and improvement of NFPC's properties on technical and environmental perspective such as mechanical properties, water resistance characteristic, thermal stability and bio-degradability.

With such research and developments, various type of NFPC with different properties can be developed and applied in different field of application (Todor et al., 2018). However, in real practice, the major shortfalls of NFPC are the low compatibility between the polar nature of natural filler and hydrophobic, non-polar polymer matrix. Weaker physical adhesion and interfacial interaction between polymer and matrix become the main factors that contribute to the lower mechanical properties, higher tendency of water absorption and poor dimension stability of the final composites. To enhance and improve the properties of NFPC, chemical treatment of the natural fiber or the

addition of coupling agent are necessary to improve the adhesion between the fiber and matrix (Shesan et al., 2019).

Nevertheless, the orientation of fiber, physical properties of fiber, fiber's strength and the physical interaction property of fiber are among other few factors that could affect the performance of composite (Mohammed et al., 2015; Peças et al., 2018). Mechanical properties of composite depend on the fiber-matrix interphase. Better mechanical properties of the composite over unfilled polymer matrix were achieved in the investigation reported by Simonassi et al. (2017). In this case, better interfacial adhesion between fiber and polymer matrix promotes the stress transfer from the matrix polymer to the fiber contribute to a higher mechanical efficiency. The mechanical properties of the continuous and aligned ramie fibers reinforced polyester composites was investigated up to 30 vol% by compression molding method. Flexural, tensile and impact properties showed a positive effect as the stress transfer mechanism through the polyester/ramie fibers resists the propagation of crack.

Chollakup et al. (2010) investigates the effect of the length of the pineapple leaf fiber (PALF) with the different fiber orientation on the properties of the LDPE composite. The enhancement of the tensile strength of the composites was more significant with the longer PALF than the shorter PALF. The observation obtained from the SEM revealed that the unidirectional oriented long PALF have a better dispersion than the multidirectional short PALF which resulted in the good interfacial bonding between the PALF and the LDPE matrix polymer (Chollakup et al., 2010).

Extensive studies was conducted on the development of natural fiber based thermoplastic polymer composites. There are different types of thermoplastic in the market, the research studied on the NFPC have been comprehensive review. PP is the choice of selection among the thermoplastic available due to their distinct properties. For instance, PP possess high flame resistance, high chemical resistance, high distortion temperature and the lower melting point of PP allows fabrication of NPRC at the lower processing temperature to prevent the degradation of the natural fiber (Mallick, 2010; Thakur et al., 2014; Gowda et al., 2018).

According to the study reported by Shubhra et al. (2010), the reinforcement of jute in PP composites improved the tensile strength up to 88%, increased the young modulus up to 8% and gained 186% in impact strength. This indicated the good physical adhesion resulted in the stronger strength and better properties of the composites. In fact, many research conducted on the finding of the mechanical properties such as tensile strength, tensile modulus and impact strength of PP composites reinforced with different type of natural fiber. Thakre et al. (2018) reviewed and outlined the experiments conducted on natural fiber such as flax, bagasse, coir, wood, hemp, nut shell of argan reinforced in PP composites.

Other than that, Shubhra et al. (2011) have reviewed the mechanical properties of PP reinforced with natural fiber composites. Based on the study, flax fiber reinforced PP composites showed a highest tensile properties whereas silk fiber and calcium alginate fiber reinforced PP composites presents a higher

impact strength as compared to the other natural fiber reinforced PP composites. Figure 2.18 illustrates the comparison of the tensile strength, tensile modulus and impact properties of the natural fiber reinforced PP composites. Based on the comparison, it was observed snail shell powder reinforced PP composites demonstrated a highest tensile strength; yerba mate fiber achieved a highest impact strength and rice husk reinforced PP composites has a highest stiffness among all the other natural fiber composites (Aridi et al., 2016; Barkoula et al., 2009; Catto et al., 2019; Hassen et al., 2015; Karmarkar et al., 2007; Lee et al., 2009; Onuegbu and Igwe, 2011; Ramli et al., 2011; Samal et al., 2008; Shubhra et al., 2010; Simonassi et al., 2017; Sullins et al., 2017; Yuan et al., 2008).

Other than mechanical properties, water absorption characteristic is another important properties to determine the suitability of the composite to be used for outdoor application. This is because the moisture absorption will facilitate the fungal attack, cause the poor dimension stability and further accelerate the deterioration lead to the short service life of the composite (Yeh et al., 2015). The well-known limitation of the NFPC is the poor moisture resistance due to the hygroscopic characteristics of the natural fiber. The hydrophilic nature of natural fiber cause high affinity to water absorption resulted in higher water uptake or swelling.

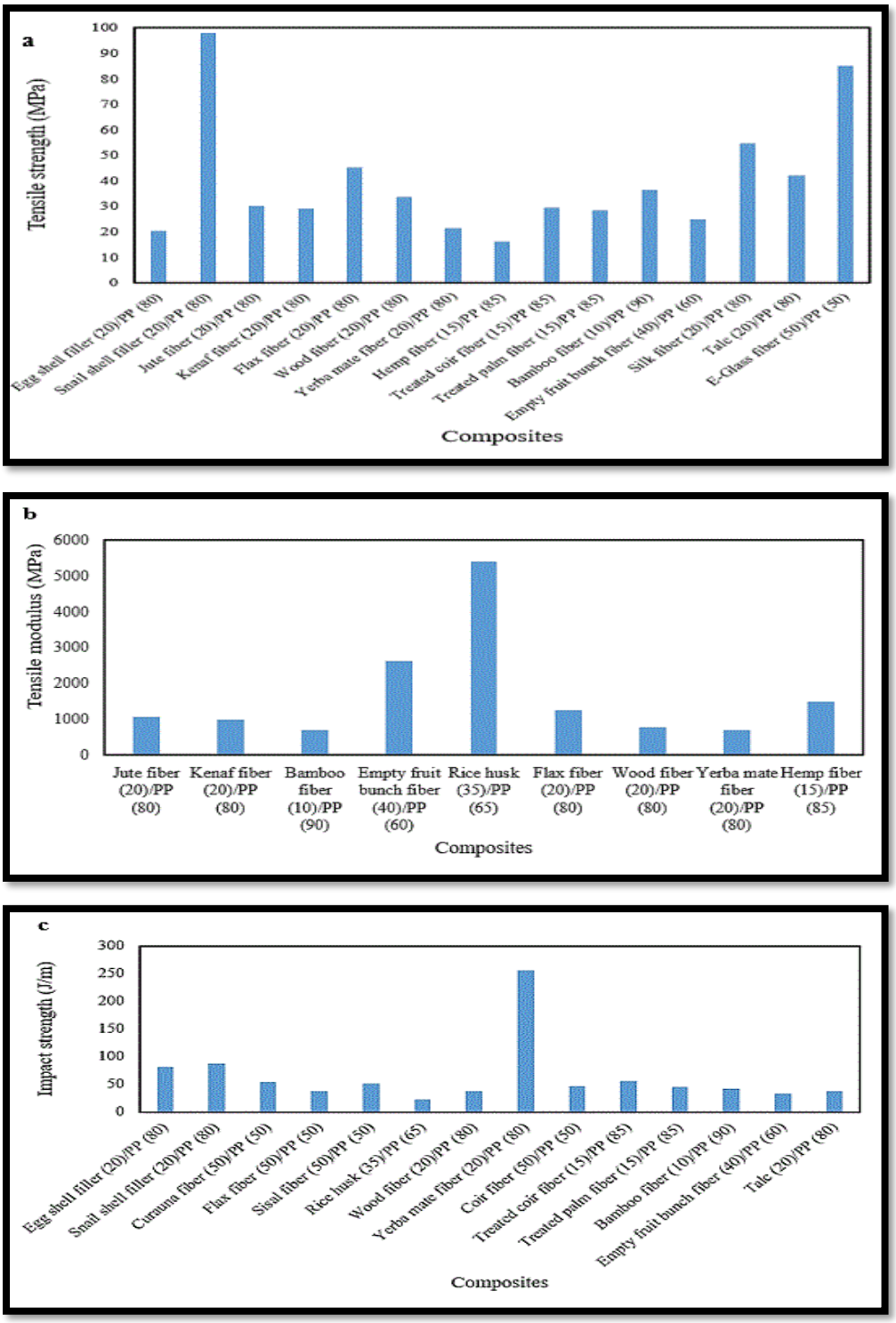

Figure 2.18: Comparison of the (a) Tensile Strength; (b) Tensile Modulus; (c) Impact Properties of Natural Fiber Reinforced PP Composites (Aridi et al., 2016; Barkoula et al., 2009; Catto et al., 2019; Hassen et al., 2015; Karmarkar et al., 2007; Lee et al., 2009; Onuegbu and Igwe, 2011; Ramli et al., 2011; Samal et al., 2008; Shubhra et al., 2010; Simonassi et al., 2017; Sullins et al., 2017; Yuan et al., 2008)

Also, natural fiber with hydrophilic nature is incompatible with the hydrophobic nature of the polymer matrix, subsequently causing the poor mechanical properties (Ku et al., 2011). Similar results were reported on the incorporation of the higher loading of natural fiber which increased the water absorption of composites (Ayrilmis et al., 2011; Kaewkuk et al., 2013; Jariwala and Jain, 2019). According to the review conducted by Dittenber and GangaRao (2012), the strength of the sisal/polyester composites was further reduced due to the moisture absorbed after soaking in water.

Furthermore, the durability of the NFPC composites is affected by the thermal stability of the composites. Thermal stability of the natural fiber itself is one of the aspects to be considered in composite processing. This is to avoid the thermal degradation of the fiber that could subsequently affect the properties and the performance of the composites (Ku et al., 2011). Another inherent limitation of the natural fiber is the low thermal stability (Begum and Islam, 2013). Generally, NFPC possess lower thermal stability as compared to the pure polymer matrix due to the presence of hemicellulose and lignin constituent in the natural fiber which has lower thermal degradation temperature (Kuciel, et al., 2014).

Similar observation was reported by Essabir et al. (2013), by which the incorporation of argan nut shell in PP composites was less thermally stable than the pure PP. In order to improve the properties of the NFPC which is comparable and competitive with the synthetic fiber reinforced polymer composites, chemical modification of natural fiber or matrix polymer is needed to improve

the physical adhesion (Lu and Oza, 2013). Study in the past showed that the thermal property of coconut fiber reinforced PP composites was improved with the addition of coupling agent which enhances the interfacial adhesion between the coconut fiber and PP (Thakre et al., 2018).

On the other hand, inducing the bio-degradability properties of polymer composites can be achieved by incorporation natural fiber into polymer matrix. NFPC offer a more environmental friendly and sustainable option in different field of application. Bio-degradability can be triggered when the NFPC is attacked by the microorganisms. Microorganisms decompose the natural fiber through the hydrolysis of carbohydrate into the digestible unit (Pandey et al., 2010). Sareena et al. (2013) monitored the biodegradation behavior of the natural rubber reinforced coconut shell and peanut shell powder composites through soil burial test for three and six month of soil burial period. Based on the study, filler content, size of the particles, filler modification are the factors that could affect the biodegradation rate of the composites. Loss of the mechanical properties was found due to the biological attack and the weight loss of the composite was more significant with the higher filler content which suggests that addition of natural filler could help to decompose the polymer composites upon disposal.

2.5.3 Application of Natural Fiber Reinforced Polymer Composites

Low density, satisfactorily properties, relatively low production cost, low carbon foot print, renewable sources of the natural fiber are the driving factors toward the utilization of natural fiber over the synthetic fiber (Ahmad et al., 2014). Adoption of NFPC in various fields of application involve different types of natural fibers such as hemp, flax, jute, kenaf, sisal, etc. have gain interest and good implication in the automobile sector, construction sector as well as exploited for packaging purposes (Peças et al., 2018).

2.5.3.1 Application of Natural Fiber Reinforced Polymer Composites in Automotive Industry

In 1940s, the utilization of the NFPC for automobile application was first produced with hemp fiber by Henry Ford. Soon or later, the NFPC emerges very rapidly due to higher demand for light weight, good specific strength and modulus with eco-friendly characteristic (Sullins et al., 2017). The growing of bio-based composited is motivated from the economical and sustainable green environment point of view. From the advantage of fuel efficiency as stated by Pandey et al. (2010), around 250 million barrel of crude oil was saved and 220 billion pounds of carbon dioxide emission was reduced per year when the automobile weight is reduced with 25%.

Germany based car manufacturer such as Mercedes, Volkswagen, Audi Group, BMW and Ford fabricated the car interior part such as seat, door panels, dashboards, door trim panel, boot linen, backrest and parcel shelves with NFPC (Sanjay et al., 2016; Witayakran et al., 2017). Glass fiber reinforced polymer composites has been replaced by flax/PP composites in Mercedes-Benz A-Class. Also, press molded flax/PP composites was used to produce the inner instrumental panel of the Smart Fortwo Coupe. Door panel was produced with polymer composites reinforced with jute fiber in Mercedes-Benz E-Class. With the 44 car interior components produced with other natural fiber, reduction of weight up to 34% was achieved as compared to the previous model (Ahmad et al., 2014).

There was 80,000 ton of natural fiber composites used in automotive sector in the year 2012 in European Union. Figure 2.19 presents the different types of natural fiber used and it could be observed that the wood and cotton fiber governed more than half as compared to the other fiber. Table 2.8 summarizes the commercially used NFPC in automotive industry.

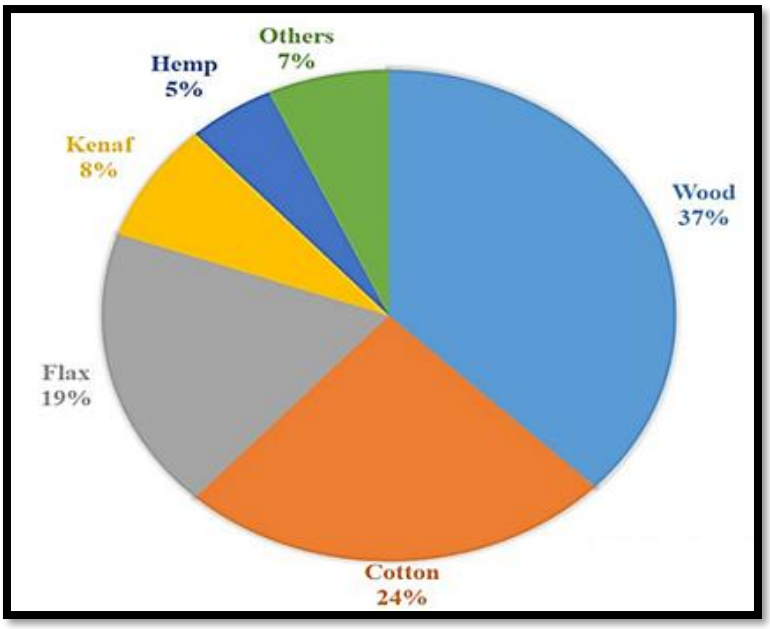

Figure 2.19: Types of Natural Fiber Used in the European Union Automotive Industry in 2012 (Witayakran et al., 2017)

Table 2.8: Application of NFPC in Automotive Industry

Fiber	Polymer	Automotive Applications	Reference
Wood fiber	Acrylic resin	Carrier for covered door panels Covered or foamed instrument panels Covered inserts (currently in production for Mercedes-Benz, Opel) Covered seat back panels (currently in production for BMW, Ford, MercedesBenz, Opel, Hyundai)	Witayakran et al. (2017); Peças et al. (2018)
Wood flour	PP or polyolefin	Carrier for covered door panels Carrier for armrest Carrier for covered inserts (currently in production for FIAT, Lancia, Alfa Romeo)	
Hemp or Flax	Epoxy resin	Carrier for covered door panels (currently in production for BMW)	

Table 2.8 continued

Fiber	Polymer	Automotive Applications	Reference
Fibrowood recycled (Wood fiber/acrylic resin, synthetic fiber)	PP granules	Plastic retainer for seat back panel	Witayakran et al. (2017); Peças et al. (2018)
Bast fiber (flax, hemp, kenaf, jute, sisal, etc.)	PP or polyester	Rear shelf trim panels (Chevrolet Impala), door panels, door bolsters, headliners, side and back walls, seat backs, rear deck trays, pillars, center consoles, load floors, trunk trim (currently in production for Mercedes-Benz, Chrysler (DCX), Ford, Honda, and Nissan)	Mohammed et al. (2015); Witayakran et al. (2017); Peças et al. (2018)
Kenaf	PP	Door inner panel “Mondeo” model from Ford	Ahmad et al. (2014); Peças et al. (2018).

Table 2.8 continued

Fiber	Polymer	Automotive Applications	Reference
Flax/sisal	Thermoset resin	In the interior door linings and panels, door panels in production for Audi	Peças et al. (2018).
Flax	Mat with PP	Seatbacks, covers, rear parcel shelves, other interior trim, floor trays, pillar panels and central consoles, floor panels for “Mondeo” model from Ford	Huda et al. (2008)
Cotton	PP/PET	Soundproofing, trunk panel, insulation	

2.5.3.2 Application of Natural Fiber Reinforced Polymer Composites in other Industry

Although the widespread use of NFPC is mainly focused on automobile sector, NFPC is also gain importance in other applications such as materials for building construction, decking, sport product, household appliance and framing. A great review has been made by Ngo (2017), reporting on the applications of NFPC in different industries. The review also reported on the prevalent usage of polyester and PP as the main materials in producing NFPC. Table 2.9 summarizes the application of different types of natural fiber and its corresponding matrix in various sectors.

Table 2.9: Applications of NFPC in Various Sectors

Fiber	Polymer	Application	Reference
Bamboo	-	Used in structural concrete element as reinforcement	John and Thomas, (2008)
Sisal fiber Coir fiber	-	Used as roofing components to replace asbesto	John and Thomas, (2008)
Flax	50% recycled resin, reinforced with flax (25%) and E-glass (25%) roving	Green wall panel	Ngo, (2017)
Wood	Wood plastic composites	Modular house construction	Ngo, (2017)
Coir	Coir and natural latex rubber	Containers, boxes, trays, packaging	Ngo, (2017)
Flax, Hemp	Epoxy	Racing bicycle	Ngo, (2017)
	PP	Cases for musical instruments	Ngo, (2017)

Table 2.9 continued

Fiber	Polymer	Application	Reference
Hemp, Jute, Kenaf	Thermoplastic polymers	Containers for shipping and storage, interior panels, load floors and underbody shields for cars and trucks, workspace panels and Furnishings for offices and homes, structural support for agricultural seedlings	Ngo, (2017)

2.6 Compatibilisation of Natural Fiber Reinforced Polymer Composites

2.6.1 Introduction

Interfacial adhesion is the dominant factor that determines the properties of a polymer composite. Typically, almost all natural fillers and fibers has a limited adhesion and interaction to hydrophobic polymers (Ali et al., 2016). Poor fibre-matrix interface across the boundary causes inefficient stress transfer and poor mechanical properties as well as weak moisture resistance of composites. Incompatibility between matrix and filler due to the different in the polarity and characteristics of filler and matrix is the main problem that influences the reinforcement of polymer by natural fiber (Kabir et al., 2012).

In this case, wettability plays a vital role in determining the interfacial adhesion and bonding between the filler and matrix. Interfacial defect resulted from the poor filler wetting by polymer matrix lead to stress concentration and weakening of filler reinforced composites when subjected to stress (Ali et al., 2016). The solution to compromise the problem stated are being dealt with today by carrying out either physical or chemical treatment of either the fillers or polymer matrix. To develop a composite with good mechanical properties, the interfacial strength between the two phases need to be optimized. Modification of filler or matrix regarded as the precursor to enhance the wettability of filler in the matrix polymer (Pickeringet et al., 2016).

2.6.2 Chemical Treatments

Based on previous researches carried out, treatment of fillers or polymer matrix using chemical are more preferred as compared to physical approaches. Extensive research has been conducted to optimize the fiber-matrix adhesion by using chemical approaches (Li et al., 2007). There are different effective methods of chemical treatments including alkaline treatment, silane treatment, isocyanate treatment, permanganate treatment, benzoylation treatment, acetylation treatment and the uses of maleated coupling agents. The most common techniques are alkaline treatment, silane treatment and the uses of maleated anhydride grafted coupling agent (Pickeringet et al., 2016).

The treatment performed with the coupling agent and compatibilizer help to enhance the compatibility and adhesion between the filler-matrix interfaces. Coupling agent is a tetra functional organometallic chemical reagents used to form chemical bridges between filler and matrix through covalent bonding, hydrogen bonding or polymer chain entanglement (Ali et al., 2016; Väisänen et al., 2016). Chemical treatment with compatibilizer can be done on either polymer or filler. For example, a short organic molecules having similar functional group as that the polymer is grafted on the fibers. The compatibilization using compatibilizer aimed to modify the characteristics of fiber to fit the characteristics of polymer or vice versa. Thus, compatibilization lowers down the surface energy of the fiber or polymer to bind to other phase, respectively. This can also reduce the polarity of the fiber or polymer at the

same time to make it more compatible with the other phase, respectively (Väisänen et al., 2016).

2.6.2.1 Alkali Treatment

Alkaline treatment is also known as mercerisation process. Of all the chemical modification methods of improving the compatibility between filler and polymer, alkali treatment is the most widely studied, applied and discussed in the past researches (Fiore et al., 2015; Ferreira et al., 2019). Sodium hydroxide (NaOH) is commonly used to modify the structure of the natural fibres (Pickeringet et al., 2016). The mechanism of alkali treatment involves the disruption of hydrogen bonding in the alkaline sensitive hydroxyl group (OH) and react to form water molecules before being removed from the structure which lead to the formation of fibre–cell–O–Na functional groups between the cellulose molecular chains as shown in Equation 2.1. The removal and replacement of hydroxyl, OH group by O-NA group result in the reduction of the hydrophilic nature of fiber could improve the adhesion between fiber and polymer which enhance the mechanical properties and moisture absorption resistance property of the natural filler and the NFPC (Kabir et al., 2012).

$$\text{Fiber-OH} + \text{NaOH} \longrightarrow \text{Fiber-O-Na} + H_2O \qquad (2.1)$$

Moreover, alkaline treatment also changes the natural filler's constituents by partially removing the hemicellulose, lignin, pectin, fat, wax and

impurities material that covers the surface of the fibre cell wall. The removal of the constituent substrates thereby increases the surface roughness of filler particles resulting in improved exposed area for better fiber-matrix interfacial adhesion (Ferreira et al., 2019).

Figure 2.20 illustrates the structure of lignocellulosic fiber before and after the alkaline treatment. Elimination of the material that hinders the crystallization of cellulose could enhance the cellulose crystallinity. Clean and uniform filler structure will have a better filler matrix interfacial adhesion. This is due to availability of more possible sites for reaction when there is more cellulose molecules exposed on the surface (Ferreira et al., 2019). Meanwhile, alkaline treatment depolymerizes the highly packed crystalline cellulose and exposes the short length crystallites for the possible interaction with polymers (Li et al., 2007).

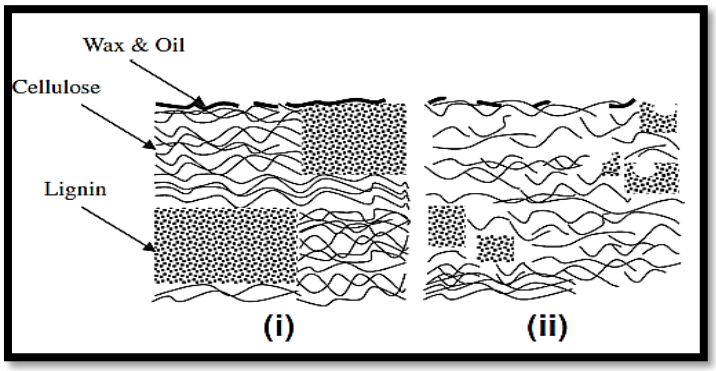

Figure 2.20: Structure of Cellulose Fibre: (i) before Treatment and (ii) after Alkaline Treatment (Kabir et al., 2012)

During the alkaline treatment, natural filler are immersed in NaOH solution with specific concentration for a particular period of time. Numerous studies have been reported on the significant improvement of the composites' properties through the alkaline treatment with different applied treatment parameters. Torun et al. (2019) reported on the surface treatment of chestnut cupula with 5 w/v % NaOH solution for 24 hours at room temperature. Similar method was adopted by Pouriman et al. (2018) on the treatment of salago fiber with 5 w/v % NaOH solution for 24 hours at room temperature. The findings showed that mechanical strength as well as water absorption resistance of the composites has been improved due to the better interfacial adhesion between the polymer matrix and treated fibers.

In another research conducted by Marques et al. (2014), treatment of curaua fibers with 5 w/v % NaOH solution for 1 hour at 80 °C has been carried out. Improvement of thermal stability, degree of crystallinity and mechanical properties up to 50% has been achieved with the addition of treated caraua fiber. Similarly, in another earlier research reported by Mishra et al. (2003), 5 w/v % alkali treatment solution of sisal fiber gave an optimum tensile and impact strengths as compared to other types of treatment method including cyanoethylation and acetylation. Excess delignification of natural fiber was reported at higher alkali concentration observed for 10% NaOH solution resulted in weakening of fiber strength.

Moreover, Asumani et al. (2012) examined the effect of concentration of NaOH (1 wt.% - 8 wt.%) treated kenaf filled PP composites for 24 hours at

45°C. The report stated that 5 w/v % NaOH aqueous solution is the optimum for the alkali stage treatment as better mechanical properties were observed. Thus from reviewing all the related research conducted on the alkaline treatment of natural fibers, it can be concluded that 5 w/v % - 8 w/v % concentration of NaOH solution are the suitable and optimum concentration for the treatment of MESSP for this research work.

Besides alkaline treatment, there are also other types of chemical treatment of natural fibers which provides different efficiency of fiber modification. For instance, work reported by Paul et al. (2010) investigates the effect of alkaline treatment, silane treatment, stearic acid treatment, benzoyl acid treatment and potassium permanganate treatment on the surface characteristics of banana fibre. It was also reported that the composites containing treated banana fibre were found to have higher tensile strength as compare to the composites containing untreated banana fibre. Meanwhile, the flexural strength and modulus of the treated fiber composite were found to be superior to that of the untreated fiber composites. Improved adhesion between treated fibers and PP facilitates the stress transfer in the composite. As a comparison, alkaline treated banana fiber composites was found to give the best mechanical properties than other method of treated fiber composite as this method showed the best efficiency to alter the surface topography of the fibers.

2.6.2.2 Silane Treatment

Silane is a hydrophobic chemical derivative of SiH_4 with different functional groups that form the bridge through covalent bonding between the hydrophilic end of natural filler and the other end which reacts with the hydrophobic groups of the polymer matrix. Silane coupling agent helps to stabilise the composites material and reduce the number of hydroxyl group of the natural fiber (Väisänen et al., 2016). The most frequently used silanes reagents are amino, methacryl and alkyl silanes. Siloxane bridges are the chemical link formed between the fiber-matrix interfaces. However, the silane treatment is more tedious not as desired as alkaline treatment due to many stages of the treatment process which may add to the treatment time and additional cost. This silane treatment involves 3 stages which is the hydrolysis, condensation and bond formation of the fibre. The formation of the silanols in the presence of moisture and hydrolysable alkoxy group is shown as chemical formulation Equation 2.2 (Ali et al., 2016; Ferreira et al., 2019).

$$CH_2CHSi(OC_2H_5)_3 \longrightarrow CH_2CHSi(OH)_3 + 3C_2H_5OH \qquad (2.2)$$

During the condensation process as depicted in Equation 2.3, the hydroxyl groups of cellulose will react with one end of the silanols and the other end of silanol will react with the functional group of the polymer matrix (Ali et al., 2016; Ferreira et al., 2019).

$$CH_2CHSi(OH)_3 + \text{Fiber-OH} \longrightarrow CH_2CHSi(OH)_2O\text{-Fiber} + H_2O \qquad (2.3)$$

The reaction of hydroxyl group with the silanol will then form a stable covalent bond to the cell wall that is chemisorbed onto the fibre surface. Also, the silane coupling agent acts as a surface coating on the micro-pores on the natural fiber's surface. Silane could penetrate into the pores and develops mechanically interlocked coatings on fiber surface. As a result, the swelling of fibers is restricted. However, silane treatment is an expensive process, the modification of fiber-matrix interface actually reduced the flexibility and young modulus of fibers which is probably the main limitation of this approach (Saha et al., 2015).

Suwanruji et al. (2016) found that silane coupling agent such as 3-aminopropyltriethoxysilane (APS) and 3-mercaptopropyltrimethoxysilane (MRPS) were effective in the modification of natural fiber-matrix interface due to the enhanced interfacial adhesion and composites strength of PALF reinforced LDPE composite. However, the deterioration of cellulose content in the fiber results in decreasing crystallinity of the treated NFPC. Thus the composites containing treated PALF possess low tensile modulus and flexural properties.

2.6.2.3 Maleated Coupling Treatment

Maleic anhydride (MA) grafted polymers are the coupling agent used to enhance the strength properties of the composites consisting of fillers. MA is normally grafted to the polymer matrix of the composites to ensure the good compatibility between the final matrix and the coupling agent (Ferreira et al.,

2019). Unlike other chemical modification, maleic coupling agent not only used to modify the filler surface but also the polymer matrix. For example PP matrix was grafted with MA to achieve the efficient interaction with the functional surface of the filler and matrix phases (Ferreira et al., 2019). Grafting of MA to PP results in maleic anhydride grafted polypropylene (MAPP) which is most popularly found in the literature (Pickering et al., 2016). MAPP not only acts as a coupling agent but it also behaves as compatibilizer in NFPC (Väisänen et al., 2016).

Furthermore, reaction between MAPP with the hydroxyl groups of natural filler surface reduces the hydrophilicity through the formation of covalent bond or hydrogen bond across the interface. Treatment between hot MAPP copolymer with natural fiber involves two steps. Figure 2.21 shows the modification mechanism which starts with the heating process under 170˚C for the copolymer activation and followed by the esterification of cellulose. This treatment helps to increase the surface energy of the filler which is nearer to the surface energy of the matrix that ends up improving the wettability and interfacial adhesion (Adekunle, 2015).

This process is much more effective as compared to other treatment methods of natural fillers. However the steps involve in the grafting is tedious and is very complex (Li et al., 2007; Adekunle, 2015). Moreover, treatment of natural filler with maleated coupling is an expensive process, the use of the hazardous chemicals and high temperature are the main drawbacks of this approach (Saha et al., 2015). Report by Bera et al. (2010) showed the

comparison between the usage of MAPP and vinyl trimethoxy silane (VTMO) as the coupling agent for the surface treatment of jute fiber. It was reported that improvement of tensile properties through the MAPP treatment was twice as obtained for composites containing silane treated jute fiber.

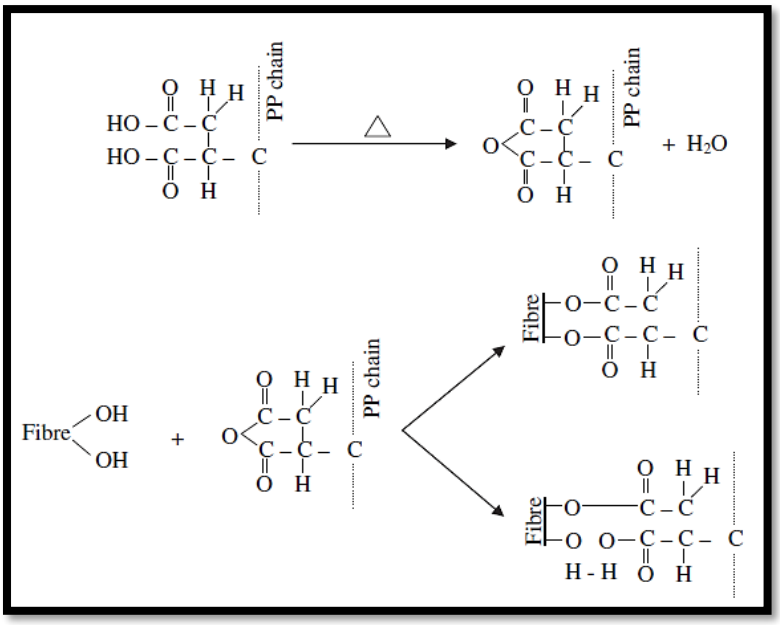

Figure 2.21: Coupling Reaction of MA, PP, MAPP and Natural Fiber (Ferreira et al., 2019)

CHAPTER 3

RESEARCH METHODOLOGY AND RESEARCH DESIGN

3.1 Overview of the Work

In this chapter, the source of raw materials used, the extraction of the natural filler and experimental steps for the preparation of biocomposites were elaborated. Figure 3.1 outlines the experiment flowchart.

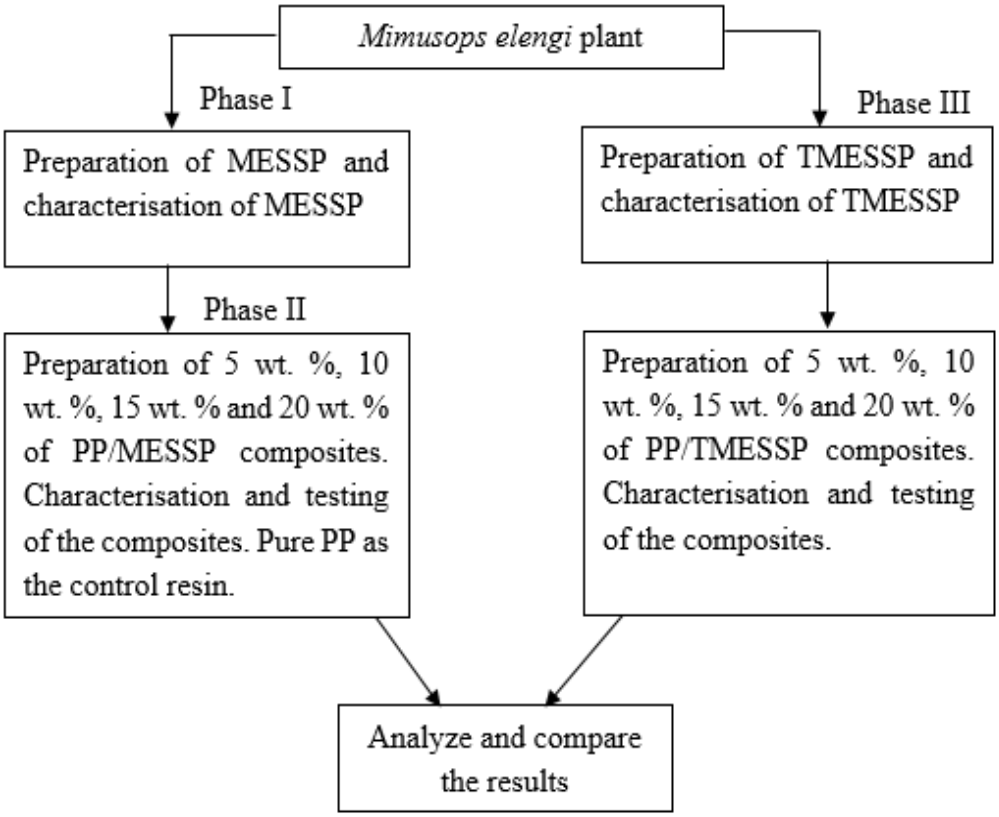

Figure 3.1 Experiment Flow

Besides, this chapter also briefs the instrumentation used, standard techniques for characterisation and testing carried out on *Mimusop elengi* seed shell powder (MESSP), treated *Mimusop elengi* seed shell powder (TMESSP), MESSP filled PP (PP/MESSP) composites and TMESSP filled PP (PP/TMESSP) composites. In order to achieve the research objectives, qualitative and quantitative research approach were applied through the analysis from numerical data collected. The basic concepts and the groundwork was obtained in the literature review for understanding the current trends and the research work done.

3.2 Raw Materials

3.2.1 Polypropylene (PP)

PP homopolymer was purchased from Lotte Chemical Titan (M) Sdn. Bhd, Pasir Gudang, Johor, Malaysia and used as polymer matrix to produce the composites. The tradename of PP purchased was Titanpro® 6331 with the chemical abstract service (CAS) registry number 9003-07-0 which can be used for closures, housewares, toys, games, pill boxes, containers, healthcare devices, syringe barrel, pen cap and pen body. Table 3.1 summarizes the properties of PP as per specification provided by the supplier.

Table 3.1: Properties of PP

Properties	PP
Appearance	White pellet
Density (g/cm^3)	0.99
Melting point (°C)	160 – 165
Melt flow index (g/min)	1.4
Deflection temperature at 0.46 MPa (°C)	99
Water Absorption after 24 hours (%)	0.02

3.2.2 Sodium Hydroxide

Sodium hydroxide (NaOH) was purchased from Lab Medical Science in the form of white pellets. MESSP surface modification was conducted in an alkaline treatment with NaOH. For NaOH solution preparation, distilled water was used. The amount of NaOH needed was weighed to prepare the alkaline aqueous solution with 5 w/v % - 8 w/v % concentration. Table 3.2 presents the physical properties of NaOH as provided by the supplier.

Table 3.2: Physical Properties of NaOH

Physical properties	NaOH
Appearance	White pellet
Density (g/ cm^3)	2.13
Melting point (°C)	318
Boiling point (°C)	1388

3.2.3 Miscellaneous Materials

Acetone, ethanol, nitric acid and sulfuric acid was used as chemical reagents to determine the weight percentage of the chemical constituents present in MESSP. Acetone and ethanol were supplied by Lab Medical Science whereas, nitric acid was purchased from Synertec Enterprise whereas sulfuric acid was supplied by Biotek Abadi Sdn Bhd. Table 3.3 shows the properties of the acetone and ethanol and Table 3.4 depicts the properties of the nitric acid and sulfuric acid respectively.

Table 3.3: Properties of the Acetone and Ethanol

Physical properties	Acetone	Ethanol
Density (g/cm^3)	0.791	0.789
Boiling point (°C)	56	78.3
Flash point (°C)	-17	14

Table 3.4: Properties of Nitric Acid and Sulfuric Acid

Physical properties	Nitric acid	Sulfuric acid
Density (g/cm^3)	1.48	1.84
Boiling point (°C)	120.5	290

3.3 Experimental Design and Methodology

This section discussed the extraction of *Mimusops elengi* seed shell powder (MESSP). The methodology explains the method used to determine the cellulose, lignin and extractive content in MESSP, the procedures for the preparation of PP/MESSP and PP/TMESSP composites. Lastly, the instrumentation and methods used for the characterisation and testing of the composites were explained.

3.3.1 Extraction of MESSP

MESSP was obtained from the seeds of ripe fruits of *Mimusops elengi* plants which can be found at Taman Kampar Perdana, Kampar, Perak (Google map coordinate: 4º20’20”N, 101º9’9”E). The fruits were collected and the seeds were separated from the ripe fruits. The seeds were oven-dried at 50 °C for 24 hours until it changes into brownish color indicating dried seed (Osman and Zakaria, 2012). Dried seed shells were obtained by crushing the seed and removing the kernel. Next, the seed shells were grinded and sieved to < 45 µm

particle size using a sieve shaker (RX-29-10). Preparation steps of MESSP from *Mimusops elengi* fruit are illustrated in Figure 3.2 (Muniyadi et al., 2018).

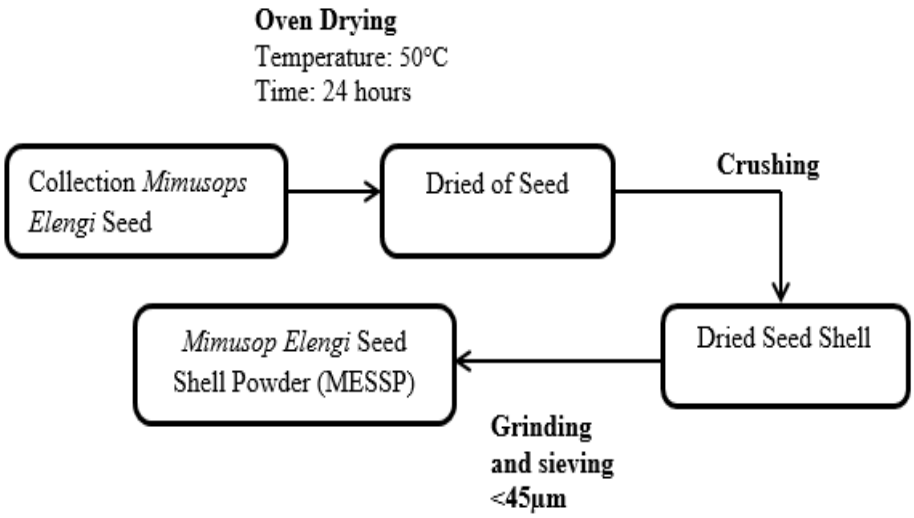

Figure 3.2: Flow Chart of MESSP Preparation

3.3.2 Chemical Composition Analysis

The chemical composition including cellulose, hemicellulose, lignin and the extractives contents were determined for MESSP and TMESSP. In order to determine and compare the cellulose content of MESSP and TMESSP, cellulose analysis through the Kurschener and Hoffer method was conducted. These method allowed the measurement of percentage dry basis of cellulose (Zhang et al., 2011). Amount of extractive in biomass was determined from solvent extraction by using the extractor Soxhtec HT2. Acetone was used as solvent for extraction. 150 ml of acetone was measured and added to 1g of MESSP. The temperature was maintained at 90°C, the residence time and the rising stages

were 4 hours and 20 minutes respectively. The sample was air dried before oven-dried again at 105 °C. The extractives content was measured by calculating the differences in weight before and after the extraction (Blasi et al., 1999; Ayeni et al., 2015). The percentage of extractives (A) was calculated using Equation 3.1 as follow:

$$A = \frac{W_{\text{before extraction}} - W_{\text{afetr extraction}}}{1} \times 100\% \quad (3.1)$$

According to Kurschener and Hoffer method, cellulose was determined by means of nitric acid-ethanol mixture (Kürschner et al., 1933; Zhang et al., 2011). The ratio was 1:4 respectively. A mixture solution of 80 ml of 95% ethanol and 20 ml of concentrated nitric acid was used as the solvent and added to 1g of MESSP (Vijay et al., 2019). The residence time for the reflux was 1 hour, the temperature was maintained at 90 °C. The reflux was conducted in the constant level of boiling water bath. This method makes use of three cycles of 1 hour reflux treatment. This was explained as there was the lignin left after two reflux whereas the most of the lignin was removed at the third time of reflux results in a more constant composition obtained. After the reflux, the residue was oven dried at 105 °C. The weight of the residue ($W_{cellulose}$) was measured after cooling in the desiccator (Pardee, 1937; Manimaran et al., 2019). Percentage of cellulose (B) was calculated using the Equation 3.2.

$$B = \frac{W_{\text{cellulose}}}{1} \times 100\% \quad (3.2)$$

Quantification of lignin content of MESSP was determined based on Klason lignin method according to the TAPPI-T222 om-02 standard. 1g of MESSP was hydrolyzed with 15 ml of 72 wt.% sulfuric acid for 2 hours in the water bath at 19-21 °C. After 2 hours, 545 ml of water was added to dilute the solution to 3% concentration sulfuric acid. The diluted solution was further boiled for 4 hours by using the reflux condenser. The residue was cooled before the filtration. The weight of the crucible was recorded, $W_{crucible}$. The crucible with the residue was dried at 105 °C for 24 hours (Zhang et al., 2011). The weight of the crucible with the dried residue, (W_{cr}) were measured. The correction for ash in lignin was performed by placing the crucibles and residue in the muffle furnace at 575 ± 25 °C for 4 hours. After that, the crucible was removed and cooled in a desiccator for 1 hour before the weight of the crucible and the ash, W_{Ash} were recorded. The percentage of acid insoluble lignin (C) content was calculated based on Equation 3.3.

$$C = \frac{(w_{cr} - w_{Crucible}) - (w_{Ash} - w_{Crucible})}{1} \times 100\% \quad (3.3)$$

Equation 3.4 was used to calculate the hemicellulose content. (Blasi et al., 1999; Li et al., 2004; Lin et al., 2010).

$$\text{Percentage of Hemicellulose (\%)} = 100 - A - B - C \quad (3.4)$$

Hemicellulose content was calculated by difference, assuming that extractives, hemicellulose, lignin, and cellulose are the only constituents of the entire biomass. Same procedures were repeated with the TMESSP in order to

compare the amount of composition available with the MESSP. The experiments were repeated twice to obtain the average composition of each constituent of MESSP and TMESSP.

3.3.3 Chemical Treatment of MESSP

MESSP was chemically treated with NaOH, concentration range from 5 w/v % to 8 w/v % in intervals of 1 w/v % NaOH aqueous solution. Solution of MESSP ratio was maintaining at 1:15 ratio (Luna et al., 2015). MESSP was immersed in the alkaline solution for 24 hours at room temperature (Torun et al., 2019). After the treatment, TMESSP was washed with deionized water to remove excess alkali until a neutral state obtained (pH=7). TMESSP was oven-dried at 80 ºC for 24 hours (Kabir et al., 2012).

3.4 Preparation of PP/MESSP Composites

Melt mixing followed by compression molding technique were used to fabricate the three types of samples including control PP resin, untreated MESSP filled PP composites (PP/MESSP) and TMESSP filled PP composites (PP/TMESSP). Prior to the compounding process, PP resin and MESSP powder were pre-dried in vacuum oven for 24 hours at 80 °C to ensure the completely removal of moisture. PP pellet and MESSP were blended according to the compounding formulation as shown in Table 3.5. PP pellet and MESSP were

blended according to the compounding formulation as shown in Table 3.5. Three compounding were prepared for each loading of MESSP filled PP composites as well as TMESSP filled PP composites.

Table 3.5: Compounding Formulation of PP/MESSP Composites

Sample	Designation	PP (wt. %)	MESSP (wt. %)	TMESSP (wt. %)
1	PP	100	0	-
2	PP/M5	95	5	-
3	PP/M10	90	10	-
4	PP/M15	85	15	-
5	PP/M20	80	20	-
6	PP/TM5	95	-	5
7	PP/TM10	90	-	10
8	PP/TM15	85	-	15
9	PP/TM20	80	-	20

PP pellets and MESSP were pre-mixed before discharged into the hopper. The processing temperature was fixed at 180 °C for 8 minutes with the mixing speed of 60 rpm in a Brabender internal mixer (Plastograph ® EC 815652, Duisburg, Germany) with co-rotating blades and a mixing head with volumetric capacity of 50 cm^3. Thereafter, PP/MESSP composites were compression molded into thin composite sheets by hot pressing at 180 °C using a hydraulic hot and cold press machine GT-7014-A30C with the 0.5 mm thickness mold. The composites was preheated for 12 minutes before it was

compressed with the holding time of 4 minutes followed by cooling for another 2 minutes. The feasibility study of the composite preparation was conducted and was found to be optimum at 20 wt. % MESSP loading. The saturation point was achieved and an immiscible mixture was produced beyond saturation point.

3.5 Characterisation of MESSP, TMESSP, PP/MESSP and PP/TMESSP Composites

This section outlines the techniques to characterise the fillers and the composites in comparison to the control samples (neat PP).

3.5.1 X-Ray Fluorescence (XRF) Analysis

The measurements of elemental composition of MESSP were investigated through the X-ray fluorescence technique using the benchtop Energy Dispersive X-ray Fluorescence (ED-XRF) elemental analyzer, Rigaku NEX QC. Quantification analysis of the elemental compositions of MESSP was conducted at RGS Corporation Sdn. Bhd. located at Seri Kembangan, Selangor Malaysia. MESSP prepared had three replicates for the XRF analysis.

3.5.2 Fourier Transform Infrared (FTIR) Spectroscopy

The FTIR spectra of MESSP and TMESSP were analyzed using a Perkin Elmer FTIR- spectrometer to identify and compare the chemical functional groups of MESSP and TMESSP. FTIR analysis was carried out to determine the absorption band at mid-IR spectrum ranging from 400 – 4000 cm^{-1}, with a 4 cm^{-1} resolution and 16 scans. Analytical grade KBr pellets was mixed with MESSP and TMESSP to form the finely ground specimen before pressed into a thin KBr pellet. A minimum of 5 scans were conducted for MESSP and TMESSP respectively.

3.5.3 Attenuated Total Reflectance-Fourier Transform Infrared Spectroscopy (ATR- FTIR)

ATR-FTIR analysis of MESSP, PP/MESSP and PP/TMESSP composites were acquired on Perkin Elmer RXI IR spectrophotometer to identify the possible chemical bonds and functional groups available. ATR-FTIR spectra were measured in the range of 400 - 4000 cm^{-1} and obtained with the accumulation of 16 scans at a resolution of 4 cm^{-1}. The composites was placed on the ATR-crystal, the composites sheet were pressed against the crystal prior to the scanning.

3.5.4 Density Test

Density measurement was conducted to compare density of MESSP with other natural fillers reported in the literature review. The density of MESSP and TMESSP were examined using a gas pcynometer from Micromeritic. Helium was employed in the density test. The test was conducted using a 10 cm^3 chamber insert at 10 times number of purges. The test was conducted at GAT Scientific Sdn. Bhd. located at Shah Alam, Selangor, Malaysia. Five replications of density test were carried out.

3.5.5 Particle Size Analysis (PSA)

Measurement of the individual particles size distribution, mean particles size as well as the specific surface area of the MESSP and TMESSP were performed in PSA through the Malvern Mastersizer particle size analyzer (Hydro 2000 MU, Malvern Instrument Ltd, Malvern, UK). Prior to the analyzing, the refractive index of MESSP was measured by using a digital refractometer (300034, Sper Scientific Ltd., Scottsdale, AZ, USA). Three replication of the analysis has been conducted for each TMESSP and MESSP to obtain the mean values.

3.5.6 Scanning Electron Microscope (SEM) Analysis

SEM was conducted to examine the morphology of MESSP and TMESSP, soil buried composites as well as the tensile fracture surface of the

composites. In order to minimize the extent of sample arcing and avoid the build-up of electrostatic charge, the fracture surfaces or the sample's surface to be examined were mounted on the disc before coated with a thin layer (15 nm) of a platinum with the density of 21.45 g/cm^3 by mean of a vacuum sputter coater (JFC-1600, Jeol, Akishima, Japan). SEM analysis was performed using a scanning electron microscope (JOEL JSM 6701-F, Jeol, Akishima, Japan) at an accelerating voltage of 4 kV. SEM analysis was conducted to compare the surface morphology of MESSP and TMESSP as well as to study the dispersion of MESSP and TMESSP in PP matrix, compatibility between the matrix-filler system and the extent of soil-burial degraded of the composites.

3.5.7 Thermogravimetric Analysis (TGA)

TGA was conducted using a Mettler Toledo thermal analyser to study the thermal stability of MESSP and TMESSP as well as the composites. This analysis was performed using a 70 mg alumina crucible. Sample weighing approximately 10 mg to 12 mg of MESSP was placed inside the crucible before submitted to the temperature run. The samples was placed inside a tube furnace under the nitrogen atmosphere (flow of 50 mL/min) from 30 °C to 600 °C at 20 °C /min heating rate. TGA measure the thermal decomposition of the samples by mean of weight percentage of the samples as function of the temperature. Three replications of TGA test were performed for each loading of MESSP filled PP composites as well as TMESSP filled PP composites.

3.6 Testing of PP/MESSP Composites

3.6.1 Processing Torque

As mention earlier, the optimum mixing process was carried out for a duration of 8 minutes. The development of the processing torque over the time was displayed and recorded on the liquid crystal display (LCD) unit. The process ability of MESSP in PP matrix can be analyzed from the processing torque graph plotted. The torque value recorded at the end of 8 minutes time was taken as the stabilization torque. As mentioned in the preparation of the composites, three compounding were prepared for each loading of MESSP. Thus, there were three set data of processing torque collected for each loading of the composites.

3.6.2 Mechanical Properties

The standard mechanical properties were determined with the American Society for Testing and Materials (ASTM) standard for plastics. Tensile strength, tensile modulus, elongation at break and the impact properties were the mechanical properties studied.

3.6.2.1 Tensile Properties

Tensile properties of neat PP were compared with PP/MESSP and PP/TMESSP composites according to ASTM standard test method (D638) under ambient condition. Dumbbell-shaped specimens were cut by using a

dumbbell cutter (Leader Technology Scientific (M) Sdn.Bhd., Balakong, Malaysia). Dumbbell-shaped specimens were prepared and labeled for each loading of the composites. Ten specimens of each loading of PP/MESSP and PP/TMESSP composites were run to determine the mean values of the data. Tensile test was performed at crosshead speed of 20 mm/min by using a light-weight tensile tester (Tinius Olsen H10KS-0748, Salfords, UK). The weight load cell used for all specimens are 450 N. The specimen was subjected to 1200 mm of extension range with a 26 mm of gauge length.

3.6.2.2 Impact Properties

The impact properties of neat PP, PP/MESSP and PP/TMESSP composites were analyzed through the Izod impact tests according to ASTM D256 testing standard. This test was performed at Zwick Impact tester with a pendulum load of 12.5 J released on the notched samples of 64 mm length, 12.7 mm width and 3 mm thickness to measure the impact energy (Joule) required to fracture the specimens. The impact strength of the specimen was evaluated using Equation 3.5. Five replication were conducted for each loading of MESSP filled PP composites.

$$\text{Impact strength} = \frac{\text{Impact load}}{\text{thickness of the specimen x pendulum load}} \qquad (3.5)$$

3.6.3 Differential Scanning Calorimetric (DSC)

A thermoanalyzer (Mettler- Toledo International Inc., Schwarzenbach, Switzerland) was used to determine the melting point and the degree of crystallinity of the PP/MESSP and PP/TMESSP composites. Approximately 3-5 mg of the samples were measured and encapsulated in a hermetically sealed aluminum pan. The samples were examined under the presence of the flow of nitrogen (10ml/min) at a heating rate of 10 °C /min. The sample was heated up from room temperature, 25 °C to 300 °C and then cooled back to 25 °C. The degree of crystallinity of the PP/MESSP composites were then calculated using Equation 3.6 (Faria et al., 2006, Huang et al., 2018).

$$X_c^m = \frac{\Delta H_m}{W_p \times \Delta H_{100}} \times 100\% \quad (3.6)$$

Where:

X_c^m: Degree of crystallinity of PP phase

ΔH_m : Melting enthalpy of composite

ΔH_{100}: Melting enthalpy of 100% crystalline PP (207 J/g)

W_p: Weight fraction of PP matrix in the composite

3.6.4 Water Absorption Test

Water absorption test was done according to ASTM standard test method D 570-98. For each loading of PP/MESSP composites, five samples were prepared. The composites were cut into dumbbell-shape samples. The samples were first oven-dried at 50 ± 3 °C for 24 hours and cooled in the desiccator before weighing to the nearest 0.001g using an electronic analytical and precision balance (Sartorius M-pact AX224, Sartorius AG, Germany) and recorded as initial weight (W_i). The specimens were then immersed in the distilled water and rest on edge to ensure specimens were completely immersed in the container. The specimens were immersed for 24 hours at room temperature, 25 °C. After 24 hours, the specimens were removed at a time and the surfaces were wiped off using the tissue, weighed again and recorded as W_f. Water absorption percentage of the composites were calculated using the weight difference between the specimen before and after the immersion in water using the Equation 3.7 as follows,

$$\text{Water Absorption Percentage (\%)} = \frac{w_f - w_i}{wi} \times 100\% \qquad (3.7)$$

Where

W_i = initial weight of the samples, g

W_f = weight of the sample after immersion, g

3.6.5 Soil Burial

Bio-degradability test namely soil burial test was conducted. For each loading of PP/MESSP composites, five dumbbell-shaped samples were weighed, recorded as B_i and buried in compost black soil (Tesco brand) at a depth of 5 cm in the containers. Soil burial tests were carried out at ambient temperature (25 - 30 °C) where the containers were exposed to the real weather condition which placed in Faculty of Engineering and Green Technology (FEGT), Universiti Tunku Abdul Rahman, Kampar, Perak. The samples were taken out from the soil after 2, 4 and 6 months, washed with distilled water and then were oven-dried at 70 °C for 24 hours to remove the moisture (Obasi et al., 2013). The weights of the dried samples (B_f) were recorded. The weight loss percentage was calculated using Equation 3.8 (Siakeng et al., 2020). The condition of the samples were visually inspected to observe the changes that can linked to the surface degradation. The surface morphology of the samples before and after the soil burial test were compared using SEM. The tensile properties of the buried samples also tested with the same method as mentioned earlier.

$$\text{Weight Loss (\%)} = \frac{B_i - B_f}{Bi} \times 100\% \tag{3.8}$$

Where

B_i = initial weight of the samples before soil burial test, g

B_f = weight of the sample after soil burial test, g

CHAPTER 4

RESULTS AND DISCUSSIONS

This chapter focuses on the analysis of feasibility study of different loading of *Mimusops elengi* seed shell powder (MESSP) as the biofiller in polypropylene (PP) composites, characterisation of MESSP as well as the testing on MESSP filled PP (PP/MESSP) biocomposites. The effects of the MESSP filler content on the processability, physio-mechanical properties, thermal properties, water absorption resistance as well as the bio-degradability properties were investigated. Moreover, the influence of alkali treatment of MESSP on the processability, physio-mechanical properties as well as water uptake resistance of PP composites were compared and analyzed.

4.1 Characterisation of MESSP

MESSP was characterised in order to study the physical and chemical properties as well as the feasibility study of MESSP as a potential biofiller in PP resin. The physical properties such as density, particle size and distribution, particle shape, surface morphology and thermal decomposition were evaluated. Meanwhile, the chemical properties such as elemental composition and functional group were also evaluated.

4.1.1 X-Ray Fluorescence (XRF) analysis

XRF spectrometry is one of the approach to determine the inorganic elemental composition. The total organic compound, inorganic compound and the loss of ignition of MESSP were 79.4 wt. %, 18.7 wt. % and 1.90 wt. % respectively. It was observed that the elemental composition by the XRF was only a minor contribution of the total weight of MESSP as lignin, hemicellulose and cellulose were the major composition as shown in FTIR analysis (Thyrel, 2014). Chemical elements of the periodic table present in MESSP, except for gases was identified through XRF (Morgan et al., 2015; Presle et al., 2017). Table 4.1 shows the XRF analysis of MESSP (Abhulimen and Orumwense, 2017). XRF analysis revealed that MESSP contains each of these elements; calcium (Ca), potassium (K), sulfur (S), iron (Fe), titanium (Ti), chlorine (Cl), rubidium (Rb), phosphorus (P), silicon (Si), aluminium (Al), magnesium (Mg), sodium (Na) and fluorine (F). The main elements that present in MESSP were Ca, K, S, Fe, Ti and Cl. Si, Al, Mg, Na and F were found in minor (trace) quantities. Similar observation was reported by Bashir and Manusamy (2015), as the major constituents present in the egg shell powder were Ca, K, S, Fe and Cl. Besides, several other research works also confirms that these elementals are the common components in natural filler such as in activated charcoal, rice husk and egg shell powder (Tahir et al., 2016). Meanwhile, the element such as Ti which was detected as one of the main element in MESSP could be sourced from usage of commercial fertilizers. According to Lyu et al. (2017), Ti is a beneficial element that is vital for plant growth and is mainly sourced from the commercial fertilizers. Thus, this suggest that the presence of Ti is due to the Ti

uptake from fertilizers to the *Mimusop elengi* plants which accumulate on the seed shells. There were no high percentages of hydrophilic elements such as Si and Al detected in MESSP. Si and Al are the common hydrophilic elements present in many natural fillers which results in incompatibility to hydrophobic polymers. Thus, the absence of these elements showed that MESSP could be compatible to the hydrophobic PP matrix (Ismail and Muniyadi, 2011).

Table 4.1: XRF analysis of MESSP

Component	Chemical Name	Weight Percentage (wt. %)
CaO	Calcium oxide	31.2
K_2O	Potassium oxide	23.4
SO_3	Sulfur trioxide	14.8
Fe_2O_3	Ferric Oxide	11.3
TiO_2	Titanium oxide	10.9
Cl	Chlorine	3.53
Rb_2O	Rubidium Oxide	3.21
P_2O_5	Phosphorus pentoxide	1.64
SiO_2	Silicon dioxide	trace
Al_2O_3	Aluminium Oxide	trace
MgO	Magnesium monoxide	trace
Na_2O	Disodium oxide	trace
F	Fluorine	trace

4.1.2 Attenuated Total Reflectance-Fourier Transform Infrared Spectroscopy (ATR-FTIR)

ATR-FTIR analysis was carried out to determine the chemical functional groups on MESSP. Figure 4.1 depicts the ATR-FTIR spectrum of MESSP.

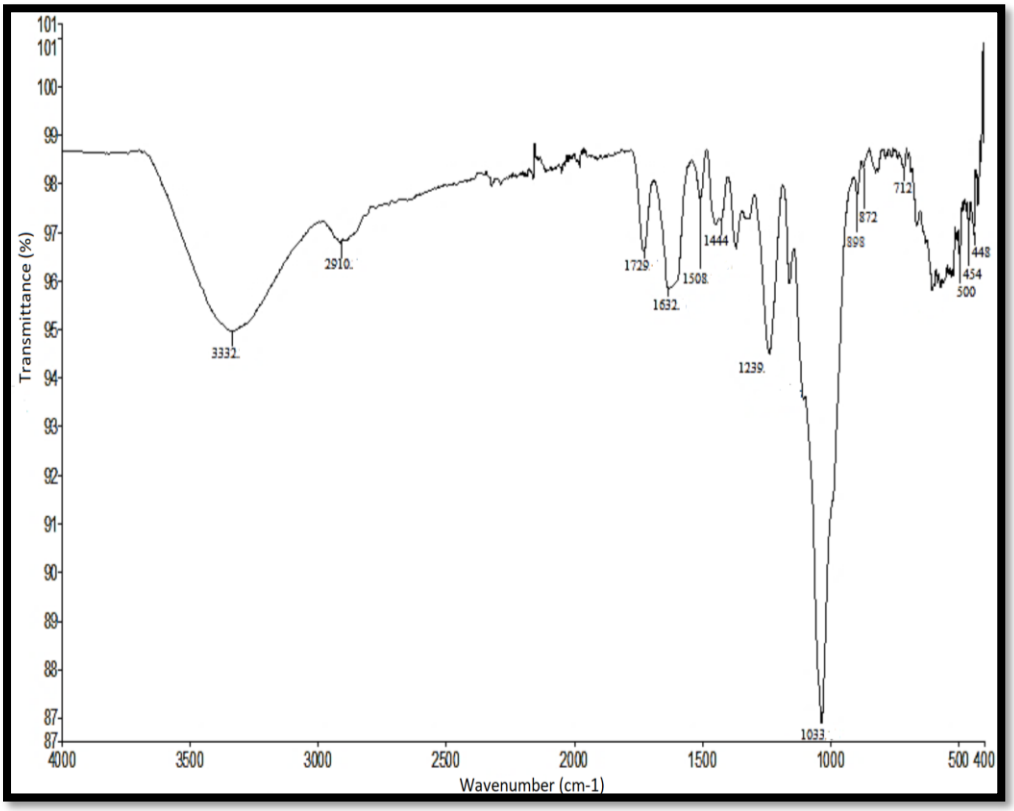

Figure 4.1: ATR-FTIR Spectrum of MESSP

A strong and wide vibration band located at peak 3332 cm^{-1} was observed confirming the present of hydroxyl group (OH) (Ooi et al., 2011). The presence of OH groups revealed that MESSP surface contains hydrophilic characteristics and could prevent strong adhesion to the polymer matrix despite the absence of chemical elements which depicts the hydrophilic characteristics

of MESSP. The characteristic band that appeared in the range from 3000 cm^{-1} to 2800 cm^{-1} attributed to the stretching of the C-H group which appeared at 2910 cm^{-1} in MESSP (Stuart, 2004). The absorption band appeared within 1730 cm^{-1} to 1740 cm^{-1} was due to the presence of C=O stretching in the acetyl groups of hemicellulose where the peak at 1729 cm^{-1} was found in MESSP (Alemdar and Sain, 2008). The peak occurred at 1632 cm^{-1} was due to the absorbed moisture by the H-O-H bending in cellulose (Fan et al., 2012; Muniyadi et al., 2018). The existence of the peak at 1508 cm^{-1} was corresponded to the C=C vibration of aromatic skeletal found in lignin (Shi et al., 2004). The peak detected at 1239 cm^{-1} could be corresponded to C-O stretch acetyl group in lignin or corresponded to O-H phenolic in lignin (Muniyadi, 2018). A peak found at 1033 cm^{-1} which within the range from 1000-1150 cm^{-1} was assigned to the C-O-C and C-O groups from main carbohydrates of cellulose and lignin (Koay et al., 2013).

The presence of Ca element as discussed in XRF was proved with the peaks displayed at 1444 cm^{-1}, 872 cm^{-1}, 712 cm^{-1} and 500 cm^{-1}. Similar peaks were observed in the study conducted by Zaki et al. (2006) where the calcium oxide spectrum displayed a medium doublet centred around 1444 cm^{-1} and a weak absorption at 878 cm^{-1}. In addition, the absorption band in the region of 875 cm^{-1} and 500 cm^{-1} were corresponded to the Ca-O stretching vibration (Galván et al., 2009; Sumathi, 2017). Infrared spectrum of MESSP at approximately 898 cm^{-1} could be attributed to the presence of ferric oxide in the form of goethite which could be found in soil (Betancur et al., 2012). According to Lu et al. (2008), the absorption band in the range 500-1000 cm^{-1} is attributed

to the vibration of Ti-O bond. Appearance of Ti-O frequency absorption was noted at 448cm^{-1} and 454 cm^{-1} respectively (Silva, 2009; Choudhury and Choudhury, 2012). Band deriving from K-O stretching vibration could be observed at the mode above 200 cm^{-1} from Raman spectra which conducted at high pressure (Krobok and Holzapfel, 1994). ATR-FTIR analysis confirms the presence of most of the chemical elements as determined through XRF analysis.

4.1.3 Particles Size Analysis and Density Test

Particles size is one of the crucial factors that can affect the processing and the properties of any composites. The size of any particles is measured in the unit micron meter. Despite the fact that the irregular size of the particles, the number is often named as the mean particles sizes which the average is determined either by weight percent or number percent. Particle size of MESSP was measured with a particle size analyser correlated with the particle morphology examined through SEM. Based on Figure 4.2, the particle size distribution of MESSP appeared to fall in the ranges from 0.02 μm to 1.445 μm. MESSP has relatively narrow particle size distribution which may lead to a more uniform pore structure as compared to particles having broader particle size distribution (Bjørk et al., 2012). Majority of the particles size govern almost 99% was in the range of 0.03-0.24 μm. The mean particle size was found to be 0.092 μm. According to Kamalbabu and Kumar (2012), bigger particles size of cuttlebone in the composites caused the uneven particles dispersion in the matrix polymer whereas the smaller particles size presented the higher

tensile strength and young modulus of the reinforced composites due to the good interaction in the filler-matrix phases.

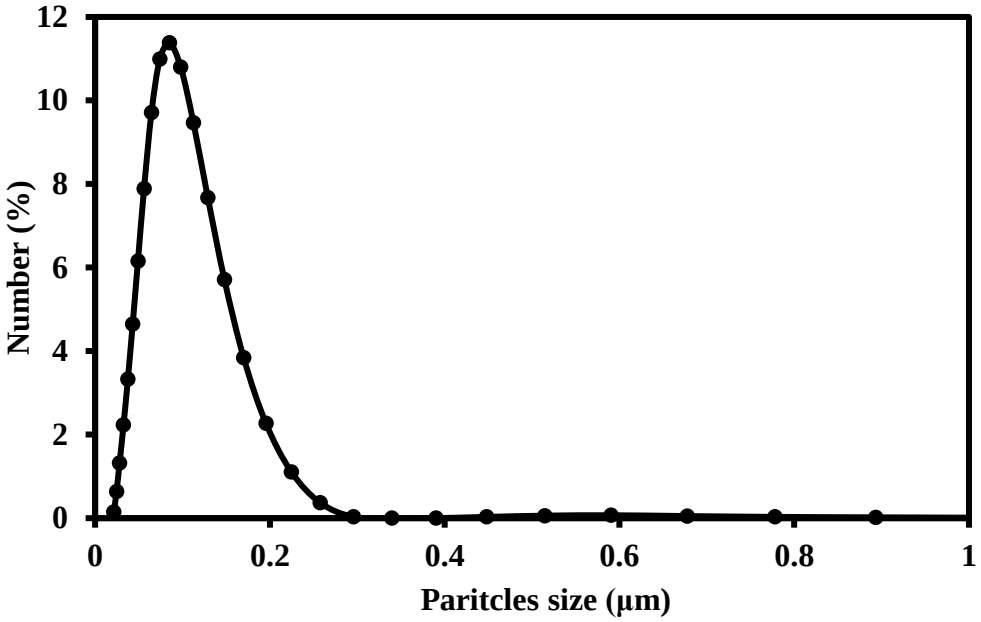

Figure 4.2: Particle Size Distribution of MESSP

The specific surface area of MESSP was found to be 29.1 m^2/g. Specific surface area is generally referred to the total surface area exposed of finely divided filler to interact with polymer matrix. Smaller particle size has more total surface area which increase the area of composite interface which facilitate the mechanical bonding between matrix and filler. This could be observed in the study reported by Nasution et al. (2016), where incorporation of finer cockleshell powder in the polymer matrix resulted in the higher impact strength. Thus, the results obtained from particle size analysis proved that particle size distribution, mean particle size and specific surface area of MESSP fulfils the required characteristics of a filler material to produce a polymer composite with enhanced properties.

When considering the density of a composite material, lightweight natural fibre is preferred and is more competitive and advantageous over the synthetic fibres which are relatively denser. The lower density of natural fiber is more favourable to produce lightweight composites with high specific properties application (Kocaman and Ahmetli, 2016). Table 4.2 shows the comparison of MESSP's density to other existing natural fibres and synthetic fiber which have been studied previously by other researchers. The density of MESSP is the lowest as compared to the existing natural and some synthetic fibres. This suggests a greater potential of MESSP to replace other natural and synthetic filler in large volume for commercial application. The incorporation of the lower density filler with the matrix yielding the lower weight composites (Sathishkumar et al., 2013).

Table 4.2: Comparison in Density Properties of MESSP with Natural Fiber and Synthetic Fiber

Types of Fiber	Fiber	Density (g/cm^3)	Reference
Natural Fiber	MESSP	0.46 ± 0.0004	
	Cellulose Fiber	0.98	(Sozen et al, 2017)
	Wood Flour	0.99	(Sozen et al., 2017)
	Flax	1.40-1.60	(Truong et al., 2009)
	Jute	1.30	(Kumar and Anandh, 2017)
	Bamboo	0.60-1.10	(Naidu et al., 2017)
	Cotton	1.50-1.60	(Pickering et al., 2016)
	Eggshell	2.49	(Boonprasert and Tangboriboon, 2017)
Synthetic Fiber	Carbon	1.40	(Gon et al., 2012)
	E-glass	2.50	(Gon et al., 2012)
	Kaolin	2.60	(Wardhana et al., 2014)

4.1.4 Scanning Electron Microscopy (SEM) Analysis

The morphological properties of MESSP such as particle shape, surface morphology and particle structure were analysed using a scanning electron microscopy (SEM). Figures 4.3 (a) and (b) shows the SEM micrograph of MESSP at 200x and 1000x magnifications, respectively. From the micrographs, it can be seen that MESSP particles were irregular in shape and size and can be categorized as particulate fillers. The particles were loosely arranged and tend to appear as an individual particles or smaller aggregates. This observation revealed that MESSP particles are not tightly bound and can be easily dispersed in polymer matrix at lower processing torque. Agglomeration of fillers affects the mechanical properties of polymer composites as it can act as stress concentration point and weakens the composite structure (Lu et al., 2010).

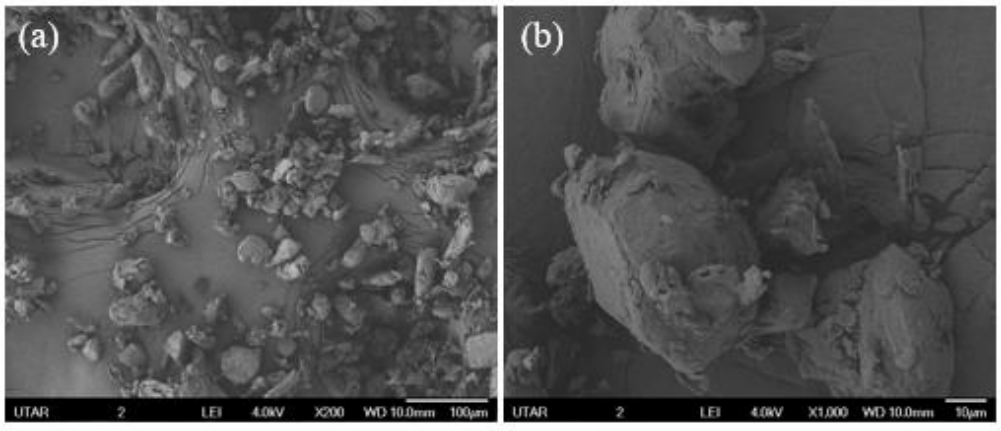

Figure 4.3: Micrographs of MESSP at (a) 200x and (b) 1000x Magnification

4.1.5 Thermogravimetric Analysis (TGA)

The thermal stability of the lignocellulose-filled polymer matrix composite is mainly affected by the thermal characteristic of the matrix and filler itself. Thermal stability is one of the important parameter to determine the processing condition and the servicing conditions of NFPC. According to Osman and Zakaria (2012), virgin PP which is a widely used polymer matrix in NFPC and showed a single-mass loss step with the maximum decomposition rate at 490 °C. Thus, high thermal stability of the filler is essential in order to maintain the high thermal stability of the polymer composite produced using PP as matrix. The thermal stability of MESSP has been evaluated through thermogravimetric analysis and the thermal decomposition percentage of MESSP over a range of temperature was shown as in Figure 4.4. The combustion characteristic of the sample was reflected on the weight loss through out the burning process (Wang et al., 2011; Cao et al., 2017).

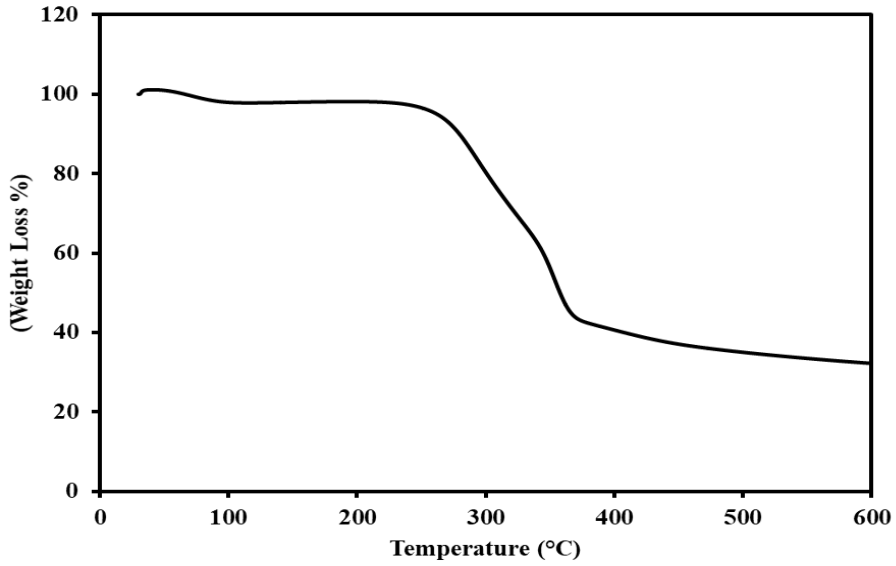

Figure 4.4: Thermal Decomposition of MESSP

Figure 4.4 shows two-step decomposition stages of MESSP. The initial weight loss was corresponded to volatilization of water or moisture from the MESSP before it reached a constant weight plateau. Approximately 1.4 % of weight loss was recorded at 84 °C. MESSP was thermally stable at the processing temperature of the filler filled polymer composites as there was only 1.9 % of its initial weight loss at 180 °C. The weight loss was clearly observed at the second stage of decomposition which occurred at 276 °C to 500 °C where there was approximately 66 % weight loss of MESSP recorded. This can be associated with the decomposition of the organic compound such as hemicellulose, lignin and cellulose at this stage. At this temperature, MESSP starts to decompose and become thermally instable (Balakrishna et al., 2013).

The maximum weight loss rate occurred at 365 °C and the weight loss become constant when the temperature was beyond 498 °C. This shows that MESSP can withstand high temperature above 498 °C with 33 % residue left based on the raw TGA data as shown in Figure 4.4. Study reported by Ong and Charoenkongthum (2002) revealed that banana starch used as filler were thermally instable because there was only 2 % of the filler remained as residue at 600 °C. The report proved that natural fillers are not thermally stable and is not suitable for high temperature processing. However, decomposition of MESSP shows that about 30 wt. % of MESSP was remained as residue upon heating up to 600 °C. High thermal stability of MESSP results in lower rate of decomposition at higher temperature and confirms that MESSP has better thermal stability and can be processed at higher temperature as similar to the processing temperatures of most of the polymers.

4.2 Characterisation and Testing of MESSP/PP Composites

4.2.1 Attenuated Total Fourier Transform Infrared Spectroscopy (ATR-FTIR)

The ATR-FTIR spectra of neat PP are found in the literature showing the absorption band with aliphatic C-H stretching between 3000 and 2800 cm^{-1}, CH_3 asymmetric deformation and CH_3 symmetric deformation at 1457 and 1375 $cm^{-1,}$ respectively. The absorption band appeared at 1165 cm^{-1} was due to the bending vibration of tertiary carbon, 950 cm^{-1} was attributed to CH_3 rocking vibration, 841 cm^{-1} and 813 cm^{-1} were corresponded to CH_2 rocking vibration (Butylina et al., 2012; Catto et al., 2019).

Figure 4.5 illustrates the spectra of PP/MESSP composites at various MESSP loading. Overlapped ATR-FTIR spectrums of neat PP and PP/MESSP composites were similar showing that the interactions among the PP molecules are dominant. This is due to stronger interaction between the PP chains as compared to the interaction between PP chain and MESSP particles, and interaction in-between MESSP particles (Ooi et al., 2011). It can be also seen that there were no new peaks that appeared or disappeared as the spectra of PP/MESSP composite were compared with spectrum of neat PP. This indicates that there were no chemical interaction or new chemical bonding formed between PP and MESSP. On the other hand, there are some changes in the intensity of peak that can be observed in the region of 3650 cm^{-1} - 3200 cm^{-1} and the absorbance peak at 1632 cm^{-1} that corresponded to the O-H groups and

moisture where the intensity of the O-H group absorbance appeared higher in PP/M15 and PP/M20 composites. This indicates the presence of the moisture in the specimen contributed by the higher hydrophilic properties of the composites at higher loading of MESSP (Catto et al., 2019).

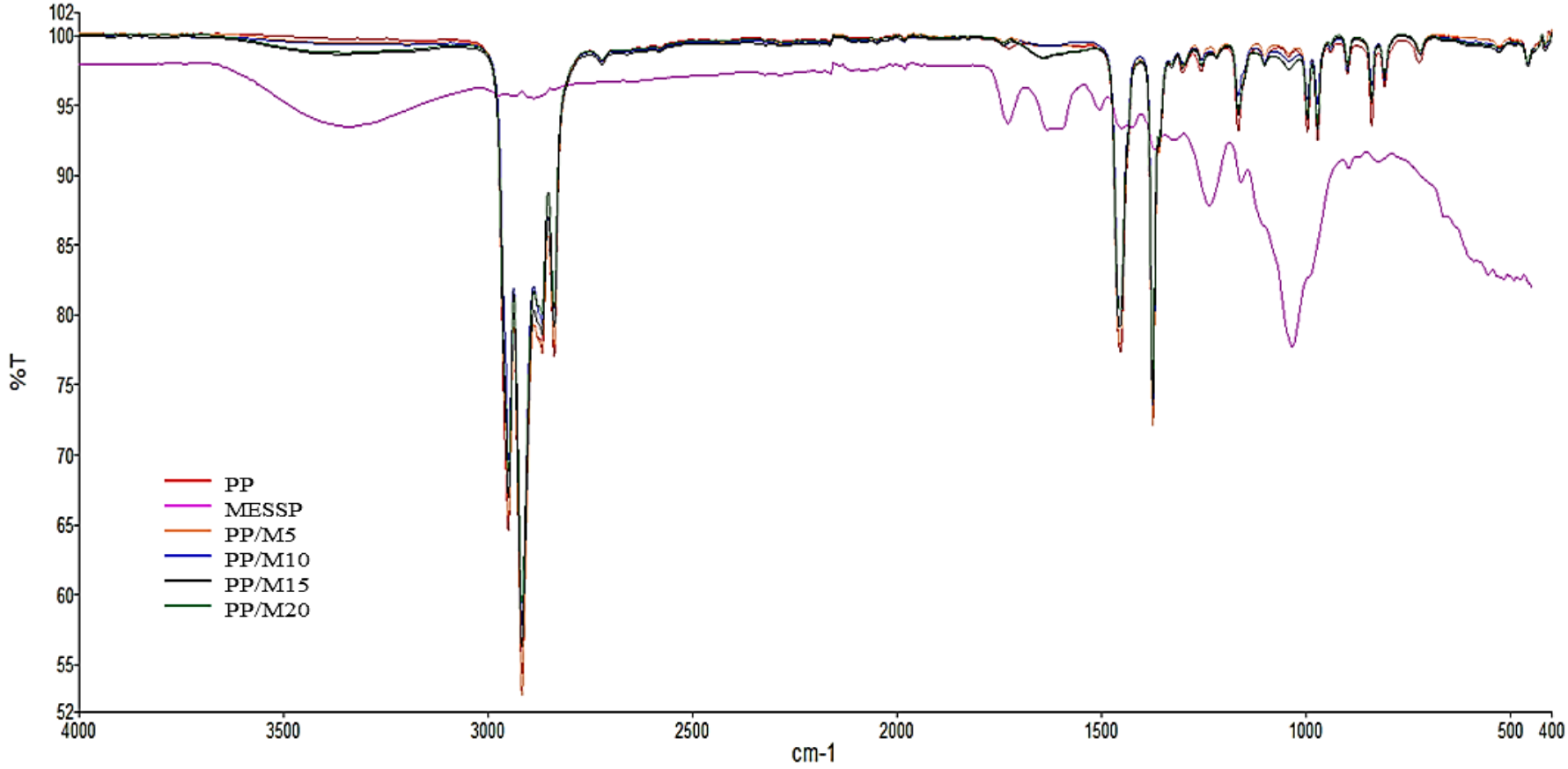

Figure 4.5: ATR-FTIR Spectra of Neat PP, MESSP and PP/MESSP Composites

4.2.2 Thermogravimetric Analysis (TGA)

Thermal stability is an important parameter which can affect the processability of composites. TGA as shown in Figure 4.6 (a) illustrates the thermal stability of the MESSP and PP/MESSP composites. Meanwhile, Figure 4.6 (b) displays the derivative thermogravimetric (DTG) curves that present three thermal stages (Santos et al., 2018). Table 4.3 presents the temperature to which the samples were reduced by 10 wt. % corresponding to the decomposition process, the maximum decomposition temperature (T_{max}) as well as amount of the residue remained (Kumar et al., 2019). Neat PP and the composite show similar thermal behavoiur up to 280 °C; beyond that, thermal decomposition of PP/MESSP composites shifts to lower temperatures as shown in Figure 4.6 (a) owing to removal of the less thermally stable organic compounds present in MESSP in second stage of decomposition (Stelescu et al., 2017). Hemicellulose, cellulose and lignin constituent in MESSP have different decomposition resistance toward high temperature. Based on Figure 4.6 (b), two peaks are observed in second stage of decomposition from 280 °C to 385 °C which involve the decomposition of hemicellulose and cellulose whereas lignin undergoes slow decomposition from 280 °C to 490 °C (Balakrishnan et al., 2013). As reported by Cordeiro et al. (2014), this temperature range (280 °C) marks the decomposition of organic constituent of the fillers. On the other hand, the T_{max} as present in the DTG thermogram analysis is related to the polymer decomposition. Decomposition of PP polymeric chains occurred with a T_{max} around 465 °C and completed upon 600 °C. Addition of MESSP for PP composites was found to improve thermal stability of the composites by 5 °C as

T_{max} increase with the increasing of MESSP amount. Final residua of PP and PP/MESSP composites are 0.34 wt. %, 1.26 wt. %, 2.34 wt. %, 3.83 wt. % and 5.37 wt. % respectively. Based on the graph shown in Figure 4.6 (a), MESSP possess a better thermal stability as compared to neat PP at temperature beyond 480 °C. This suggests that the MESSP was slightly less combustibility than neat PP beyond the 480 °C and the composites with higher loading of MESSP exhibits higher thermal stability as more residue was remained upon heating up to 600 °C.

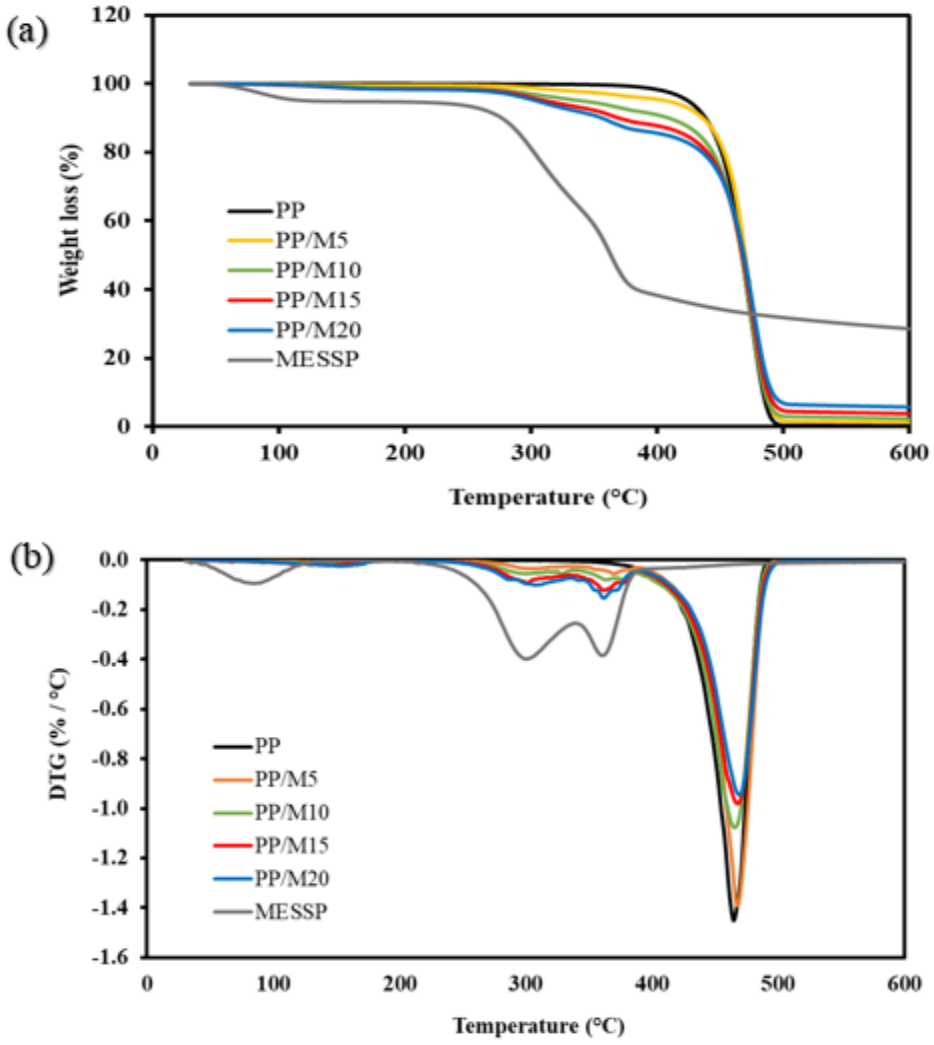

Figure 4.6: (a) TGA and (b) DTG Curves of MESSP and PP/MESSP Composites

Table 4.3: TGA Data of PP/MESSP Composites

Code of specimen	T_{onset} 10% (°C)	T_{max} (°C)	Residue @ 600°C (wt.%)
PP	438.64	465.33	0.34
PP/ M5	436.68	468.33	1.26
PP/ M 10	409.59	466.33	2.34
PP/ M15	370.18	468.33	3.83
PP/ M20	356.71	470.00	5.73
MESSP	277.16	362.00	28.59

4.2.3 Processing-ability

Process-ability of polymer composite is one of the indications to determine the feasibility of MESSP to be used as filler for PP. The processing torque reveals the rheological behaviour and the stiffness of the composite (Aho, 2011). The process-ability of PP/MESSP composites was evaluated based on the processing torque obtained through mixing process.

In general, an increasing torque value were observed upon polymer discharged into the mixing chamber, resulted from the mixing of PP pellet with the MESSP until the peak value know as loading torque was achieved. This was attributed to the resistance exhibited by the shearing action of un-melted PP pellets against the rotors. Thus, with increasing MESSP loading from 0 wt. % to 20 wt. %, the amount of PP was reduced and this results in lower shearing

action that responsible for the reduction of loading torque. The reduction in amount of PP discharged in the mixing chamber created lower melt viscosity and lower shear exerted to the rotor reflecting the low torque values (Cao et al., 2012).

Meanwhile, at all MESSP loading, PP/MESSP composites become completely homogeneous and achieved a constant torque value at the end of mixing which was known as stabilization torque. Stabilization torque is the result of homogeneous dispersion of filler in polymer composites and thus achieving constant torque confirms good dispersion of filler in polymer matrix (Pang et al., 2015). Besides, the research study by Mittal (2016) reported that lower stabilisation torque also implies better process-ability as well as good and homogeneous dispersion of filler in PP matrix.

By comparing the stabilization torques with increasing MESSP loading as shown in Figure 4.7, it can be seen that stabilization torque were increased slightly. This was due to the increased mobility restriction of polymer chains with increasing of MESSP loading in PP matrix. More shear was required to overcome the physical restriction created by MESSP which in turn increased the viscosity of PP. Thus, slightly higher shear was required to homogeneously disperse larger amount of MESSP in PP matrix (Koay and Husseinsyah, 2016).

Besides, the dispersion of MESSP in PP matrix was found to be affected by the amount of filler loading. The increment of the stabilisation torque from 0 wt. % to 15 wt. % MESSP loading was not significant but a sharp increase

was clearly observed at 20 wt. % MESSP. At higher filler loading, MESSP started to aggregate and created higher viscosity eventually caused higher flow resistance and stabilisation torque of the mixture. However, 0 wt.% to 15 wt.% of MESSP loading still possess processing advantage as the different of processing torque of PP/MESSP was insignificant as compared to neat PP.

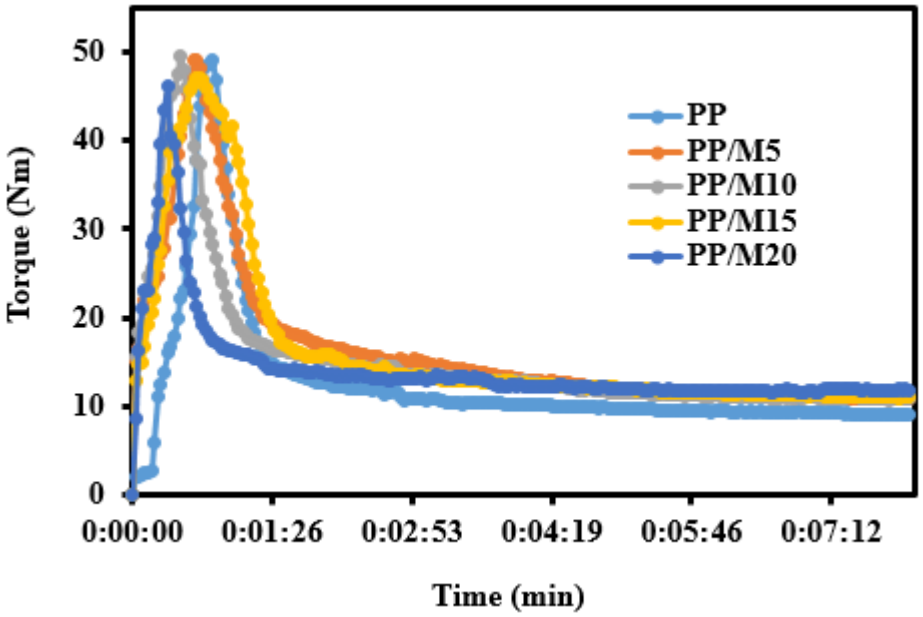

Figure 4.7: Processing Torque of PP/MESSP Composites

Table 4.4 summarizes the processing torques of PP/MESSP composites with various MESSP loading, respectively. Processing torque study reveals that addition of MESSP up to 20 wt. % loading does not significantly influence the processing condition of PP matrix. There were only slight increase in the processing torque values which did not require any modification of the processing condition. Thus, PP/MESSP composites can be processed at similar processing conditions as that of neat PP.

Table 4.4: Processing Torque Values of PP/MESSP Composites

MESSP Loading (wt. %)	Processing Torque	
	Loading Torque (N)	Stabilization Torque (N)
0	49.20	9.00
5	49.21	10.77
10	49.61	10.79
15	47.02	11.00
20	46.07	11.80

4.2.4 Differential Scanning Calorimetric (DSC)

Figure 4.8 displays the melting characteristic of melt mixed specimens of neat PP and its composites. Neat PP and its composites exhibited similar thermal profile.

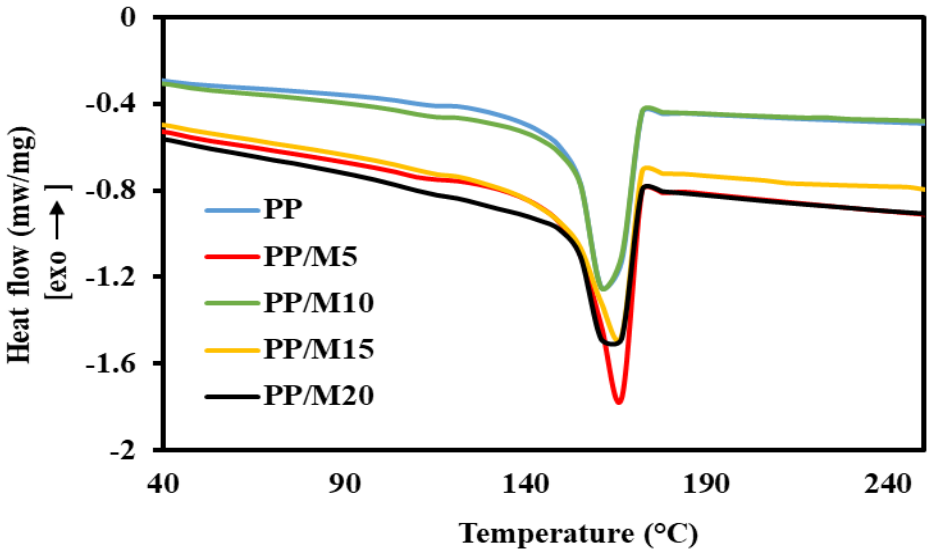

Figure 4.8: Heating Curve of PP/MESSP Composites

The melting profile of PP in different specimen differs slightly by 1 to 3 °C. DSC result shows that there was no distinctive change on the melting temperature, T_m of PP matrix with the increasing MESSP loading. This indicates that the addition of MESSP has relatively little effect on the crystallization of PP during melt mixing process.

Table 4.5 shows the thermal characteristics of neat PP and PP/MESSP composites obtained at different MESSP loading through DSC analysis. It was noticed that PP/M5 and PP/M10 composites show slightly higher heat of fusion (ΔH_m) and degree of crystallinity (X_c^m) values as compared to PP/M15 and PP/M20. MESSP presents two competing role in the composite that affects the degree of crystallization which is acting as nucleating agent at lower filler loadings and retards crystalline growth at higher filler loading. Thus, it suggests that at 5 wt. % and 10 wt. %, MESSP exhibit a nucleating effect which promotes the crystallization and further increase the degree of crystallinity of the composites.

Besides, it was also found that crystallisation temperature (T_c) shift to higher temperature with the addition of MESSP up to 10 wt. %. MESSP. Incorporation of MESSP induced the crystallization of PP chains through nucleation activity resulted of the higher T_c. This result is in line with the observation reported by Faria et al. (2006), the increased T_c with the addition of *Dwarf Cavendish* filler on PP composite. It was reported that lignocellulose filler is an efficient nucleating agent which promotes crystallization of the polymeric matrix and results in increased T_c of the composite system.

On the other hand, at higher loading, MESSP tend to retard the crystallization of PP chains and results in gradual reduction of T_c and X_c^m. At higher MESSP loading of 15 wt. % and 20 wt. %, the segmental mobility of PP chains were reduced and it inhibits the rearrangement of PP chains to form crystalline structure. The MESSP particles tend to move in between the PP chains and reduce the rearrangement of the chains to form crystalline phase. This effect becomes more prominent with increasing amount of filler. Other researchers also reported on similar observation by which presence of filler could results in PP chains to entrap and reduce the regularity of chain rearrangement to form crystalline structure (Papageorgiou et al., 2013; Mustapa et al., 2014; Wang and Ying, 2014).

From the thermal characteristics study, it can be observed that addition of MESSP insignificantly affects the melting and crystallization temperature of the PP matrix. Thus, PP/MESSP composites can be processed at similar temperature as that of the neat PP.

Table 4.5: DSC data of PP/MESSP Composites

Composite Code	W_p	T_m (°C)	T_c (°C)	ΔH_m(J/g)	X_c^m (PP phase)
PP	1.00	164.41	125.24	71.62	34.60
PP/ M5	0.95	162.58	125.90	69.65	35.42
PP/ M10	0.90	163.73	126.06	67.45	36.21
PP/ M15	0.85	165.03	126.01	63.31	35.98
PP/ M20	0.80	165.38	125.95	57.84	34.93

4.2.5 Tensile Properties

Figure 4.9 (a) displays the tensile strength of MESSP/PP composites. Addition of higher loading of MESSP reduced the tensile strength of the composites. Tensile strength of the composites is affected by the interfacial interaction and the compatibility between PP and MESSP. Incorporation of MESSP did not increase tensile strength and this implies that the bonding between filler and matrix is weak that ease the detachment of MESSP from PP when the composite was subjected under pulling (Gulitah and Liew, 2018). As discussed in ATR-FTIR analysis, there was only physical interaction and no chemical bonding between PP and MESSP. Physical interaction phenomena between MESSP and PP can be seen through SEM analysis which will be discussed in the following section. Degree of detachment depends on filler/matrix interaction. MESSP were fractured in lower loading and tend to pull out from PP matrix at higher loading. The former shows the better physical interaction while the occurrence of latter is a sign of weaker interaction.

Low wetting behaviour of PP can be seen at 20 wt. % of MESSP when aggregation occur leading to a lower tensile strength (Kim et al., 2008). Notably, 30 wt. % and 40 wt. % of MESSP content were failed to obtain for the PP/MESSP composites. It was discovered that immiscible mixture was obtained due to the improper mixing of the MESSP in the PP matrix. Filler-filler interaction was more significant at higher MESSP loading where aggregation happened and further promotes the stress-concentrated. When the composites were unable to withstand the forces, detachment of MESSP from PP matrix

occurred (Balakrishna et al., 2014). Similar observation was reported by Onuegbu and Igwe (2011) indicated that the dispersion of filler is also a factor that is responsible for the tensile properties. In addition, the poor adhesion between filler and matrix is also caused by the incompatibility between the polar natures of natural filler and nonpolar of thermoplastic polymer. Difference nature of the filler and matrix causes the filler weakly compatible to the matrix resulted in weakening the tensile strength of the composites (Zainudin et al., 2014).

However, all the PP/MESSP composites exhibited greater tensile modulus as compared to neat PP. Based on Figure 4.9 (a), tensile modulus increased with the increasing of the MESSP loading. It was found that the presence of MESSP enhances the rigidity and stiffness of the PP composites which due to the crystallinity of the cellulose structure in natural filler contribute to the stiffness properties (Balakrishna et al., 2014). The elongation at break of neat PP was 30.6 % and experienced a drop with the increasing of MESSP loading. This exhibited similar trend as tensile strength which the poor elongation of PP/MESSP composites was affected by the weak interaction between fiber/matrix composites (Vu et al., 2018). Moreover, restriction of polymer chain mobility caused by the presence of MESSP reduces the flexibility which in turn reduces the elongation at break as reflected an increasing stiffness of the composite as shown in Figure 4.9 (b). Similar behaviour was reported for polymer composites containing durian seed flour, cellulose fiber extracted from rice straw and rice husk powder which all showed increased modulus and

reduction in elongation at break of the polymer composites with the increasing filler loading (Premalal et al.,2002; Osman and Zakaria, 2012; Vu et al.,2018).

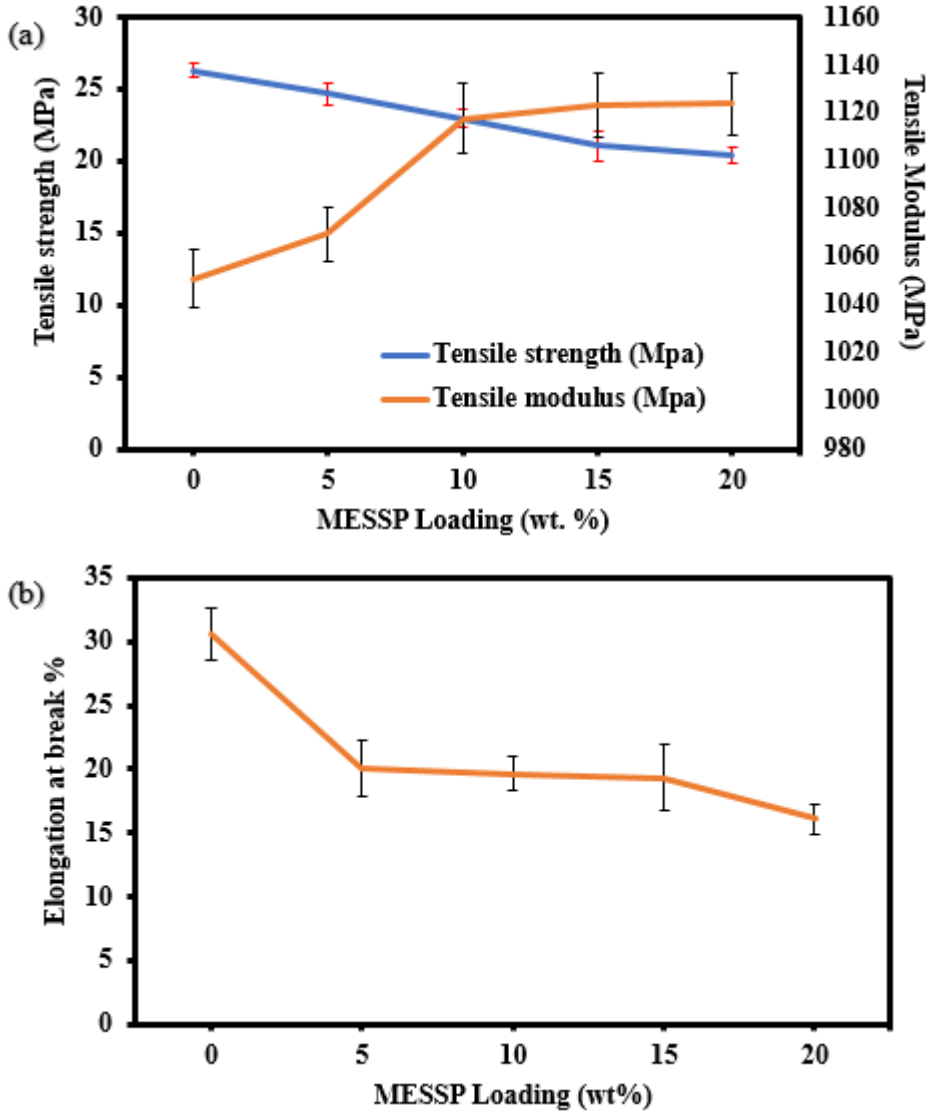

Figure 4.9: (a) Tensile Strength, Tensile Modulus and (b) Elongation at Break of PP/MESSP Composites

Table 4.6: Tensile Properties of PP/MESSP Composites

Filler loading (wt. %)	Tensile Modulus (MPa)	Tensile strength (MPa)	Elongation at Break %
0	1050.71± 12.08	26.31± 0.48	30.60± 2.11
5	1069.57± 11.54	24.67± 0.71	20.08± 2.17
10	1117.83± 14.35	22.98± 0.58	19.66± 1.37
15	1123.33± 13.72	21.04± 0.65	19.33± 2.55
20	1124.00± 13.08	20.39± 0.53	16.08± 1.21

4.2.6 Impact Properties

Notched IZOD impact tests were carried out on neat PP and PP/MESSP composites to compare the resistance of the material to the indentation and fracture due to the impact force (Premalal et al., 2002). The impact strength of the MESSP filled PP composites were higher than neat PP as illustrated in Figure 4.10. The impact energy for neat PP was 21.07 J/m and increased drastically to around 31.20 J/m, 39.73 J/m, 44.53 J/m and 45.87 J/m for PP/MESSP composites, respectively. Generally, the values obtained from impact strength were inversely proportional to the values obtained from tensile strength. In spite of the slightly lower tensile strength of PP/MESSP composites, MESSP exhibited better impact properties at higher filler loading than neat PP. Higher impact strength was obtained with higher MESSP loading shows the significant effect of MESSP loading on the impact properties of the PP/MESSP composites.

There are literally several factors that could affect the impact properties of the composites. For instances, toughness properties of the reinforcement, the nature of the interfacial region and also the frictional work involve in fiber matrix decohesion (Wambua et al., 2003; Nasihatgozar et al., 2016). Energy is dissipated by fiber fracture or fiber pull out from the polymer matrix which known as debonding. As compare to fiber fracture, debonding dissipate more energy exhibited a sign of weak bonding (Paul et al., 2010; Nasihatgozar et al., 2016).

When the interfacial region of the composite is weak, crack propagation along the fibre matrix interface will happen before debonding. More energy capacity of the composites is needed in order to produce the new rough surfaces in the separation of MESSP from the PP matrix. Thus, with the increase of MESSP loading, it can be expected that the greater impact strength of the composite is measured due to more energy is consumed for debonding (Paul et al., 2010; Indira et al., 2013; Zaman and Beg, 2014).

Weaker interfacial adhesion was observed at higher MESSP loading as more filler pull out from then matrix. This phenomena was the main failure mechanism lead to the lower tensile strength. The explanation of lower interfacial bonding herein in line with the impact properties of the composites. Similar result reported for coir/PP composite with low tensile strength but higher impact strength (Wambu et al., 2003; Malkapuram et al., 2009).

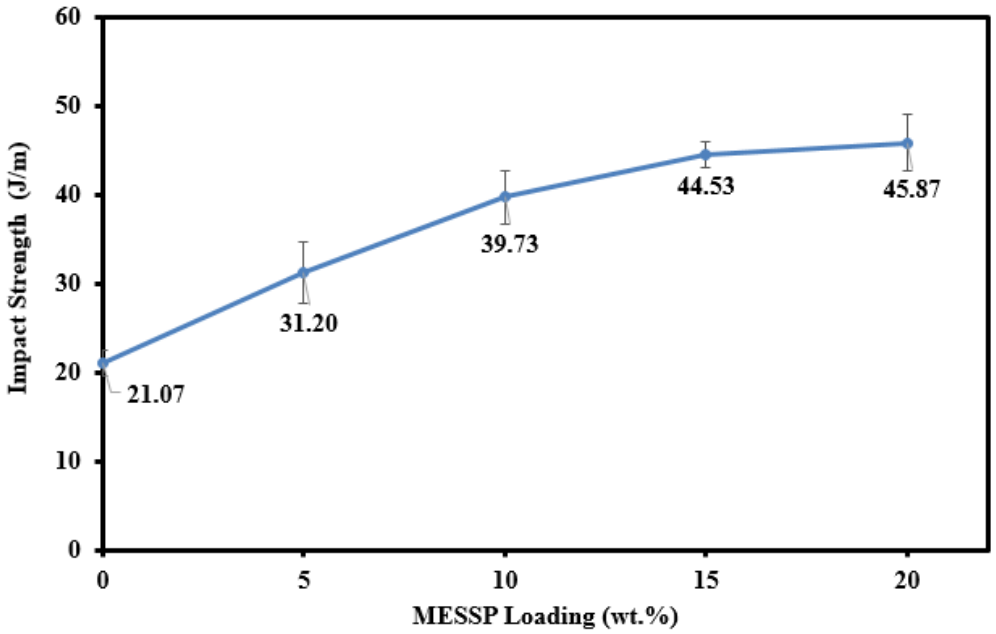

Figure. 4.10: Impact Strength of PP/MESSP Composites

4.2.7 Scanning Electron Micrograph (SEM)

Filler pull out as result of the formation of voids is a sign of weak interfacial adhesion between the filler and matrix. Voids were formed due to the detachment of MESSP from PP matrix as circled in Figure 4.11. This observation was more prominent at higher loading of MESSP. More voids were formed at higher MESSP content due to the aggregation of filler. The aggregation of filler become the stress concentration which lead to the filler-matrix separation as evidenced by the reduction of tensile strength of PP/MESSP composites (Sarifuddin et al., 2013).

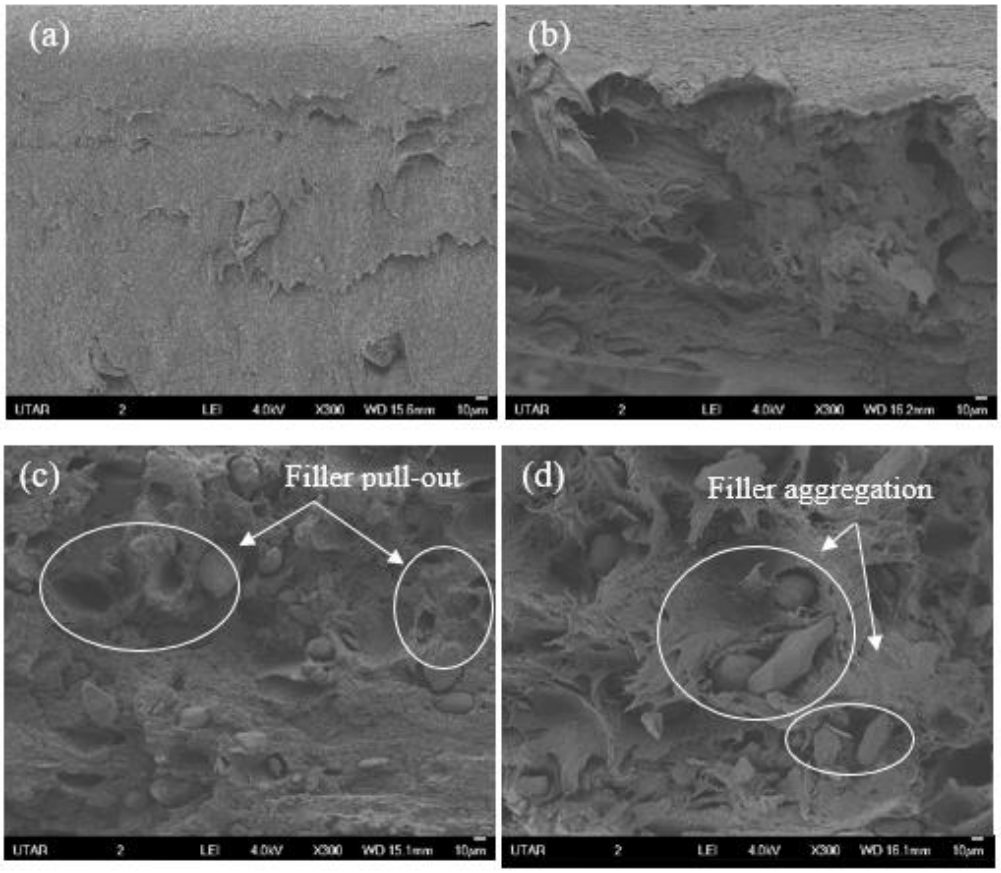

Figure 4.11: SEM Micrograph of Tensile Fracture Surface of (a) PP/M5 (b) PP/M10 (c) PP/M15 (d) PP/M20 at 300x Magnification

Figure 4.12 (a) presents the fracture surface of neat PP. Fibrous structure of PP matrix indicated the deformation of PP matrix. The fibrous structure seems to have decreased with the increasing of MESSP loading. This was due to the MESSP restricted the mobilization and the deformation of PP polymer chains, as reflected in brittle deformation of the composition lead to the increasing of tensile modulus and decreasing of elongation at break of the composites (Premalal et al., 2002, Vu et al., 2018). Figure 4.12 (b) to (d) show the morphology of the tensile fractured surfaces of PP composites at various MESSP loading.

Figure 4.12 (b) shows the good matrix tearing which was due to the stress distribution between MESSP particles in PP matrix resulting in crack propagation along the filler matrix surface. Moreover, MESSP particles tend to be embedded in PP matrix as shown in Figure 4.12 (b) whereas in Figure 4.12 (c) and (d), MESSP tend to be exposed on matrix surface and eventually fractured under pulling force. The former incident displays stronger interfacial adhesion as compared to latter with filler loading of 15 wt.% and 20 wt. % (Kim et al., 2008; Zaman and Beg; 2014; Kolawole et al., 2017).

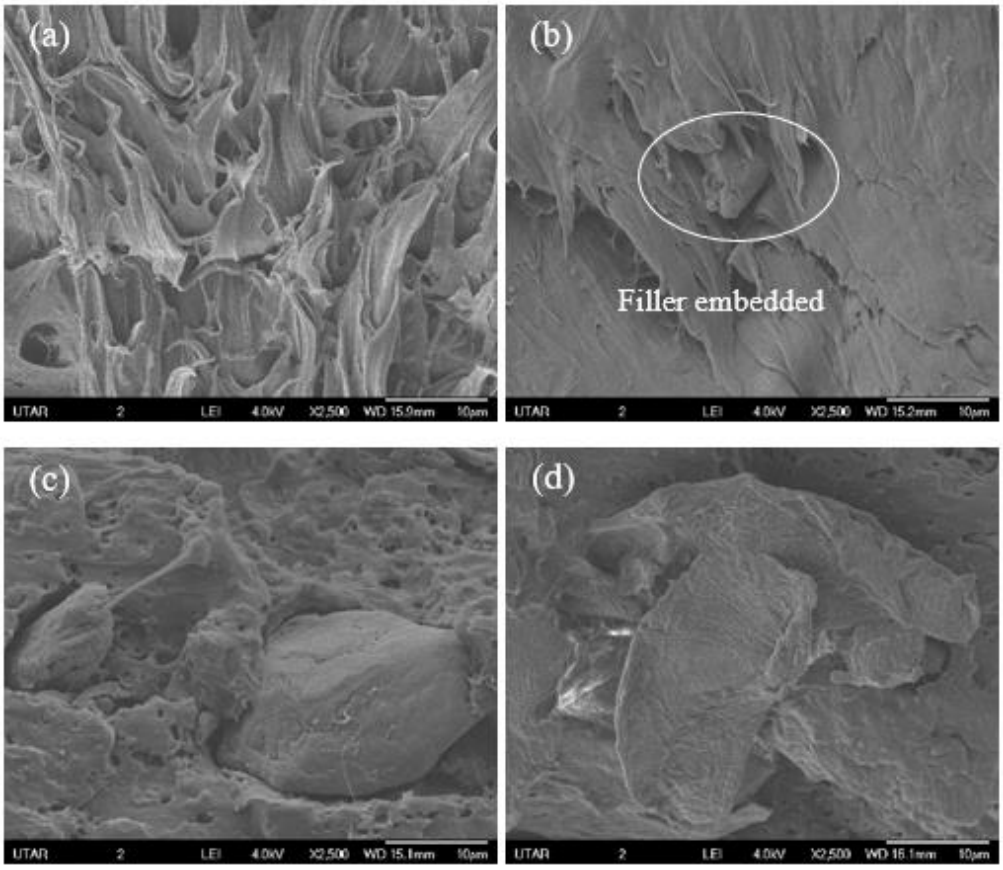

Figure 4.12: Comparison of Surface Fracture of: (a) PP (b) PP/M5 (c) PP/M15 and (d) PP/M20 at 2500x Magnification

4.2.8 Water Absorption

Figure 4.13 presents the plots of the evolution of the water uptake of PP/MESSP composites immersed in water as a function of MESSP loading. It was observed that the specimen without MESSP attained the lowest water absorption (around 0.08%) whereas the water uptake of PP/MESSP composite increased as MESSP loading was increased to 20 wt.% (PP/M20) reaching a percentage of water absorption around 1%. Basically, water permeability capability of natural filler depend on several factors such as presence of voids on filler's surface, particles size, porosity and the structural composition (Ogah et al., 2015; Acevedo et al., 2016; Dhanola et al., 2018; Wechsler et al., 2019).

The tendency of water absorption properties increased with addition of MESSP loading can be explained with the presence of hydroxyl group in filler which possess the hydroscopic nature, promoted the formation of hydrogen bonding between the water molecules and the hydroxyl groups on the cellulose structure of natural filler (Dhanola et al., 2018; Wechsler et al., 2019). Similar result was obtained by Demir et al. (2006), which showed an increase in water absorption of the kenaf fiber filled polymer composite. The amount of water absorbed by the composite increased with the increasing filler loading due to more free hydroxyl group were available at higher filler loading which comes in contact with water through hydrogen bonding which resulted more water uptake and weight gain in the composites.

It could be noted that the presence of voids were more pronounced due to the aggregation observed at the higher loading of MESSP as illustrated in SEM micrographs (Figure 4.11 (d)). Higher MESSP content resulted in higher voids entrapped caused by the weak adhesion between interfacial areas of MESSP filler and hydrophobic PP matrix causing the retention and accumulation of water within the composites. (Santiagoo et al., 2011; Balakrishna et al., 2013; Sarifuddin et al., 2013; Alias et al., 2019). However, the water absorption of PP/MESSP composites slightly increased when compared to the neat PP as shown in Figure 4.13.

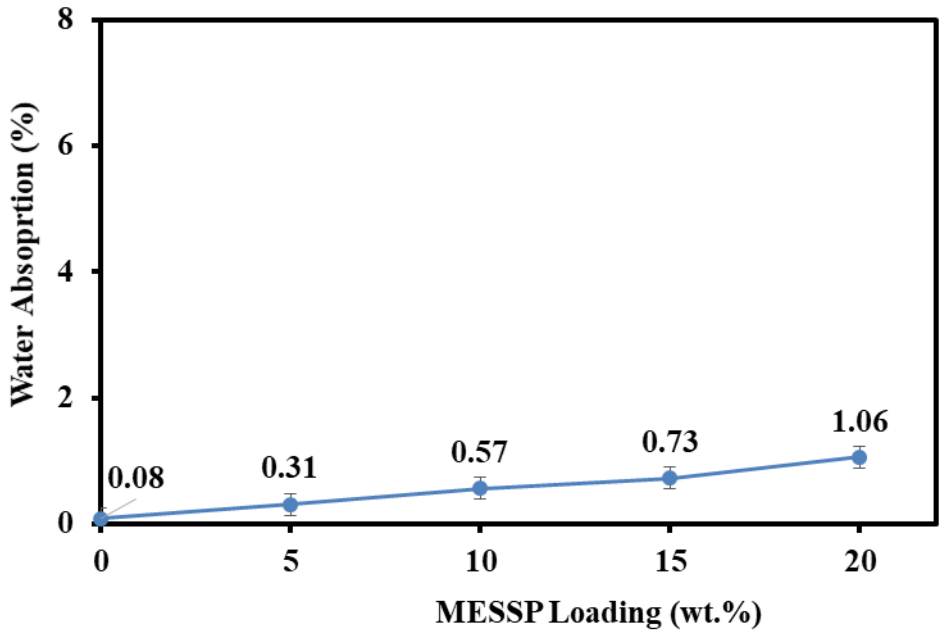

Figure 4.13: Water Absorption Percentage of PP/MESSP Composites

4.2.9 Soil Burial Test

4.2.9.1 Weight Loss

Soil burial test was conducted in the realistic environment to observe the possible biodegradation takes places with the present of microorganism (Alshabanat, 2019). Variation of weight, discolouration based on the visual inspection, crazing of the composite's surface, loss of tensile properties were used to analyse the extent of deterioration. The results were collected consecutive for every 2 months up to 6 months' time (Shah et al., 2008). The weight loss of the samples as the function of the MESSP loading is shown in Figure 4.14.

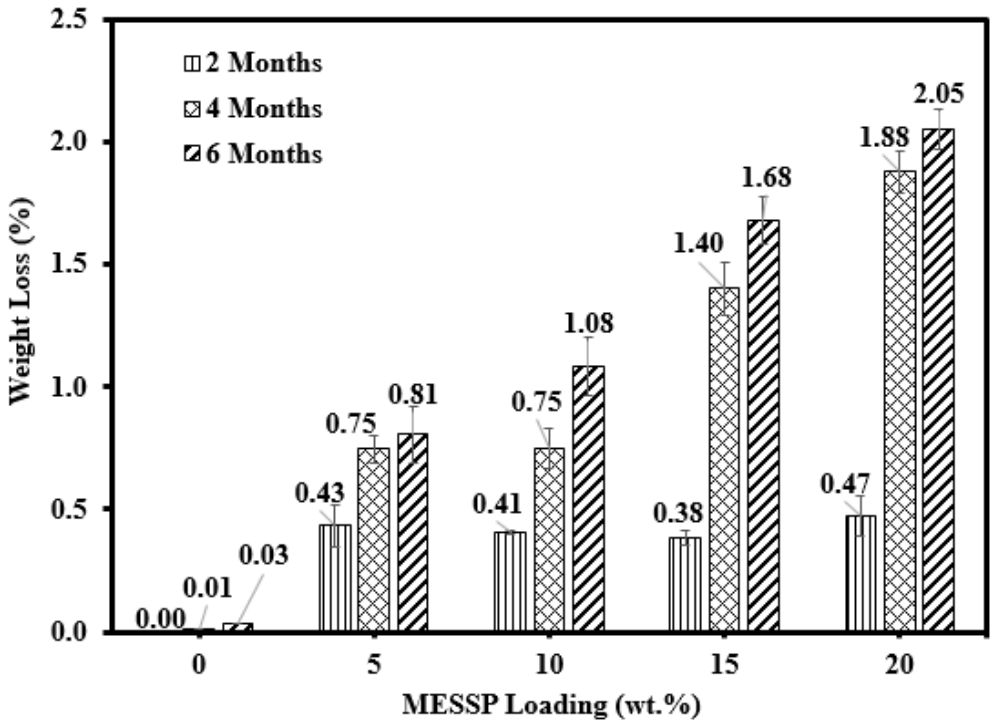

Figure 4.14: Percentage Weight Loss of PP/MESSP Composites versus MESSP Loading

From the study, it was noticed that all the composites experienced a significant weight loss as compared to neat PP. Neat PP showed the minimal weight loss ranging between 0.01- 0.03% throughout the soil burial test due to the high hydrophobic properties that show the high resistance toward the biodegradation (Shah et al., 2008). Out of the three period of time recorded, the weight loss of the samples buried for 2 months was the least and less significant. Prominent variation of the weight loss was clearly observed in 4 and 6 months of soil burial.

For instance, at the same loading of MESSP (20 wt.%), the weight loss of the PP/M20 composites increased from 0.5 % to 2.1 % which soil buried for 2 month and 6 months respectively. This phenomena was attributed to the higher biodegradation rate caused by the attachment of the microorganism in degrading the composites. The presence of MESSP served as the food source for the growth of the microorganism in polymer composite. This evidence was further supported in the SEM micrographs to be disccused latter that showed the microbial attack and the migration of the microorganism on the surface of MESSP. This finding was consistent with the previous studies reported that presence of the microorganisms such as fungi was crucial for the biodegradation to take places which resulted the weight loss of kenaf fiber reinforced polymer composites (Hidayat and Tachibana, 2012).

Other than that, the evolution of weight loss degree of the composites was higher with the increasing MESSP loading. This indicated that MESSP favours the biodegradation process as more weight loss was observed in the

composite with higher MESSP loading. Similar finding was reported by Nourbakhsh et al. (2014) by which there was no weight loss observed from the neat PP but the PP with the highest natural fibre content contributed to the greatest weight loss which corresponded to the bio-degradability effect. According to Chee et al. (2019), hemicellulose was the constituents in the natural fibre that responsible for the biodegradation. In this work, MESSP promoted the microbial attack by interacting with the moisture in the soil resulted in the consumption by the microbe and leaching of the MESSP out from the composite (Hidayat and Tachibana, 2012; Chee et al., 2019).

4.2.9.2 Physical Appearance

Signs of the surface degradation can be indicated based on the colour changes, roughening of the surface, crazing or delamination (Shah et al., 2008). The samples collected from the soil burial test were inspected and compared with the samples before soil burial. As reported earlier**,** the most significant weight loss was observed in the PP/M20 composites with the highest MESSP content as compared to other composites. This shows the composites with higher MESSP loading were keen to biodegradation.

Figure 4.15 illustrates the physical appearance of the PP/M20 composites before and after soil burial for a period of 2, 4 and 6 months exposure in the degradation condition. As the time prolonged, the colour changes of the composites was getting prominent. The composites become paler

with the presence of the minor marked crazing observed. Moreover, the surface of the composites were getting rougher due to the surface degradation (Fakhrul and Islam, 2013). These visual changes were the signs of the any possible microbial attack. However, these changes did not confirm the biodegradation takes places in term of metabolism. Thus, SEM analysis was conducted to obtain more sophisticated evidence to determine the surface degradation phenomena of PP/MESSP composites (Shah et al., 2008).

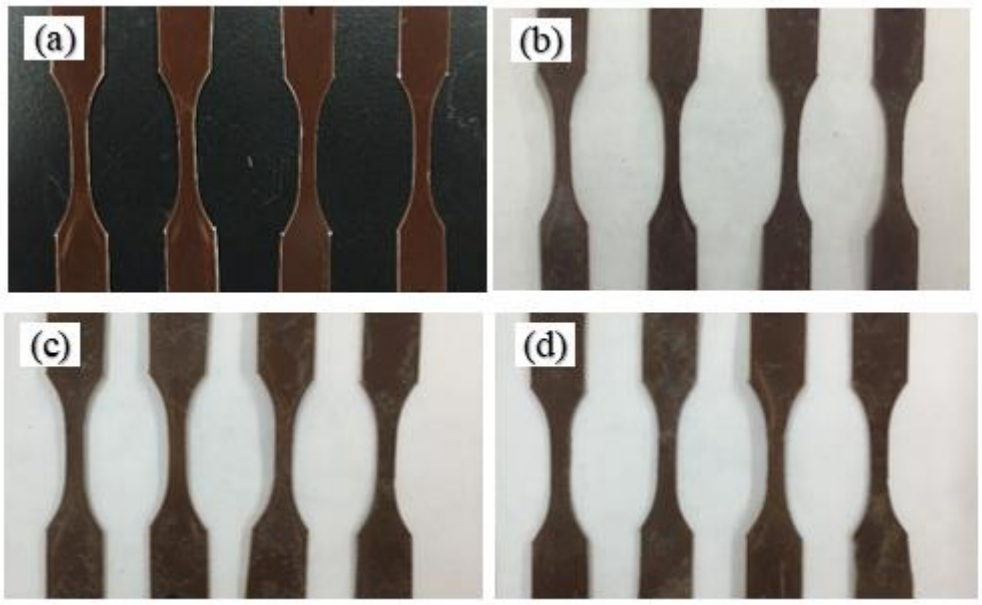

Figure 4.15: Physical Appearance of the PP/M20 Composite on; (a) 0 Month Soil Burial, (b) 2 Months Soil Burial, (c) 4 Months Soil Burial and (d) 6 Months Soil Burial

4.2.9.3 Scanning Electron Microscopy (SEM)

In order to analyse the extent of biodegradation, the composites before soil burial and the composites exposed to soil burial for 4 and 6 months were compared. It can be observed that there was no any changes of the surface of the neat PP matrix before and after soil burial up to six months, the surface of the PP matrix remain smooth as shown in Figure 4.16.

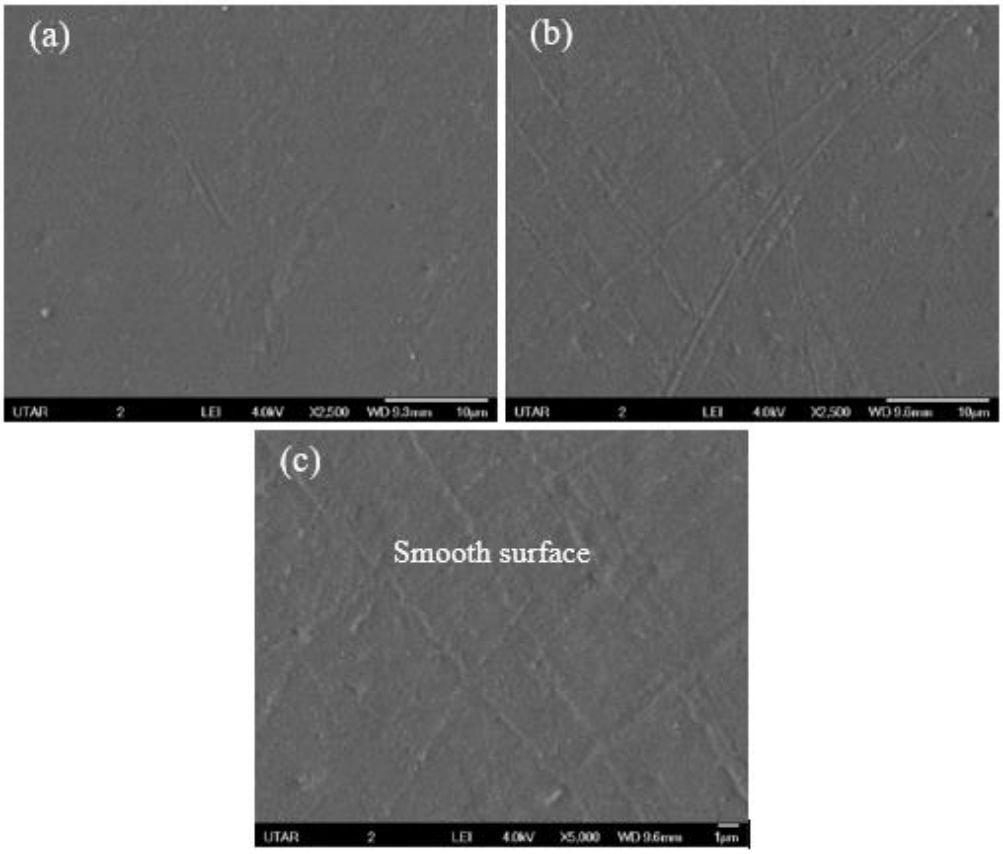

Figure 4.16: Comparison of Surface Morphology of Unfilled PP Polymer (a) before Soil Burial and after Soil Burial Test; (b) 4 Months (c) 6 Months at 2500× Magnification

In contrast, eroded surface due to the action of microbial attack was observed in the composites filled with MESSP as shown in Figure 4.17. Microorganisms were adhered and caused the damage to the MESSP's surface. Attachment of the microorganism and the formation of the micro-voids proved the presence of the biodegradation takes place in the MESSP filled PP composites as compared to unfilled PP (Luthra et al., 2020). In the case of higher loading of MESSP, the effect of biodegradation was more pronounced. This could be further supported by the rougher surface and erosion happen in the composites.

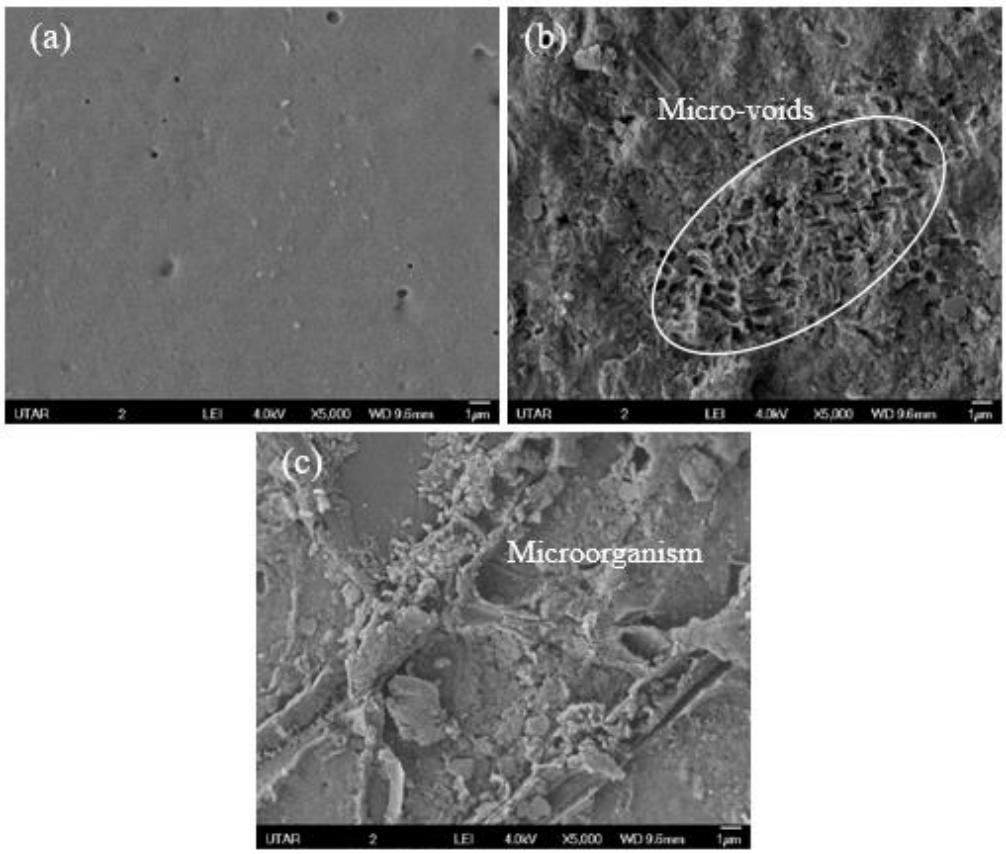

Figure 4.17: Comparison of Surface Morphology of PP/M10 Composites (a) before Soil Burial and after Soil Burial Test; (b) 4 Months (c) 6 Months at 5000× Magnification

The composites that damaged and invaded by the bacteria can be clearly visible with the formation of the holes as shown in Figure 4.18 (c) (Luthra et al., 2020). Severe degradation was more likely to takes place in the composites with higher loading of MESSP which exposed longer in the soil burial. These results were correlated to the weight loss discussed previously. Structural changes in the form of gaps and surface erosion examined from the SEM determined the surface damages of PP/MESSP composites through the action of the microorganisms (Hidayat and Tachibana, 2012).

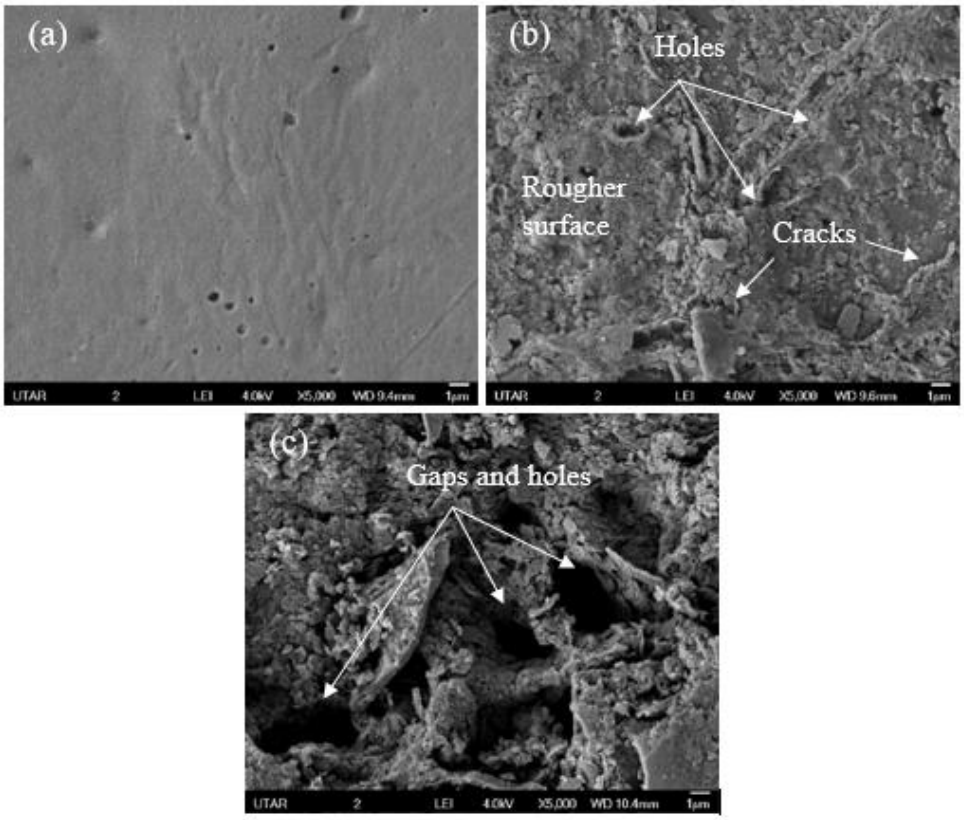

Figure 4.18: Comparison of Surface Morphology of PP/M20 Composites (a) before Soil Burial and after Soil Burial Test; (b) 4 Months (c) 6 Months at 5000× Magnification

In addition, the build-up of the bacteria can be clearly visible in Figures 4.19 (a) to (e). The weight loss of the composites that subjected to soil burial for 2 months was not prominent as compared to 4 and 6 months soil burial even though there were bacteria observed on the surface of composites. This could be explained with the three phases occurred in the biodegradation cycle as reported by Song et al., (2009). The PP/MESSP composites that soil buried for two months was considered as the early stages in the cycle where accumulation of the microbial population on the food source happened. Second stages involved the migration of microbe and the consumption on the carbon substrate for growing where this condition can be observed in the composites that subjected to 4 and 6 months soil burial. The last stages of the cycle came in when the carbon substrate was almost fully utilised by the microorganism.

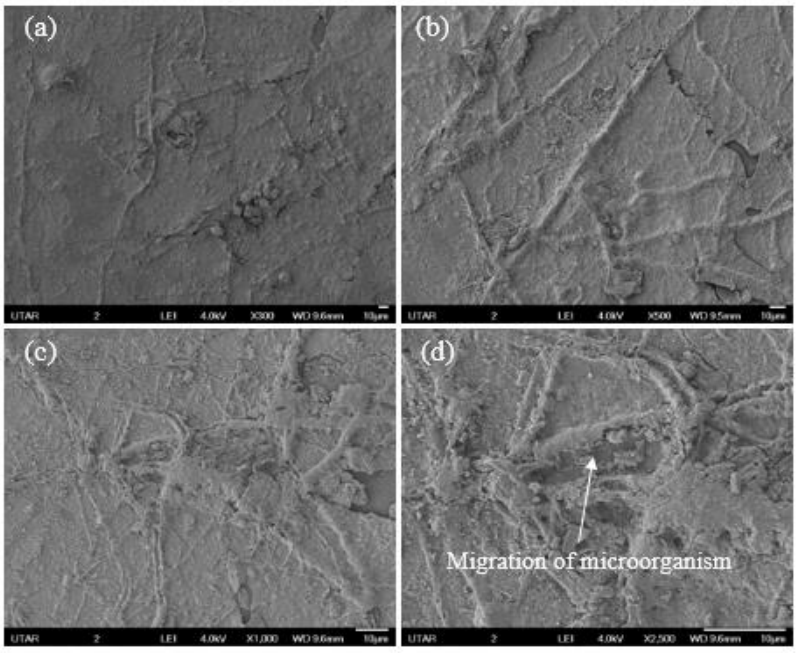

Figure 4.19: Attachment of Bacteria on the Surface of the Composites: (a) PP/M20 2 Months soil burial, (b) PP/M20 2 Months soil burial, (c) PP/M10 6 Months Soil Burial and (d) PP/M10 6 Months Soil Burial

4.2.9.4 Tensile Properties

Other than quantitatively analyzing the weight loss of the polymer, biodegradation was also characterised by the measurement of change in the tensile properties (Tareq, 2010). According to Erlandsson et al. (1997), variation in the mechanical properties was one of the indicator of degradation. Slight changes in the molar mass of the polymer would directly affect the tensile strength of the polymer as the mechanical properties was very sensitive to the changes of the weight.

Figures 4.20 presents the tensile properties of the PP/MESSP composites before and after the soil burial test. The influence of soil burial by mean of the humidity, the present of microorganism, climate changes over the characteristic of the composites varied depending on the burial time (Vasile et al., 2018). Based on the result collected, more variation in the tensile properties in the composites except for neat PP were observed with the longer soil burial period due to the higher biodegradation rate. This result was in line with the results discussed in the weight loss of the PP/MESSP composites. Meanwhile, all the MESSP filled PP composites experience the deterioration in tensile strength for the 6 months soil burial ranging from 1.49 % to 11.25 %. With the increment of soil burial period, the composites with 20 wt.% MESSP content showed deterioration of 2.42 %, 6.84 %, and 11.25 % in the order of 2, 4 and 6 months of the corresponding initial strength respectively. Similar observation was reported in the previous study where significant loss in the tensile properties of the soil buried sago starch filled LLDPE composites (Danjaji et al., 2000).

Moreover, the loss of the elongation of break ranging from 2.35 % to 30.98 % was observed in the soil burial test. As expected, the tensile modulus experience the similar trend with tensile strength. The reduction of the tensile modulus were 1.04 % and 6.78 % for the 6 months soil burial period. This phenomena again indicated the loss of the tensile modulus was attributed to the weight loss. The good correlated between the weight loss and the loss of tensile properties reflect the improved bio-degradability of the PP/MESSP composites (Shah et al., 2008).

The reduction in the tensile properties was evidenced in the SEM micrograph that show the leaching of the MESSP due to the consumption of MESSP by the microbe as shown in Figure 4.21. According to the study reported by Moharir and Kumar (2018), microorganisms able to attack the carbohydrate polymers, hydrolyses and break down the polymer into digestible units by using the enzymes. These microbial action were physically weaken the structure and strength of the composites. MESSP contains hydrophilic substituents such as cellulose and hemicellulose which facilitated the moisture absorption were more prone to biodegradation. This was because the moist environment accelerated the growth of the microorganism resulted in the degradation through the hydrolysis by enzyme (Shah et al., 2008; Fakhrul and Islam, 2013). Soil microbe feed on the MESSP leading to the weakening of the structural and mechanical properties (Obasi, Igwe and Madufor, 2013).

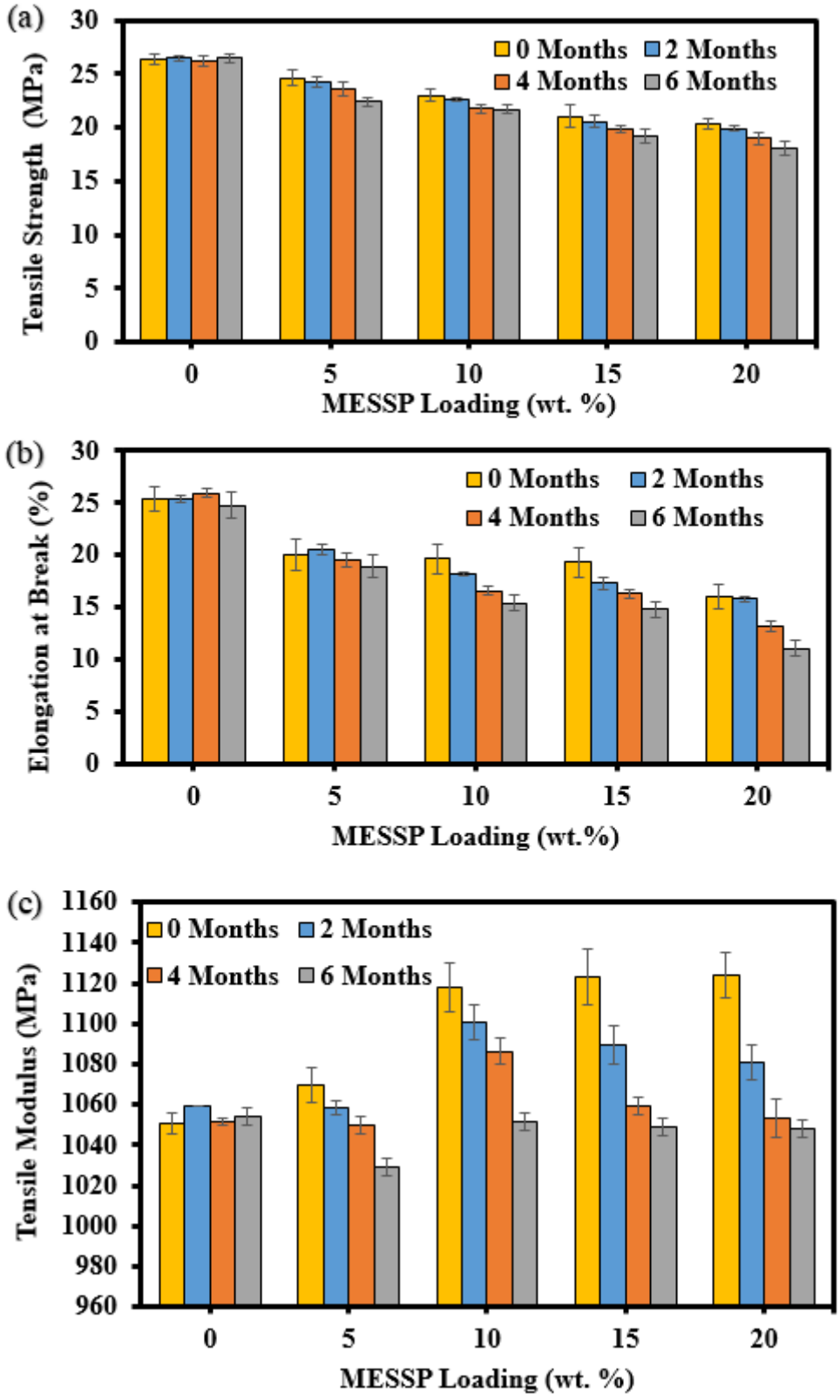

Figure 4.20: (a) Tensile Strength, (b) Elongation at Break, and (c) Tensile Modulus of PP/MESSP Composites before and after Soil Burial

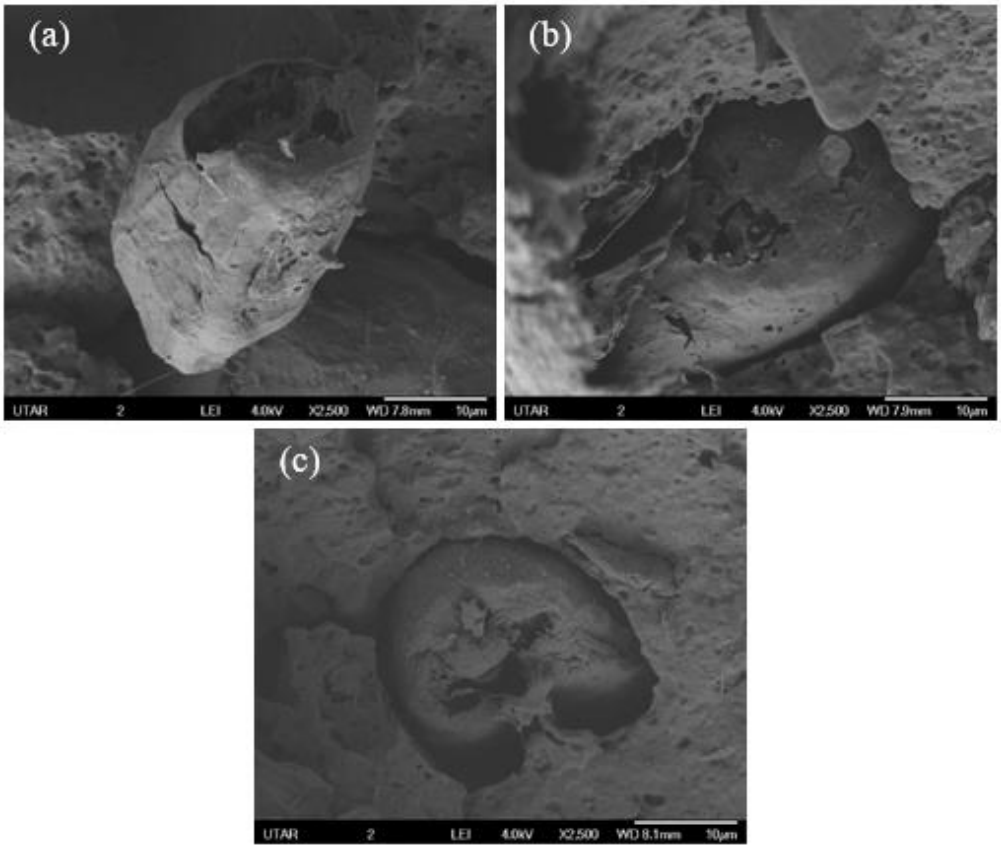

Figure 4.21: SEM Tensile Fracture of PP/MESSP Composites after Soil Burial Test

4.3 Characterisation of TMESSP

4.3.1 Fourier Transform Infrared Spectroscopy (FTIR)

The hydrophilic nature of natural fibres is the main shortcoming that caused to the poor bonding with the hydrophobic polymer matrix. Improvement in the compatibility could be achieved with surface modification or treatment of either filler or the polymer matrix (Mohanty et al., 2002). In this research, it was found earlier that MESSP contains hydroxyl functional group and results

in reduction in tensile properties and increased water absorption of the PP/MESSP composites. Thus, surface treatment of MESSP was conducted using NaOH which is the simple and most affordable chemical treatment method as found through literature review of the past work. FTIR is one of the well adapted characterization approach to study the water absorption characteristic of natural fiber or polymer based on the chemical functional group of the material. Both qualitative and quantitative analysis of moisture absorption mechanism can be obtained from the spectral. Spectral information enabled the hygroscopic analysis with the identification of main chemical functional group such as the OH band intensity (Celino et al., 2003; Chand and Fahim, 2008).

FTIR analysis was performed to study the effect of NaOH concentration range from 5w/v % – 8 w/v % on the functional group of TMESSP. Figure 4.22 presents the FTIR spectra of MESSP and TMESSP. It could be noticed that there were reduction in the intensity of the spectra band corresponded to the O-H group in the range of 3200- 3600 cm^{-1} in cellulose of TMESSP at the peak of 3337 cm^{-1}. This suggested the reduction of the OH functional group reduced the hydrophilicity of the MESSP (Rashid et al., 2016). Moreover, the transmittance intensity at the peak of 2920 cm^{-1} was also reduced. This suggested the removal of the hemicellulose constituents such as the acetyl group (methyl C-H stretching) during the MESSP surface modification (Ouarhim et al., 2018). In addition, it can be realised that the transmittance peak of 1730 cm^{-1} shown in the MESSP was no longer exists in the TMESSP. This was due to the constituents of hemicellulose that absorbed in the carbonyl region were soluble in the NaOH solution (Sepe et al., 2018). According to Elkhaoulani et

al., (2013), the disappearance of peak of 1730 cm^{-1} was due to the removal of waxes and pectin from the natural filler. The removal of the extractives was further supported in the results reported in chemical composition analysis.

The intensity of the band at peak of 1632 cm^{-1} in the MESSP was much higher as compared to TMESSP. The decrease in the intensity shows the absorbed moisture by the hydroxyl group in the cellulose were greatly reduced during the NaOH treatment (Krishnudu et al., 2019). The appearance of the small bump at 1508 cm^{-1} in MESSP was not exists in TMESSP due to the removal of the constituent including the aromatic ring stretching and C-C vibration presence in the lignin (Sudha and Thilagavathi, 2015). The strong peak at 1239 cm^{-1} observed in MESSP was not available in TMESSP. This was due to the lignin and hemicellulose were partially removed upon the NaOH treatment (Ouarhim et al., 2018, Sgriccia et al., 2008). In addition, the loss of the carboxylate substituent from the hemicellulose or lignin has reduced the band intensity at peak of 1033 cm^{-1} (Sudha and Thilagavathi, 2015). The disappearance of the peak at 899 cm^{-1} from TMESSP indicated the dissolution of the amorphous cellulose during the filler modification (Yoon et al., 2014).

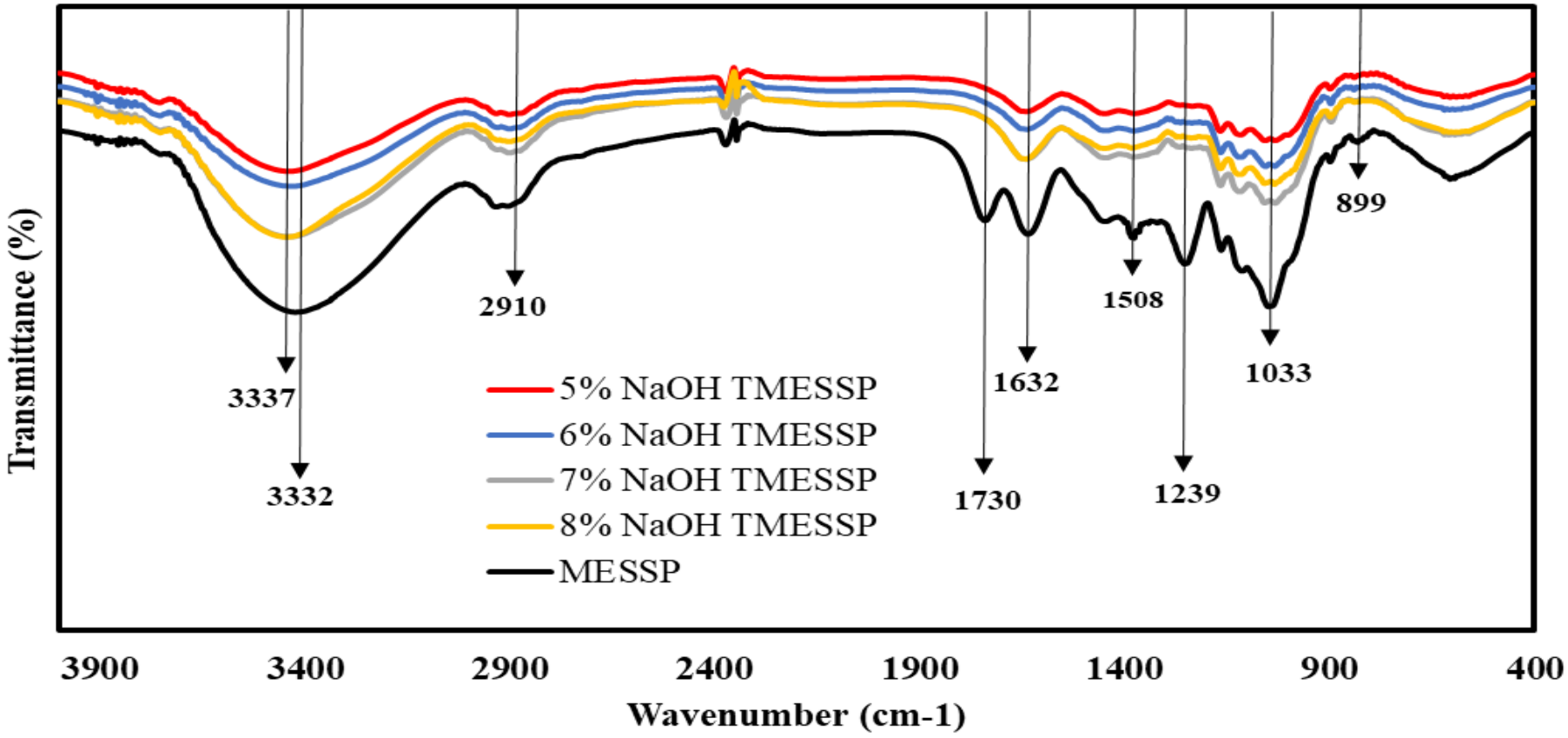

Figure 4.22: Comparison of Spectra of MESSP and TMESSP

4.3.2 Particles Size Analysis (PSA)

The size distribution of TMESSP were also analysed to study the effect of NaOH concentration on the particles size of the filler. The comparison of the particles size distribution of MESSP filler are shown in Figure 4.23. It was noticed that the MESSP and the 5 w/v % NaOH TMESSP were more homogenous with a narrower particles size distribution as compared to that of the 6 w/v % - 8 w/v % NaOH TMESSP (Pongdong et al., 2016). Moreover, the graph was shifted to the right (larger particle size) with the increasing of the NaOH concentration. This showed the TMESSP at the higher NaOH concentration (6 w/v % - 8 w/v %) would have the larger particles size as compared to the MESSP and 5 w/v % NaOH TMESSP. This could be supported with the mean particles size of the MESSP as tabulated in Table 4.7.

As mentioned before, alkaline treatment of natural fibers has bleaching effect that removes the cementing materials such as wax, oil and impurities. This results in smaller particles with higher surface area and a rougher surface of the natural fiber. Slightly higher particles size of TMESSP over the MESSP as shown in Table 4.7. The possibility is due to the swelling effect of the alkali liquor (Fareez et al., 2018; Xu et al., 2020). However, the particles sizes of MESSP and different concentrated TMESSP did not show any statistically significant different suggested that the mild alkaline treatment did not led to the obvious effect in the particles size over varying the concentration in 1 w/v % of NaOH aqueous solution (Alharbi et al., 2020). The significant effect of the alkaline treatment can be observed from FTIR, surface morphology analysis

through SEM and also the chemical composition analysis. Among the four samples of NaOH TMESSP, 5 w/v % NaOH TMESSP has the closer mean particles size to the MESPP, also the highest specific surface area observed despite the specific surface area of the TMESSP experienced a decreasing trend with the increasing NaOH concentration. Higher specific surface area of the filler would has a better filler dispersion which distributed more homogenously as compared to the bigger sizes of the filler particles (Nourbakhsh and Karegarfard, 2009).

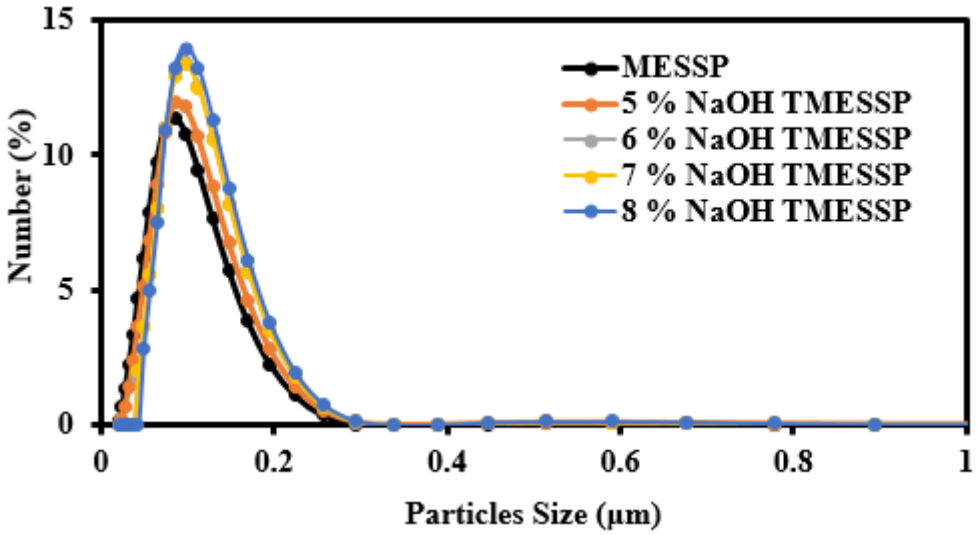

Figure 4.23: Particle Size Distribution of MESSP and TMESSP

Table 4.7: Summarises of the Properties of the MESSP in term of the Mean Particles Size and the Specific Surface Area

	Mean particles size (μm)	Specific surface area (m^2/g)
MESSP	0.0919	29.1
5 w/v % NaOH TMESSP	0.0991	26.3
6 w/v % NaOH TMESSP	0.1092	24.0
7 w/v % NaOH TMESSP	0.1089	24.8
8 w/v % NaOH TMESSP	0.1128	24.5

As reported in the literature review, the mechanical properties of composites are closely related to the filler loading and filler's size. For instance, Onuegbu and Igwe (2011) studied the effect of particle size and the filler loading on the mechanical properties of the snail shell powder filled PP composites. Better strength properties could be observed with the higher filler content as well as the smaller particles size of the snail shell powder. Along with this, the higher impact strength of the snail powder reinforced PP composite was observed with the smaller the particle size of the filler. Besides, better filler dispersion and the filler matrix interaction could be achieved with smaller particles sizes where the stress transfer could be propagated along the filler-matrix phase. In the study, a higher mechanical properties of snail powder reinforced PP composites than a talc filled PP composites was identified showed a remarkable performance of the NFPC over the synthetic fiber polymer composites (Onuegbu and Igwe, 2011).

4.3.3 Scanning Electron Micrograph and Density Test

Morphology study and textural properties of TMESSP and MESSP were analysed based on the SEM micrograph. Figures 4.24 (a) and (b) reveal the randomly oriented distribution of MESSP and TMESSP. However, the significant different was seen from the dispersion of filler. MESSP exhibits loosely bounded aggregate structure whereas TMESSP tend to be more individual particles which suggest that TMESSP can be well dispersed in PP matrix as compared to MESSP.

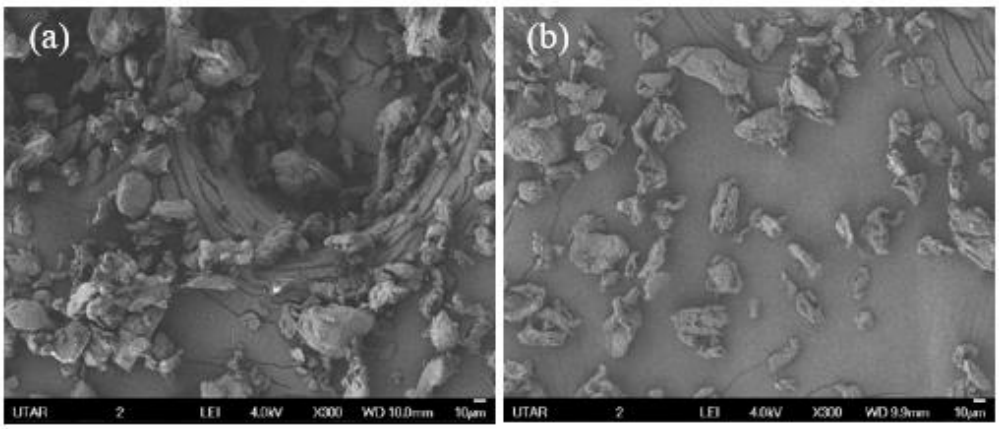

Figure 4.24: Micrographs of (a) MESSP and (b) TMESSP at 200x Magnification

The higher magnification of the SEM micrograph as present in Figures 4.25 (a) to (e) show the morphological change occurred during the filler modification. The surface appearance of MESSP was smooth as present in Figure 4.25 (a) can be accounted to the wax layer, impurities and fatty deposit. (Carvalho et al., 2010; Sudha and Thilagavathi, 2015; Torun et al., 2019). Figures 4.25 (b) to (e) illustrate the surface of TMESSP at the higher

magnification. The surface was clean and also showed a relatively rough surface with some micropores due to the dissolution of the cementing materials such as lignin, hemicellulose, wax, impurities and the hydroxyl ions from the cell wall of MESSP. In meantime, the coarser surface with pores of TMESSP provided more surface area for polymer adhesion and physical interaction. Thus, the higher amount of cellulose exposed on the MESSP surface could facilitate physical interaction via polymer chain entanglement or interlocking (Ouarhim et al., 2018; Abdullah et al., 2019). Similar observation was reported by Abdullah et al. (2019), the rough surface provides anchorage points between the fiber and matrix that promote both physical interaction and bonding reaction. According to Suradi et al. (2010), treatment of the oil palm fiber has increased the porosity and the effective surface area that could resulted in better packaging of the cellulose chain that further enhanced the crystallinity of the fibres.

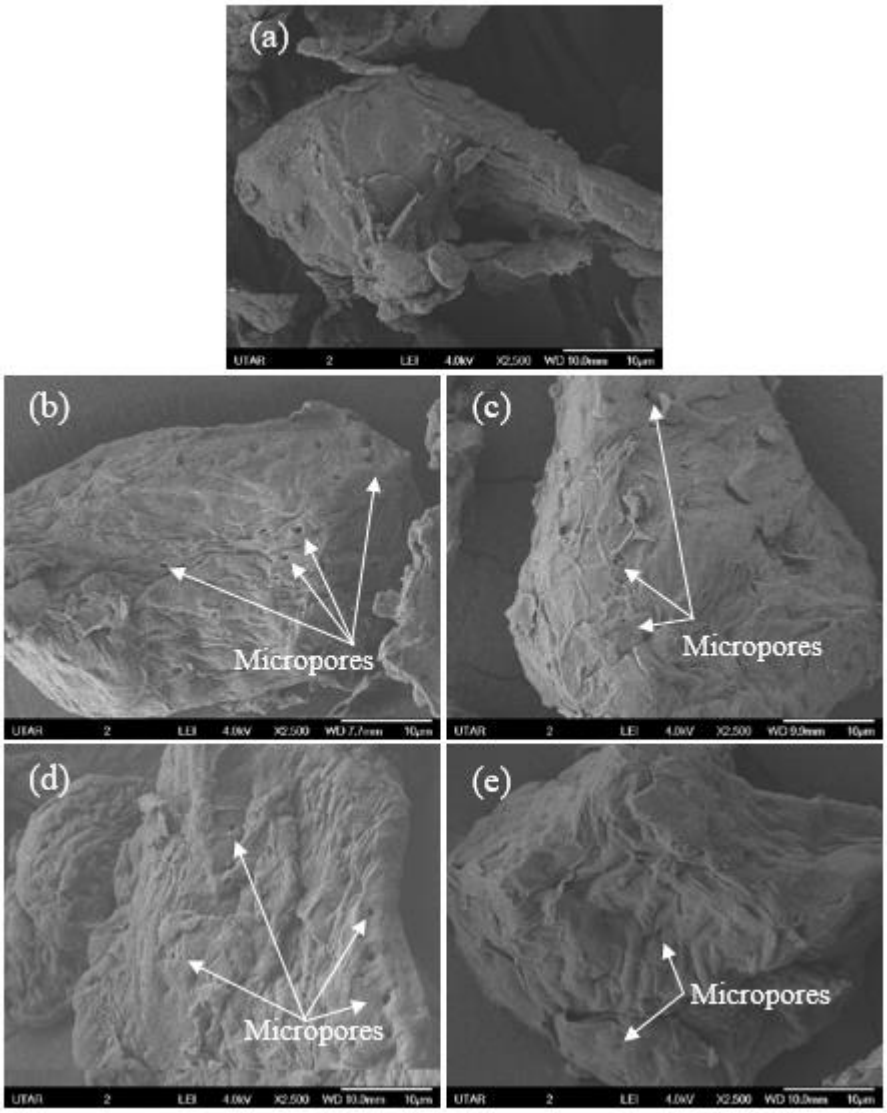

Figure 4.25: SEM Micrographs of (a) MESSP (b) 5 w/v% NaOH TMESSP (c) 6 w/v% NaOH TMESSP (d) 7 w/v% NaOH TMESSP (e) 8 w/v% NaOH TMESSP at 2 500x Magnification

The effect of NaOH treatment with different concentration on the functional, structural and morphological changes of MESSP was studied. Based on the FTIR, PSA and SEM results, 5 w/v % NaOH TMESSP was selected to proceed with the preparation of PP/TMESSP composites. This was due 5w/v % concentration of NaOH solution was the most effective to reduce the hygroscopic properties of MESSP as compared to the 6 w/v % - 8 w/v %

concentration aqueous solution. Among the TMESSP, PSA revealed that 5 w/v % NaOH TMESSP possess the smallest mean diameter and the largest specific area which the surface area available for the possible interaction with the polymer.

The density of the MESSP and TMESSP (5 w/v % NaOH TMESSP) were 0.46 g/cm^3 and 0.44 g/cm^3 respectively. It can be observed that the density of MESSP decrease slightly after the treatment. Similar result was reported by Pitchayya et al. (2020), the alkaline treated red banana peduncle fibres has the lower density than the untreated fibres. The alkali treatment has reduce the filler-filler interaction and results in increased free volume and loose packing of the filler particles in the natural filler led to the reduction in density of the filler (Ren et al., 2019). The TMESSP was observed to have some pores on the structure as shown in SEM image in Figure 4.26. The presence of the porous structure on MESSP caused to the small decrement of the density of the TMESSP (Sari et al., 2016).

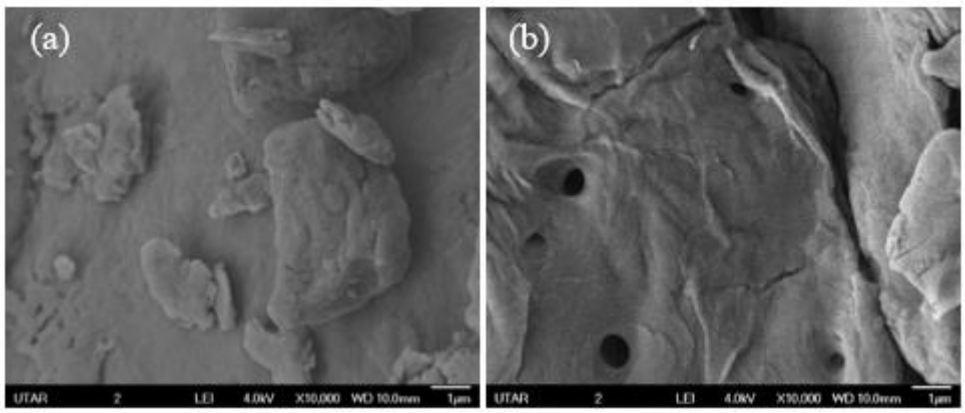

Figure 4.26: SEM Micrograph of (a) MESSP (b) 5 w/v% NaOH TMESSP at 10 000x Magnification

4.3.4 Chemical Composition Analysis

The chemical composition analysis was carried out to measure the content of cellulose, hemicellulose, lignin and the extractives contents of MESSP and 5 w/v % NaOH TMESSP. Based on Table 4.8, the results show the MESSP has 36.96 wt. % cellulose, 30.37 wt. % lignin, 24.69 wt. % hemicellulose and 7.98 wt. % extractives. Meanwhile, 5 w/v % NaOH TMESSP consisted of 54.43 wt. % of cellulose, 26.63 wt. % lignin, 18.93 wt. % of hemicellulose with no extractives found. Fat, fatty acid, steroid, waxes and other organic compound are mostly found in the extractive from plant (Mansor et al., 2019).

The comparison of the chemical composition of MESSP with other natural fiber was tabulated in Table. 4.9. TMESSP showed higher cellulose content as compared to 65% of the natural filler reported in the table. It was stated by Manimaran et al., (2019) that the presence of wax in the natural filler is the key reason for poor interfacial bonding due to the restriction of interaction between the filler and matrix. It was also noticed that the NaOH TMESSP become an extractive free biomass with a higher weight percentage of cellulose. Amount of cellulose content available is the crucial factor that could affect the mechanical properties of the NFPC.

As reported by Venkateshwaran and Elayaperumal (2010), composites incorporated with the alkali treated fiber usually has the better mechanical properties due to more cellulose exposed for the chain interlocking with the

polymer matrix. NaOH treatment of the natural fiber has a better water absorption resistance as compared to the untreated fiber (Thiruchitrambalam and Shanmugam, 2012). In short, NaOH treatment was proved to be effective on partially removing the non-cellulosic compound including the extractives, hemicellulose and lignin from MESSP.

Table 4.8: Chemical Composition of MESSP

	MESSP (wt. %)	TMESSP (wt. %)
Cellulose	36.96 ± 0.14	54.43 ± 0.06
Lignin	30.37 ± 0.08	26.63 ± 0.15
Hemicellulose	24.69 ± 0.16	18.93 ± 0.24
Extractives	7.98 ± 0.03	0.01 ± 0.00

Table 4.9: Comparison of Chemical Composition of MESSP with other Natural Fiber

Natural Fiber	Cellulose (%)	Hemicellulose (%)	Lignin (%)	Extractives (%)	Reference
MESSP	36.96	24.69	30.37	7.98	Current work
TMESSP	54.43	18.93	26.63	0.01	Current work
Untreated areca palm leaf stalk fibers	57.49	18.34	7.26	-	Shanmugasundaram et al.
Alkali treated areca palm fibers	68.54	6.13	5.87	-	(2018)
Almond shell	50.7	28.9	20.4	2.5	
Walnut shell	25.6	22.1	52.3	2.8	Demirbas, (2006)
Hazelnut shell	26.8	30.4	42.9	3.3	
Sunflower shell	48.4	34.6	17	2.7	
Pineapple leaf	66.2	19.5	4.28	-	
Corn stalk	39.0	42	7.3	-	Daud et al. (2014)
Napler Grass	12.4	68.2	10.8	-	

Table 4.9 continued

Natural Fiber	Cellulose (%)	Hemicellulose (%)	Lignin (%)	Extractives (%)	Reference
Eucalyptus wood powder	41	31	29	-	Zhang et al. (2011)
Empty fruit bunch	26	43	24	7	Yang et al. (2006)
Palm kernel shell	22	26	46	6	

4.3.5 Thermogravimetric Analysis (TGA)

Figure 4.27 shows the comparative weight loss for TMESSP and MESSP. Similar trend can be observed for the thermal decomposition of both MESSP and TMESSP. In the first decomposition step that corresponding to the evaporation of moisture, MESSP has a slightly higher degradation as compared to TMESSP. This was due to reduction in OH groups with NaOH treatment thus the particles tend to absorb less moisture and the reduction in first stage which was due to moisture absorbed was lesser.

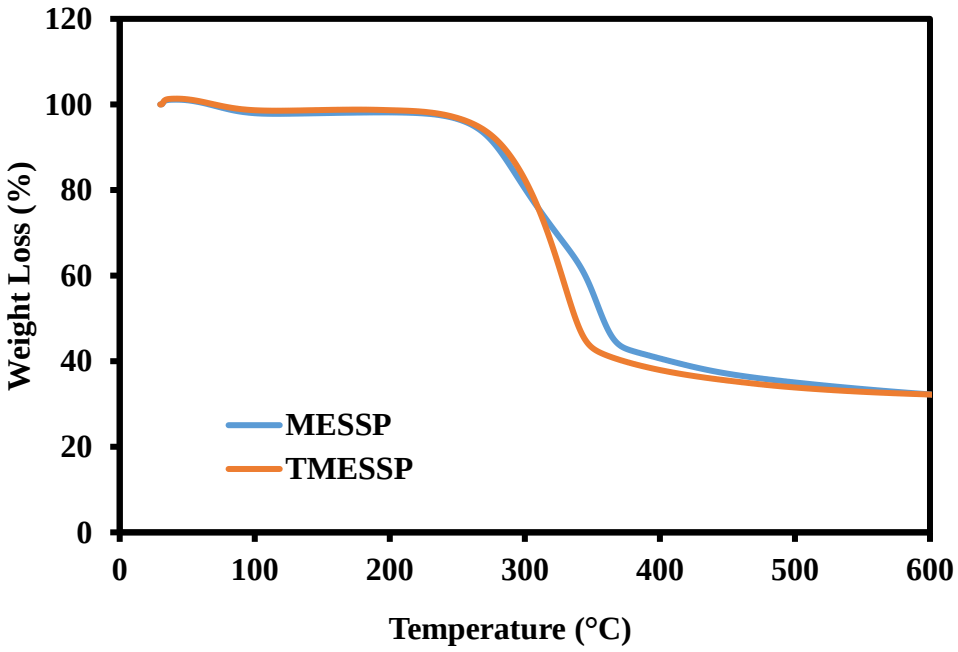

Figure 4.27: Comparative TGA Curves for MESSP and TMESSP

As mentioned earlier, large amount of weight loss taken place in the second stage of the decomposition which was associated to the decomposition of cellulose, hemicellulose and lignin. This particular stage involves the two

range of decomposition; first was the decomposition of hemicellulose and cellulose around of 230 – 360 °C where second stage was the decomposition of lignin from 360–440 °C (Elkhaoulani et al., 2013). As reported by Monteiro et al. (2012), maximum decomposition of hemicellulose was found at 290 °C. Figure 4.28 suggests the removal of the thermally unstable hemicellulose from the MESSP has improve the thermal stability of TMESSP up to 300 °C. Moreover, the disappearance of the second main peaks of around 250-320 °C as observed in the MESSP (Figure 4.28) indicated the effective elimination of the non-cellulosic constituents from the MESSP upon the NaOH treatment (Hou et al., 2014). However, it can be observed that the TMESSP was less thermally stable than the MESSP at higher temperature. This phenomena was due to the removal of the lignin that was more thermally stable causing the TMESSP to be less thermally stable as compared to MESSP at higher temperature (around 320 °C) (Ouarhim et al., 2018).

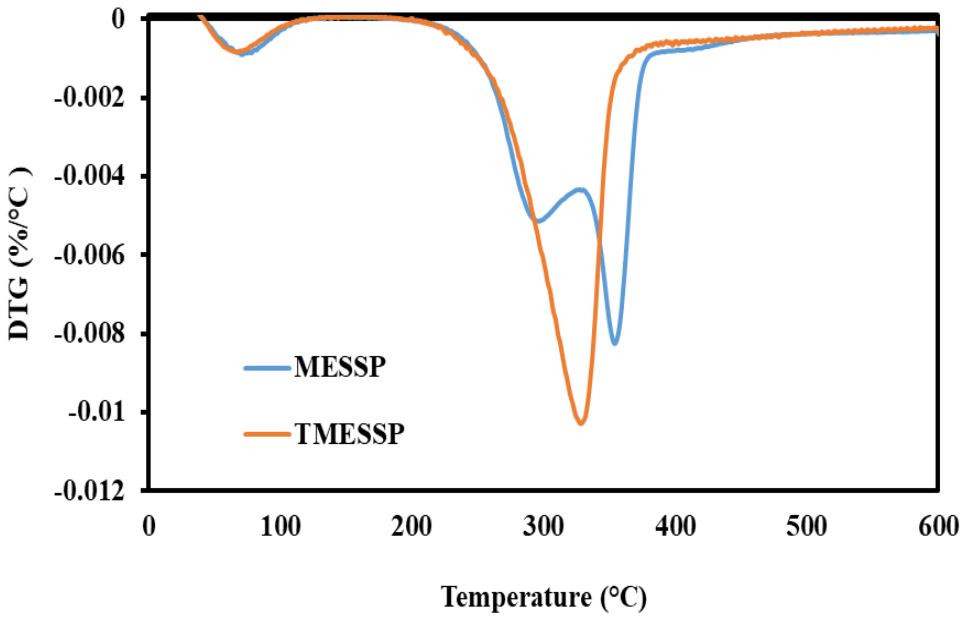

Figure 4.28: Comparative DTG Curves for MESSP and TMESSP

4.4 Characterisation and Testing of PP/TMESSP Composites

4.4.1 Attenuated- Fourier Transform Infrared (ATR-FTIR) Analysis

ATR-FTIR analysis was conducted to compare the chemical functional group present between the PP/MESSP and PP/TMESSP composites. Based on Figure 4.29, it was observed that there was no significant different between the ATR-FTIR spectra of the PP/MESSP and PP/TMESSP composites. However, the most noticeable different was the peaks at 3332 cm^{-1} that corresponded to the hydroxyl group was less intense and almost diminished in the PP/TMESSP composites upon the surface modification of composites.

Moreover, the reduction of the intensity at the peak 1623 cm^{-1} that was attributed to the moisture absorption by the O-H stretching in cellulose was reduced greatly in the PP/TMESSP composites. This suggests that the effect of the NaOH treatment of MESSP was clearly noticeable to reduce the inherent hydrophilicity properties of the MESSP that corresponded to the disappearance of the hydroxyl group.

According to Nurazzi et al. (2019), alkali treated sugar palm fiber was more compatible to the polymer matrix due to the reduction of hydrophilic properties of the fiber which resulted in the better interfacial bonding between filler and polymer matrix. Thus, this suggested that the the surface modification of MESSP has the potential to facilitate the compatibility and enhance the interfacial adhesion between the TMESSP and PP matrix phases.

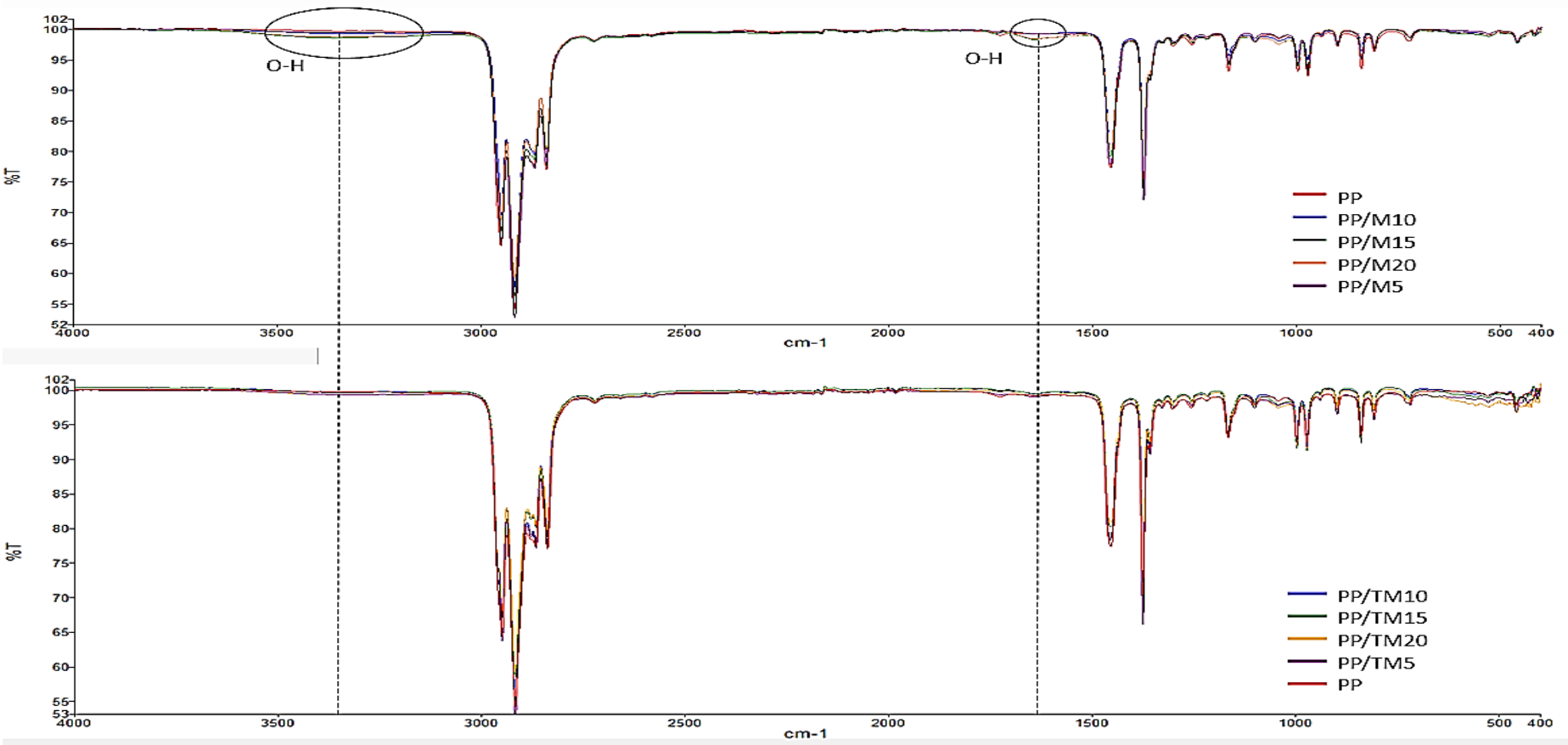

Figure 4.29: Comparison in ATR-FTIR Spectra of the PP/MESSP and PP/TMESSP Composite

4.4.2 Processing-ability

Figure 4.30 presents the processing torque as the function of time for the PP/TMESSP composites with different TMESSP loading. As mention earlier, the torque increase rapidly until the highest torque value which known as loading torque was the shear force created during the mixing before PP was melted. Reducing of the viscosity of PP was represent by the gradually decrease of torque until the stabilisation torque was observed that indicated the homogenised of the mixture. Similar trend was observed between the PP/MESSP and PP/TMESSP composites.

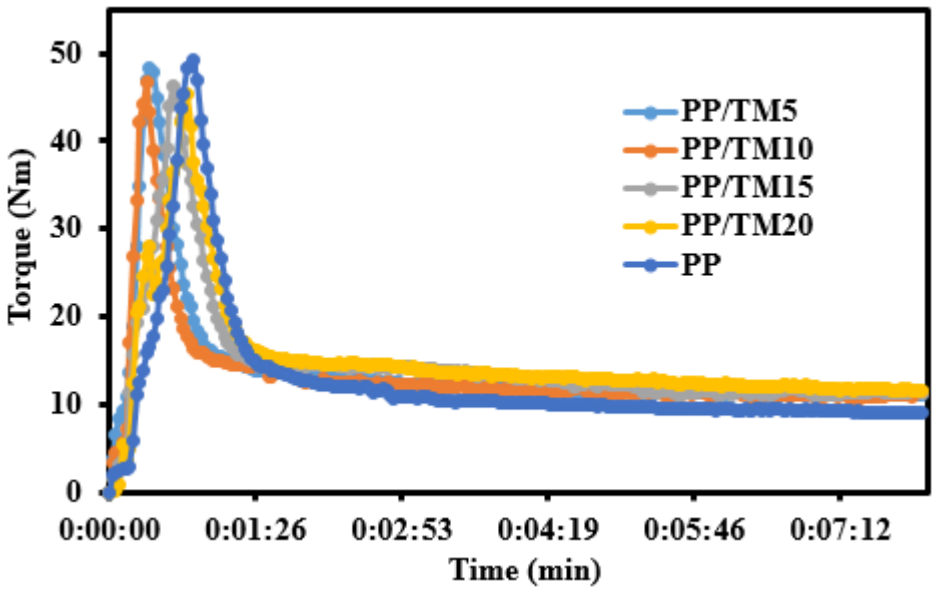

Figure 4.30: Processing Torque of the PP/TMESSP Composites

Table 4.10 summarises the processing torque obtained through the mixing process for both PP/TMESSP and PP/MESSP composites with different filler loading. At the same loading of the MESSP, it was discovered that that loading torque of the PP/TMESSP composites was lower as compared

PP/MESSP composites. The effect of mercerisation removed the hemicellulose and lignin that cementing the surface of MESSP has reduced the viscosity that was accountable for the processing of the composites. Thus, the lower processing torque observed for the PP/TMESSP composites indicate that the incorporation of TMESSP created lower viscosity than MESSP (Zaaba et al., 2016; Daud et al., 2017).

As reported by Sareena et al. (2012), specific surface area was the other factor that can affect the viscosity of the composites. In the study, peanut seed shell with the lower specific surface area imparted lower viscosity during the processing. According to the PSA result tabulated in Table 4.7, TMESSP possess a lower specific surface area as compared to MESSP. This could be the reason that leads to slightly lower torque recorded in the PP/TMESSP composites.

Furthermore, as can be seen from the Table 4.10, stabilization torque was gradually increased for both PP/MESSP and PP/TMESSP composites. However, when comparing at similar filler loading, PP/TMESSP composite shows a slightly higher stabilisation torque as compared to PP/MESSP composites at all loading. This phenomena can be explained by the increase of the viscosity caused by the good filler matrix interaction resulted in the restriction of the PP chain's flow-ability. NaOH treatment enhanced the interfacial adhesion between the PP matrix and TMESSP lead to the increase of the viscosity of the molten mixture during the mixing (Demir et al., 2006; Zaaba et al., 2016; Daud et al., 2017). Similar resulted was reported in the previous

study conducted by Santiagoo et al. (2011) involving the rice husk powder filled PP/acrylonitrile butadiene rubber with silane coupling agent where higher stabilization toque obtained due to the good bonding between the rice husk and the matrix system upon treatment.

Table 4.10: Comparison of Processing Torque of PP/MESSP and PP/TMESSP Composites

Composites	Processing Torque			
	Loading Torque (N)		Stabilization Torque (N)	
Filler loading (wt. %)	PP/MESSP	PP/TMESSP	PP/MESSP	PP/TMESSP
0	49.20		9.00	
5	49.21	48.30	10.77	11.10
10	49.61	46.75	10.79	11.23
15	47.02	46.23	11.00	11.37
20	46.07	45.37	11.80	11.63

4.4.3 Differential Scanning Calorimetric

Table 4.11 presents the thermal characteristic of PP/MESSP and PP/TMESSP composites. As discussed earlier, the crystallization temperature (T_c) and the degree of crystallinity (X_c^m) were increased with the addition of MESSP in PP matrix revealing that ability of MESSP to act as the nucleating agent and improve the crystallization of PP matrix (Marques et al., 2014). The

crystallinity of neat PP was 34.6 %, and the crystallinity of PP/MESSP composites were ranging from 34.93 - 36.21 %, which is higher than the neat PP at all loading.

Table 4.11: DSC Results for both PP/TMESSP and PP/MESSP Composites

Composite Code	W_p	T_m (°C)	T_c (°C)	ΔH_m (J/g)	X_c^m (PP phase)
PP	1.00	164.41	125.24	71.62	34.60
PP/ M5	0.95	162.58	125.90	69.65	35.42
PP/ M10	0.90	163.73	126.06	67.45	36.21
PP/ M15	0.85	165.03	126.01	63.31	35.98
PP/ M20	0.80	165.38	125.95	57.84	34.93
PP/TM5	0.95	162.71	126.44	74.20	37.73
PP/ TM10	0.90	163.24	125.99	79.77	42.82
PP/ TM15	0.85	164.38	126.29	81.06	46.07
PP/ TM20	0.80	162.34	126.43	68.30	41.24

Figure 4.31 shows the comparative degree of crystallinity of the neat PP, PP/MESSP and PP/TMESSP composites. The crystallinity of the PP/TMESSP composites were higher that the neat PP and PP/MESSP, which ranges from 37.73 - 46.07 %. PP/TMESSP composites show better improvement on the crystallinity of the composites and the optimal was achieved at 15 wt. % loading of TMESSP. Both the observation indicated that the incorporation of MESSP and TMESSP as bio-filler facilitated the crystallization process of PP through the formation of new crystals, by which TMESSP triggers more crystalline

formation in PP as compared to MESSP (Ying et al., 2013; Marques et al., 2014). Research study conducted by Ye et al. (2015) explained that the improved crystallinity was due to the increase surface roughness of the natural filler upon the NaOH treatment. Moreover, Wang and Liu (1999) supported this by claiming that the surface topography of fillers was the main factor that inducing the nucleation of crystalline structure.

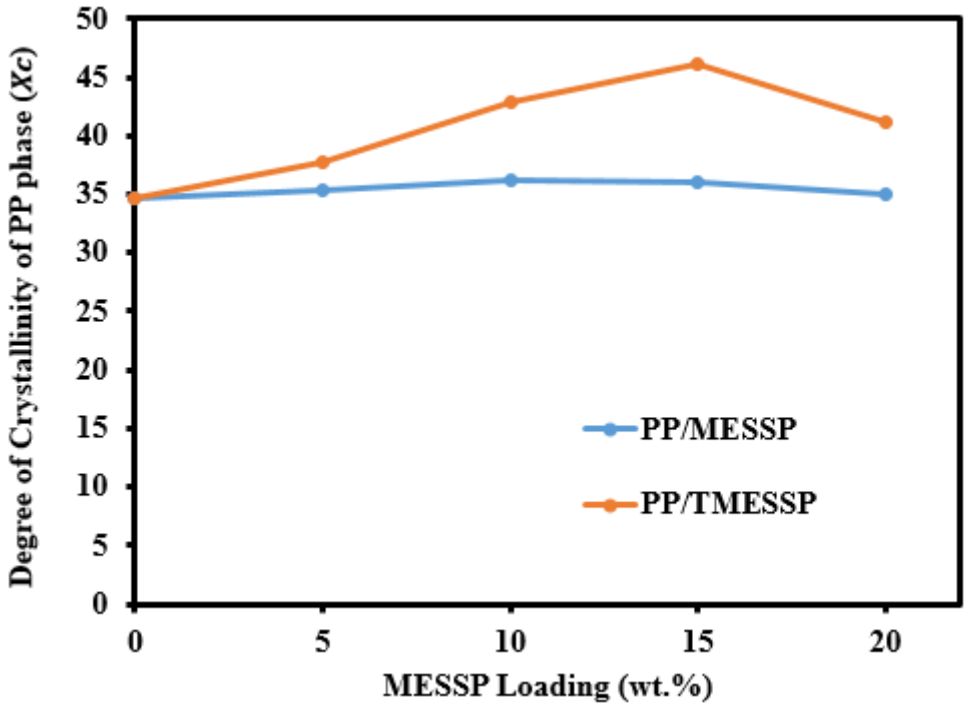

Figure 4.31: Comparison between the Degree of Crystallinity of PP/MESSP and PP/TMESSP Composites

4.4.4 Thermogravimetric Analysis

Thermal behaviour of the PP/MESSP and PP/TMESSP composites were summarised in Table 4.12.

Table 4.12: Thermogravimetric Analysis Data of PP/MESSP and PP/TMESSP Composites

Code of specimen	Weight percent at 180 °C (%)	T_{onset} 10% (°C)	T_{max} (°C)	Residue @ 600°C (wt. %)
PP	100.00	438.64	465.33	0.34
PP/ M5	99.60	436.68	468.33	1.26
PP/ M10	98.90	409.59	466.33	2.34
PP/ M15	98.50	370.18	468.33	3.83
PP/ M20	98.40	356.71	470.00	5.73
PP/TM5	100.00	416.50	453.00	5.23
PP/TM10	100.00	424.67	458.17	6.87
PP/TM15	100.00	416.33	458.33	8.01
PP/TM20	100.00	391.17	457.83	9.06

Based on Table 4.12, it can be noticed that there was no decomposition weight loss of PP/TMESSP composites at the processing temperature 180°C and this implies that PP/TMESSP were more thermally stable than PP/MESSP composites at the processing temperature. Moreover, the higher loading of PP/TMESSP composites shows a higher onset decomposition temperature than PP/MESSP composites. For instance, the weight loss at 150 °C for the PP/M15 composites has shifted to 310 °C for the PP/TM15 composites as shown in Figure 4.32.

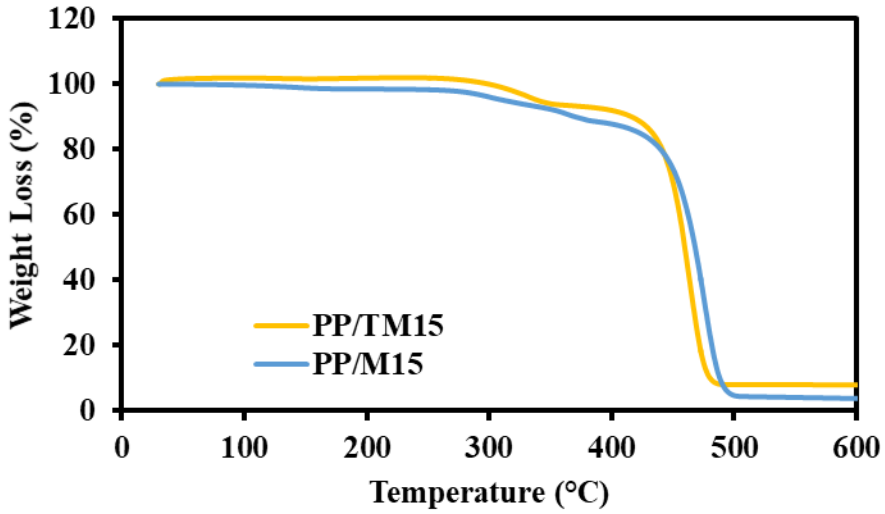

Figure 4.32: Thermal Degradation Weight Loss of PP/TM15 and PP/M5 Composites

Thus, it is clear that the addition of the TMESSP enhanced the thermal stability of the composite where the prolonged decomposition of the PP/TMESSP composites was mainly due to the elimination of the thermally less stable constituent from the MESSP and the less hydrophilicity of the TMESSP **(**Dash et al., 2000; Rashid et al., 2016). In addition, the increased of the onset decomposition temperature of the PP/TMESSP composites as compared to PP/MESSP composites suggested the closely packed cellulose chain of the TMESSP together with the PP matrix polymer has the better thermal stability up to a certain temperature (Sinha and Rout, 2009).

Generally, the PP/MESSP composites have a slightly higher thermal decomposition than the neat PP. The neat PP decomposition temperature was recorded at 465 °C by which the maximum decomposition temperature (T_{max}) has shifted to a higher temperature with the addition of MESSP. This was due

to the addition of MESSP formed the barrier to the PP polymer's exhausted gas released during the thermal process (Elkhaoulani et al., 2013; Essabir et al., 2016). However, T_{max} has shifted to a lower temperature in PP/TMESSP composites. This phenomena was due to the partially removal of the lignin from the alkaline treatment that was more thermally stable as compared to the other constituents. Thus, this resulted in PP/TMESSP composites experienced a greater weight loss and to be less thermally stable as compared to PP/MESSP composites (Ouarhim et al., 2018). This observation was in line with other studies reporting the thermal stability of the composites were decreased with the reinforcement of the treated natural filler (Ray et al., 2004; Ouarhim et al., 2018). This could be explained with the considerable effects on the MESSP upon the NaOH treatment that have improved the interaction between the filler and matrix. For instance, the reduction in the hydrophilicity of the filler, removal of the wax and impurities from the surface and the increase of the filler's crystallinity (Ray et al., 2004; Monteiro et al., 2012).

On the other hand, char yields or the residue of PP/TMESSP composites were found to be higher than the neat PP and PP/MESSP composites. This suggested that the incorporation of TMESSP into PP has enhanced the thermal stability of the composites at high temperature by preventing further decomposition of the composites (Mohanty et al., 2006; Monteiro et al., 2012).

4.4.5 Water Absorption

Figure 4.33 represents the comparative water uptake and thickness swelling of both PP/MESSP and PP/TMESSP composites as the function of filler loading.

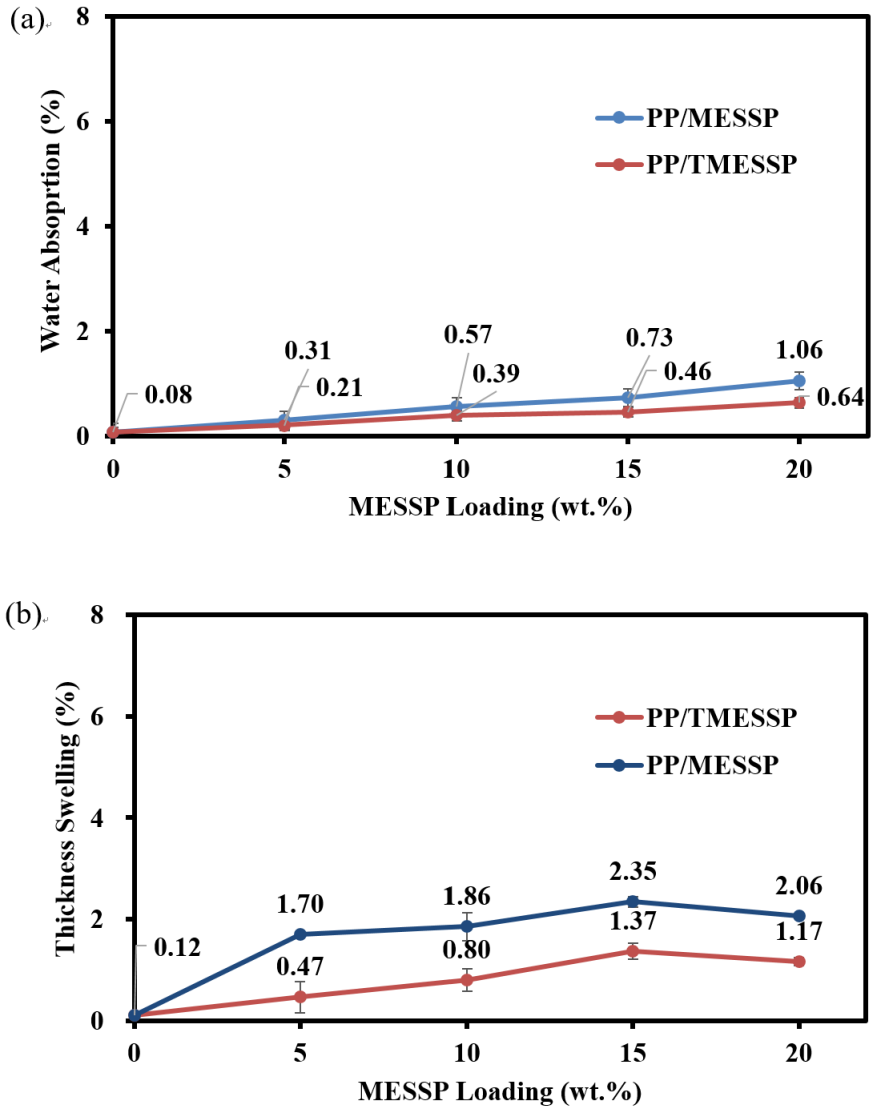

Figure 4.33: (a) Water Absorption and (b) Thickness Swelling of the PP/MESSP and PP/TMESSP Composites

Same trends were observed for PP/TMESSP and PP/MESSP composites where the addition of the filler had significantly affects the water absorption behaviour. More water uptake was observed at the higher MESSP loading. Similar observation was reported by Razavi et al. (2006), more water absorbed at the higher content of rice husk filled PP composites. This was caused by more hydroxyl group available with the higher filler loading that in contact with water through hydrogen bonding, which lead to the more water uptake. However, incorporation of TMESSP in PP polymer showed the reduction in water absorption as compared to PP/MESSP composites was due to the reduced of hydroxyl groups of MESSP and thus lower the tendency to be in contact with water. At similar filler loading, it was obvious that the treatment of MESSP with NaOH reduced the water absorption and thickness swelling of the composites. Clear indication could be made where the alkaline treatment with NaOH has enhanced the physical interaction between MESSP and PP, thus reducing the amount of water absorbed by the composites (Santiagoo et al., 2011).

Wechsler et al. (2019) reported similar findings whereby higher water absorption was observed in the higher content of peach pits reinforced in the PP composites. The reduction of the hydroxyl group in the cellulose of the TMESSP further reduced the hydrogen bonding formed with water was another justification to the decreased water uptake capacity of the PP/TMESSP composites. Better adhesion between filler and matrix has restricted the penetration and uptake of water through the voids (Demir et al., 2006).

4.4.6 Tensile Properties

The comparative study of the mechanical properties such as tensile and impact properties of PP composites was conducted upon surface treatment of MESSP using NaOH. Composites produced with MESSP affected negatively with increased filler loading. NaOH treatment of MESSP shows the positive effect on the tensile behaviour of the PP/TMESSP composites as compared to PP/MESSP composites. It was evidenced that the composites incorporated with the TMESSP has an improved tensile properties as can be seen from Figure 4.34.

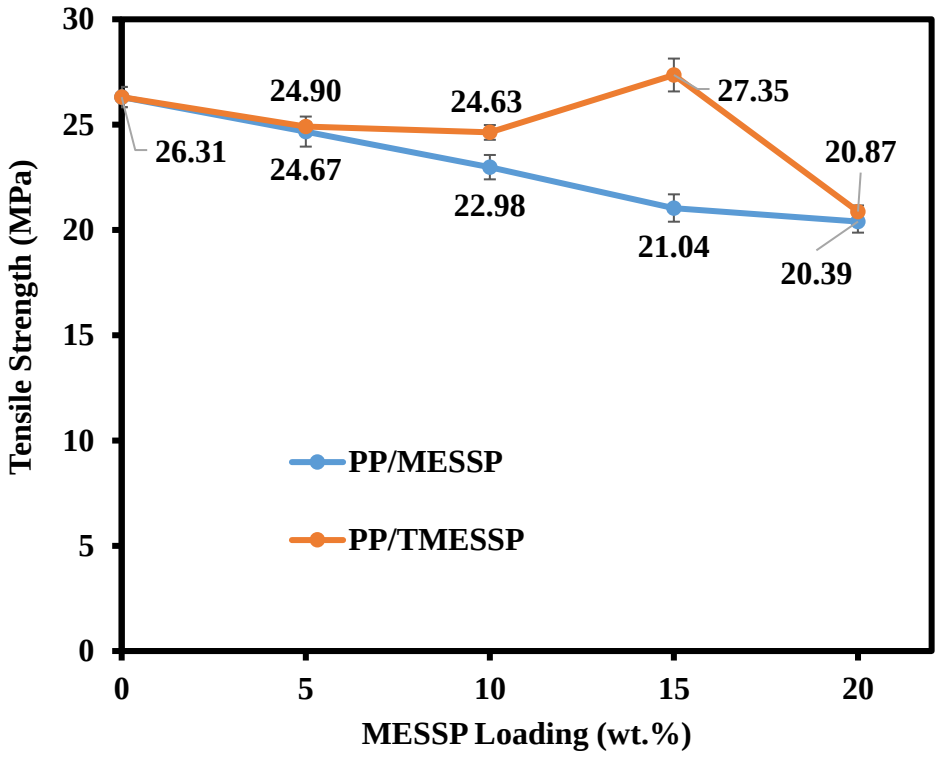

Figure 4.34: Comparison of Tensile Strength of PP/MESSP and PP/TMESSP Composites

The improvement of the tensile properties was more significant in the PP/TM15 composites. The maximum improvement of the tensile strength obtained from the PP/TM15 composites relative to the PP/M15 composites was 30 %. It was worth pointing out that the surface modification of MESSP eliminated those cementing materials that covered the surface of the filler had increased the surface roughness and exposed surface area of the MESSP for the possible physical interaction with PP matrix (Borsoi et al., 2019). As discussed earlier, the surface morphology of the TMESSP was rougher and clean upon the NaOH treatment. These properties contribute to the improved compatibility with the PP matrix where enhanced the matrix-filler interfacial adhesion resulted in a higher tensile strength of PP/TMESSP composites. According to Rajesh et al. (2015), better wettability of the alkali treated fiber in the matrix polymer was achieved leading to the higher interfacial bonding in the fiber–matrix phase. Higher tensile properties of the treated fiber reinforced composite were observed due to the better load sharing capacity.

As discussed in ATR-FTIR analysis, the hydrophilicity properties of the PP/TMESSP composites were reduced drastically as compared to PP/MESSP composites. Better compatibility and interaction between PP and TMESSP can be further verified and discussed in the SEM micrograph of the PP/TMESSP composites. This finding was consistent with the observation reported by Cai et al. (2016). 5 w/v % NaOH treated abaca fiber reinforced polymer composites gave a highest enhancement in the tensile strength due to the improved mechanical adhesion in the fiber-matrix system as compared to other concentration treated fiber. However, it was noticed that the tensile strength of

the PP/TMESSP composites deteriorates beyond the 15 wt. % TMESSP loading. At the higher loading of TMESSP, TMESSP were prone to aggregation. This phenomena was in agreement with the studies reported by Chattopadhya et al. (2009). Decrement of tensile strength of the composites at higher PALF compounding was corresponded to the weak dispersion of the fiber in the PP matrix.

Figure 4.35 presents the tensile modulus of the composites. On average, it was found that the PP/TMESSP composites have a higher tensile modulus than PP/MESSP. It was more noticeable with PP/TM15 composites where the maximum improvement exhibited was 5.3% higher than the PP/M15 composites. Improved tensile modulus attributed to the good interaction between the filler and matrix phase that facilitated the stress transfer between the two phases. Higher tensile modulus was expected when there was efficient load sharing among the interface (Asumani et al., 2012; Nopparut and Amornsakchai, 2016).

Meanwhile, from Figure 4.36, PP/TMESSP composites shows the similar trend on the elongation at break as that of the PP/MESSP composites. Elongation at break of the composites was mainly affected by the filler loading. Addition of the TMESSP reduced the elongation at break of PP/TMESSP composites. Both PP/MESSP and PP/TMESSP composites have the lower elongation at beak as compared to neat PP matrix. This was due to the structural integrity of PP being destroyed by the higher brittleness and rigidity of the MESSP (Nam et al., 2011; Torun et al., 2019).

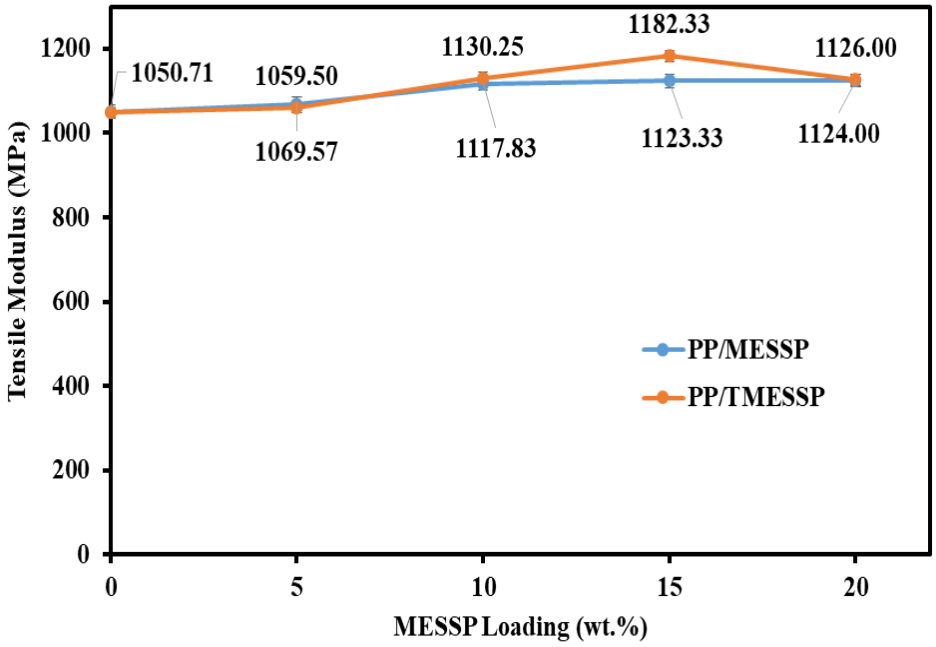

Figure 4.35: Comparative of Tensile Modulus of PP/MESSP and PP/TMESSP Composites

However, it was found that the elongation at break of the PP/TMESSP composites were higher than the PP/MESSP composites and comparable to neat PP up to 15 wt. % TMESSP loading. This could be explained with enhanced interfacial adhesion present in the PP/TMESSP composite (Mylsamy and Rajendran, 2011). The ductile nature of the PP matrix was decreased slightly with the addition of TMESSP as compared to MESSP. The elongation at break of the PP/M5 and PP/TM5 composites were reduced approximately from 34.4 % to 8.3 % respectively relative to the neat PP. The elongation at break of PP/TMESSP composites were decrease inconsiderably up to 15 wt. % TMESSP loading. This was attributed to the fracture of PP polymer occurred prior to the failure of the MESSP (Nam et al., 2011).

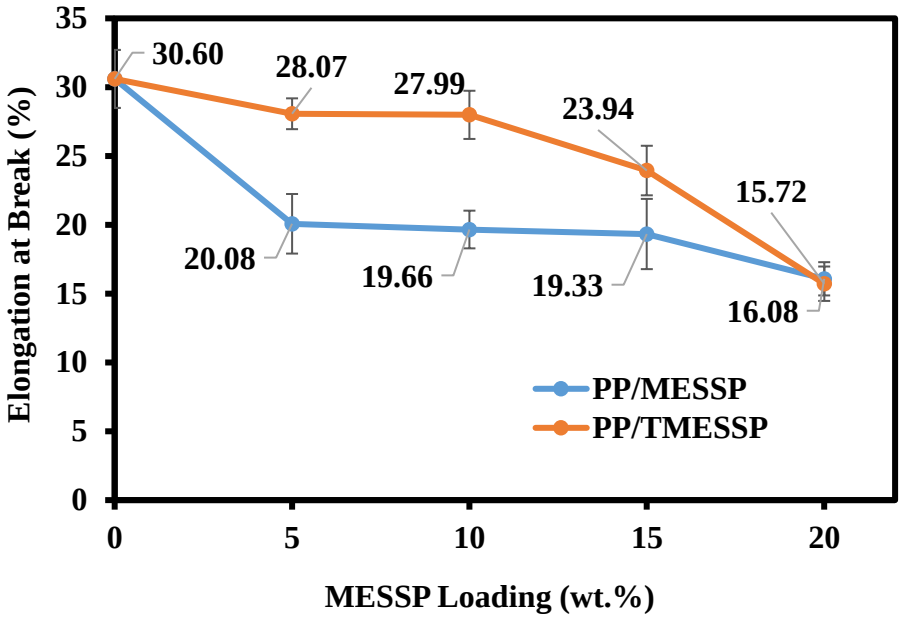

Figure 4.36: Comparative of Elongation of break of PP/MESSP and PP/TMESSP Composites

Table 4.13: Tensile Properties of PP/MESSP and PP/TMESSP Composites

Filler loading	Tensile Modulus (MPa)		Tensile strength (MPa)		Elongation at Break %	
(wt. %)	PP/MESSP	PP/TMESSP	PP/MESSP	PP/TMESSP	PP/MESSP	PP/TMESSP
0	1050.71±12.08		26.31±0.48		30.60±2.11	
5	1069.57±11.54	1059.50±16.59	24.67±0.71	24.90±0.20	20.08±2.17	28.07±1.12
10	1117.83±14.35	1130.25±15.18	22.98±0.58	24.63±0.35	19.66±1.37	27.99±1.75
15	1123.33±13.72	1182.33±18.04	21.04±0.65	27.35±0.78	19.33±2.55	23.94±1.80
20	1124.00±13.08	1126.00±29.91	20.39±0.53	20.87±0.29	16.08±1.21	15.72±1.25

4.4.7 Impact Properties

The effect of NaOH treatment of MESSP on the impact strength of PP composites was shown in Figure 4.37. Based on the literature review, decrement of the impact strength was reported with the increasing of the natural filler content due to the poor interfacial bonding of the filler and matrix interface (Bengtsson et al., 2007; Kaewkuk et al., 2013). However, from this research study, it was found that the PP/MESSP composites possess higher impact strength at the higher loading of MESSP due to more energy absorbed for the detachment of the natural filler from the polymer matrix.

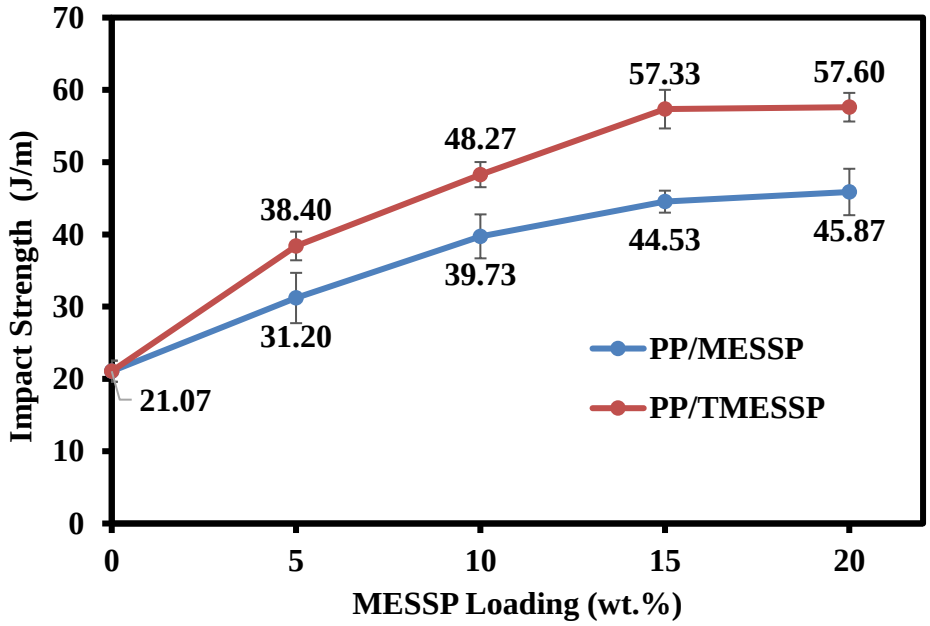

Figure 4.37: Impact Properties of the PP/MESSP and PP/TMESSP Composites

In the case of the PP/TMESSP composites, similar trend was observed. At similar filler loading, higher degree of impact strength values were obtained for the PP/TMESSP composites as compared to PP/MESSP composites. PP/TM15 composites absorbed about 28.7% more energy than the PP/M15 composites. The explanation for these situations was attributed to the removal of the lignin constituent from the MESSP upon the surface modification which was more rigid and brittle.

TMESSP that incorporated in the PP composites has a better energy absorption capability due to the enhanced mechanical bonding and bridging in the interface. Better toughness properties could be obtained when the composites were able to pass the energy through the inter-molecules where this made the composites tougher (Suradi et al., 2010). A similar result was reported by Komal et al. (2018) regarding the improvement of impact strength of the alkali treated banana fiber reinforced PP composites. According to Paul (2015), it was expected that the biocomposites to have a higher impact strength than the pure resin because the natural fibre was act as the absorbent for energy absorption. This showed the biocomposites have the higher ability to dissipate the energy through the crack propagation than the pure polymer resin.

4.4.8 Scanning Electron Micrograph (SEM)

SEM micrographs were taken to observe the fracture zone of PP/MESSP and PP/TMESSP composites. Figure 4.38 depicts the comparison of the tensile fractures of the composites. MESSP were tend to pull out and appeared on the surface of the PP polymer matrix. This failure mode was clearly shown in Figure 4.38 (a, c, e) with 5, 10, and 15 wt. % MESSP loading respectively. Also, voids and gaps were appeared between the MESSP and PP matrix when tensile stress applied. Poor interfacial adhesion between the MESSP and PP matrix was confirmed by the presence of void and gap which represented the filler debonding.

In the contrary, the enhancement of the interfacial adhesion was observed in PP/TMESSP composites. As the comparison with the PP/MESSP composites (Figure 4.38 (a)), TMESSP tend to remain intact in the PP matrix as shown in Figure 4.38 (b). This suggested a clear indication of the good interfacial adhesion of the filler in the matrix phase via mechanical interlocking mechanism. Good chain interlocking of PP polymer with the TMESSP as illustrated in Figure 4.38 (d) also suggested the effective load transfer between the fiber-matrix interfaces as evidenced from the tensile properties analysis (Kaewkuk et al., 2013). This behaviour was in agreement with the results reported previously (Komal et al., 2018).

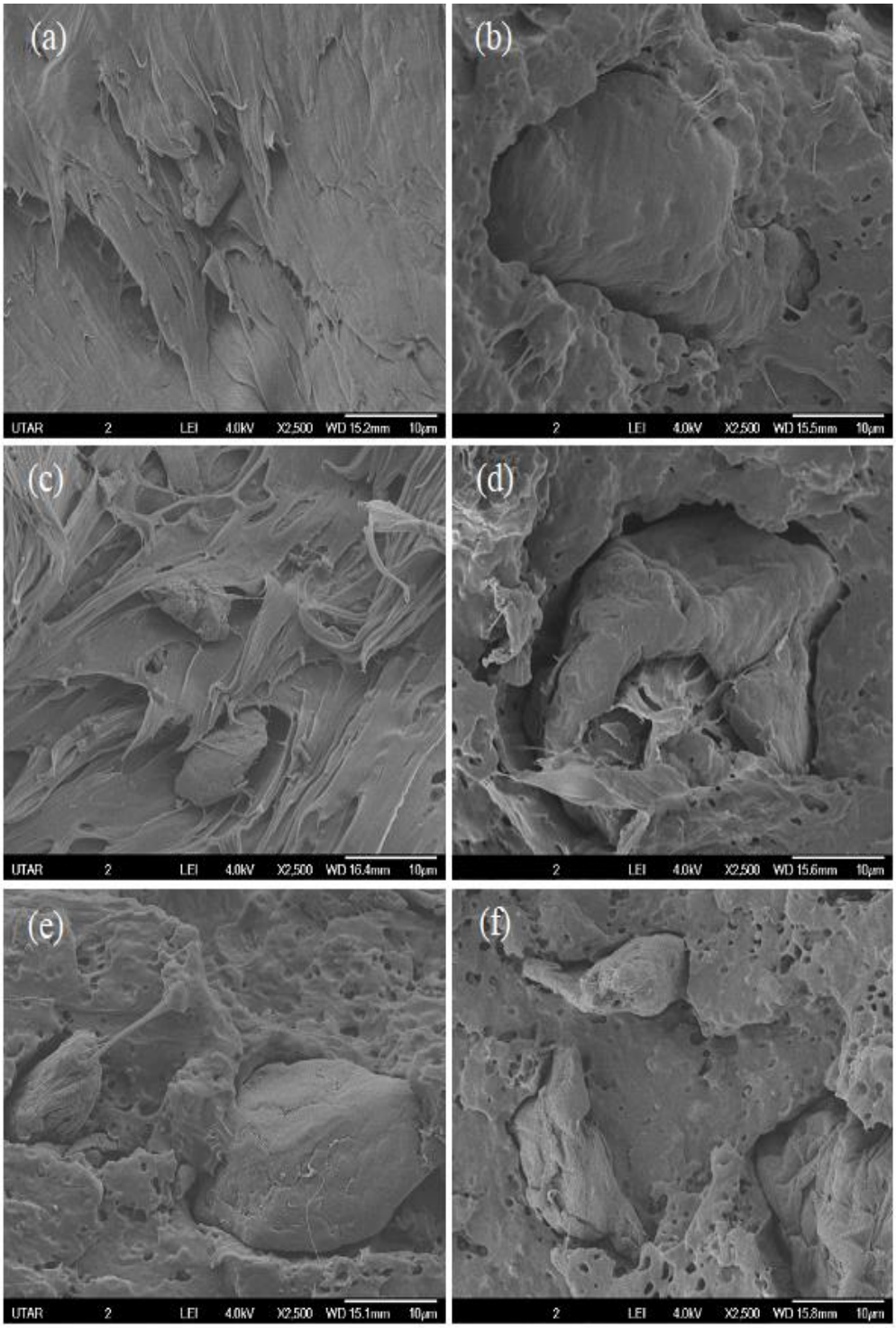

Figure 4.38: Comparative of SEM Tensile Fracture of (a) PP/M5 (b) PP/TM5 (c) PP/M10 (d) PP/TM10 (e) PP/M15 (f) PP/TM15 Composites

CHAPTER 5

CONCLUSIONS AND RECOMMENDATIONS

5.1 Conclusions

The feasibility and optimum saturation loading of MESSP in PP matrix was 20 wt. % at which immiscibility of PP and MESSP occurred beyond the saturation point. FTIR and XRF analysis revealed that MESSP was partially compatible to PP matrix due to the presence of both hydrophobic and hydrophilic elements. MESSP shows high potential to be homogeneously dispersed in PP matrix due to its narrow particle size distribution, smaller mean particle size and loosely bound aggregate structure. Thermal characteristics study showed that PP/MESSP composites have a comparable melting and crystallization temperature of the PP matrix. This implies that the fabrication of the PP/MESSP composites can be processed at similar temperature as that of the neat PP. Moreover, addition of MESSP does not affect the processability of PP as shown by the minimal changes in processing torques. Mechanical properties such as impact strength and tensile modulus of PP were improved with the addition of MESSP. However, with the increasing of the MESSP, tensile strength and the elongation at break were reduced. Morphological study indicated that the reduction in tensile properties was due to the weak filler-matrix interaction. Water uptake of the composites was increased with the increased MESSP content due to the increase of the hydrophilicity properties

as shown in ATR-FTIR analysis and penetration of water molecules through the weak interface between PP and MESSP.

Soil burial test reveals that the bio-degradability of the pure PP was improved with the addition of MESSP as evident with the degradation observed associated with the weight loss of the composites. Highest weight loss of the composites was observed which corresponded to the higher degradation rate at the higher loading of MESSP where MESSP serve as the food source for the microorganism. With the longer exposure time, PP/MESSP composites experience higher deterioration. As the evidenced from SEM images and physical appearance of the composites, attachment and the migration of microorganism as well as the presence of crazing marked were observed.

NaOH treatment of MESSP shows positive improvement with the reduction of hydrophilic properties of MESSP and an enhanced surface roughness through the removal of the extractives and impurities. FTIR proved that the wax, dirt and impurities of the MESSP was degraded in the alkali treatment. This result was correlated to the chemical composition analysis of MESSP. Besides, the treatment of MESSP has improved the processing-ability of the composites as lower processing torque were recorded. Higher degree of crystallinity of PP was observed up to 15 wt. % loading of TMESSP. In general, thermal stability of the composites were improved with the incorporation of TMESSP as compared to untreated MESSP. As the TMESSP loading increased from 0 to 20 wt. %, the tendency for the water absorption

and thickness swelling of the composites were reduced. This results are compatible with the ATR-FTIR analysis of the composites. The PP/TMESSP composites generally get lesser water absorbed due to the lower hydrophilic properties of the TMESSP as compared to MESSP. The PP/TMESSP composites resulted in the better mechanical properties as compared to PP/MESSP composites. Increased tensile properties and tensile modulus of PP composites up to the optimum 15 wt. % of TMESSP loading were obtained. Similarly, improved impact strength of the PP/TMESSP composites revealed the enhanced toughness of the composites with the higher loading of TMESSP. The SEM observation was in line with the outcome of mechanical properties due to the enhanced compatibility and interfacial adhesion between the filler-matrix phases.

Generally, the improvement on the properties of the PP/TMESSP composites can be observed with the NaOH treatment. It can be suggested that the 5, 10 and 15 wt. % TMESSP filled PP composites are the suitable candidates for the general purpose plastic product applications because the PP/TMESSP composites possess the properties in similar range and comparable to commercial PP polymer (Maddah, 2016). In addition, PP/TMESSP composite can be used in application that requires high impact strength with moderate tensile strength from household appliances to automobile part. Low cost with moderate tensile strength promote the application in houseware appliances or for the part of stationery such as decking, storage box, plastic ruler and pen cover (Girones et al., 2017). Other than that, PP/TMESSP composites shows the potential to be embraced in the non-structural purpose for the automotive

application such as door panel and floor trunk (Holbery and Houson, 2006; Ayrilmis et al., 2011; Akhtar et al., 2016). However, more characterisations, testing and improvements needed in order to determine the feasibility of the PP/TMESSP composites to be applicable in the specific field of application.

5.2 Recommendations for Future Research

From this research work, few recommendations are made for future works as listed below:

- Utilisation of the compatibiliser such as maleic anhydride grafted PP (MAPP) to increase the wettability and flowability of the PP and MESSP.

- Involve the different processing methods including extrusion or heated two roll milling that suitable for large scale of sampling and compounding.

- Study on the bio-degradability properties of PP/MESSP and PP/TMESSP composites through the respirometric test in soil for the evaluation of the biodegradation capacity through the quantification of the CO_2 produced during the biodegradation.

- A number of other analysis can be conducted such as X-Ray Diffraction

(XRD) of MESSP, flexural test and weathering test of the composites depending on the final application of PP/TMESSP composites.

REFERENCES

Abdullah, C., Azzahari, A., Rahman, N., Hassan, A. and Yahya, R., 2019. Optimizing Treatment of Oil Palm-Empty Fruit Bunch (OP-EFB) Fiber: Chemical, Thermal and Physical Properties of Alkalized Fibers. *Fibers and Polymers*, 20(3), pp.527-537.

Abhulimen, E. and Orumwense, F., 2017. Characterization and development of asbestos-free brake pad, using snail shell and rubber seed husk. *African Journal of Engineering Research*, 5(2), pp.24-34.

Acevedo, M., Tapia. A.,Correa. J., Ricardo. R and Realpe. A., 2016. Characterization of recycled polypropylene composites material reinforced with wood flour using SEPs-g-MAH as coupling agent. *International Journal of Engineering and Technology*, 8, pp. 1397-1405.

Adapa, P., Karunakaran, C., Tabil, L. and Schoenau, G., 2009. Potential Applications of Infrared and Raman Spectromicroscopy for Agricultural Biomass. *Agricultural Engineering International: the CIGR Ejournal* Manuscript 1081. XI, pp.1-25.

Adekunle, K., 2015. Surface Treatments of Natural Fibres—A Review: Part 1. *Open Journal of Polymer Chemistry*, 5(3), pp.41-46.

Ahmad, F., Choi, H. and Park, M., 2014. A Review: Natural Fiber Composites Selection in View of Mechanical, Light Weight, and Economic Properties. *Macromolecular Materials and Engineering*, 300(1), pp.10-24.

Aho, J., 2011. Rheological Characterization of Polymer Melts in Shear and Extension: Measurement Reliability and Data for Practical Processing. Degree. Tampere University of Technology.

Akhtar, M. et al., 2016. Influence of alkaline treatment and fiber loading on the physical and mechanical properties of kenaf/polypropylene composites for variety of applications. *Progress in Natural Science: Materials International*, 26, pp. 657-664.

Alabi, O., Ologbonjaya, K., Awosolu., O. and Alalade., O., 2019. Public and Environmental Health Effects of Plastic Wastes Disposal: A Review. *Journal of Toxicology and Risk Assessment*, 5(2).

Alemdar, A. and Sain, M., 2008. Isolation and characterization of nanofibers from agricultural residues – Wheat straw and soy hulls. *Bioresource Technology*, 99(6), pp.1664-1671.

Alharbi, M., Hirai, S., Hoang, A., Akioka, S. and Shoji, W., 2020. Effects of chemical composition, mild alkaline pretreatment and particle size on mechanical, thermal, and structural properties of binderless lignocellulosic biopolymers prepared by hot-pressing raw microfibrillated Phoenix dactylifera and Cocos nucifera fibers and leaves. *Polymer Testing*, 84, pp. 105510-105520.

Ali, A., Shaker, K., Nawab, Y., Jabbar, M., Hussain, T., Militky, J. and Baheti, V., 2016. Hydrophobic treatment of natural fibers and their composites—A review. *Journal of Industrial Textiles*, 47(8), pp.2153-2183.

Alias, N., Ismail, H. and Ku Ishak, K., 2019. The Effect of Kenaf Loading on Water Absorption and Impact Properties of Polylactic Acid/ Natural Rubber/ Kenaf Core Powder Biocomposite. *Materials Today: Proceedings*, 17, pp.584-589.

Alibaba.com., 2020. *Pure Indian Mimusops Elengi Herbal Extract Bulk Supply At Best Price –Buy Mimusops Elengi,Borsali Seeds,Herbal Seeds Product On Alibaba.Com* [Online]. Available at: <https://www.alibaba.com/product-detail/Pure-Indian-Mimusops-Elengi-Herbal Extract _62014001836.html?spm=a2700.7724857.normalList.6.5d0060aeYUjeWh> [Accessed 2 March 2020].

Alshabanat, M., 2019. Morphological, thermal, and biodegradation properties of LLDPE/treated date palm waste composite buried in a soil environment. *Journal of Saudi Chemical Society*, 23(3), pp.355-364.

Amir, F., Wong, K., Eldeen, I., Asmawi, M. and Osman, H., 2013. Evaluation of Biological Activities of Extracts and Chemical Constituents of Mimusops elengi. Tropical. *Journal of Pharmaceutical Research*, 12(4), pp. 591-596.

Aridi, N., Sapuan, S., Zainudin, E. and AL-Oqla, F., 2016. Mechanical and morphological properties of injection-molded rice husk polypropylene composites. *International Journal of Polymer Analysis and Characterization*, 21(4), pp.305-313.

Asumani, O., Reid, R. and Paskaramoorthy, R., 2012. The effects of alkali–silane treatment on the tensile and flexural properties of short fibre non-woven kenaf reinforced polypropylene composites. *Composites Part A: Applied Science and Manufacturing*, 43(9), pp.1431-1440.

Ayeni, A., Adeeyo, O., Oresegun, O. and Oladimeji, T., 2015. Compositional analysis of lignocellulosic materials: Evaluation of an economically viable method suitable for woody and non-woody biomass. *American Journal of Engineering Research (AJER)*, 4(4), pp.14-19.

Ayrilmis, N., Jarusombuti, S., Fueangvivat, V., Bauchongkol, P. and White, R., 2011. Coir fiber reinforced polypropylene composite panel for automotive interior applications. *Fibers and Polymers*, 12(7), pp.919-926.

Azwa, Z., Yousif, B., Manalo, A. and Karunasena, W., 2013. A review on the degradability of polymeric composites based on natural fibres. *Materials & Design*, *47*, pp.424-442.

Bajpai, P., 2018. *Wood and Fiber Fundamentals*. In: Biermann's Handbook of Pulp and Paper. 3rd ed. San Diego: Elsevier, pp.30-45.

Balakrishna, N., Ismail, H. and Othman, N., 2013. Processing, Mechanical, and Thermal Properties of Polypropylene/Rattan Powder/Talc Hybrid Composites. *BioResources*, 8(4).

Balakrishna. N., Ismail. N. and Othman. N., 2014. Polypropylene/Rattan Powder/Kaolin Hybrid Composites: Processing, Mechanical and Thermal Properties. *Polymer-Plastics Technology and Engineering*, 53 (5), pp. 451-458.

Baliga, M., Pai, R., Bhat, H., Palatty, P. and Boloor, R., 2011. Chemistry and medicinal properties of the Bakul (Mimusops elengi Linn): A review. *Food Research International*, 44(7), pp.1823-1829.

Barkoula, N., Garkhail, S. and Peijs, T., 2009. Effect of Compounding and Injection Molding on the Mechanical Properties of Flax Fiber Polypropylene Composites. *Journal of Reinforced Plastics and Composites*, 29(9), pp.1366-1385.

Bashir, A. and Manusamy, Y., 2015. Characterization of Raw Egg Shell Powder (ESP) as A Good Bio-filler. *Journal of Engineering Research and Technology*, 2(1).

Beckman, E., 2018. *The world's plastic problem in numbers* [Online]. World Economic Forum. Available at: https://www.weforum.org/agenda/2018/08/the-world-of-plastics-in-numbers [Accessed: 5 Nov. 2019].

Begum, K. and Islam, M., 2013. Natural Fiber as a substitute to Synthetic Fiber in Polymer Composites: A Review. *Research Journal of Engineering Sciences*, 2(3), pp.46-53.

Béland, S., 1990. *High performance thermoplastic resins and their composites*. Park Ridge, N.J: Noyes Data Corp.

Bengtsson, M., Baillif, M. and Oksman, K., 2007. Extrusion and mechanical properties of highly filled cellulose fibre–polypropylene composites. *Composites Part A: Applied Science and Manufacturing*, 38(8), pp.1922-1931.

Bera, M., Alagirusamy, R. and Das, A., 2010. A study on interfacial properties of jute-PP composites. *Journal of Reinforced Plastics and Composites*, 29(20), pp.3155-3161.

Betancur, A., Pérez, F., Correa, M. and Barrero, C., 2012. Quantitative approach in iron oxides and oxyhydroxides by vibrational analysis. Optica Puray Aplicada, 45(3), pp.269-275.

Bezin, F., Amornsakchai, T., Lemaitre, A., Castellant, R. and Vergnes, B. Influence of fiber content on rheological and mechanical properties of pineapple leaf fibers-polypropylene composites prepared by twin-screw extrusion. *Polymer Composites*, 40(12), pp.4519-4529.

Bhandari, N., Thomas, S., Das, C. and Adhikari, R., 2012. Analysis of Morphological and Mechanical Behaviors of Bamboo Flour Reinforced Polypropylene Composites. *Nepal Journal of Science and Technology*, 13(1), pp.95-100.

Biron, M., 2013. *Outline the actual situation of plastics compared to conventional materials*. In: Thermoplastics and Thermoplastic Composites, 2nd ed. Kidlington, Oxford, UK: Elsevier Ltd., pp.20-22.

Biron, M., 2016. *Thermoplastics: Economic Overview*. Material Selection for Thermoplastic Parts, Oxford: Matthew Deans, pp.77-111.

Bjørk, R., Tikare, V., Frandsen, H. and Pryds, N., 2012. The Effect of Particle Size Distributions on the Microstructural Evolution during Sintering. *Journal of the American Ceramic Society*, 96(1), pp.103-110.

Blasi, C., Signorelli, G., Di Russo, C. and Rea, G., 1999. Product Distribution from Pyrolysis of Wood and Agricultural Residues. *Industrial & Engineering Chemistry Research*, 38(6), pp.2216-2224.

Boonprasert, P. and Tangboriboon, N., 2017. Electromechanical-Conductive Natural Rubber Doped Eggshell and Eggshell Membrane for Drug Delivery and Actuator Applications. *Materials Science Forum*, 934, pp.43-49.

Borsoi, C., Menin, C., Lavoratti, A. and Zattera, A., 2019. Grape stalk fibers as reinforcing filler for polymer composites with a polystyrene matrix. *Journal of Applied Polymer Science*, 136(18), pp.1-10.

Butylina, S., Hyvärinen, M. and Kärki, T., 2012. A study of surface changes of wood-polypropylene composites as the result of exterior weathering. *Polymer Degradation and Stability*, 97(3), pp.337-345.

Cai, M., Takagi, H., Nakagaito, A., Li, Y. and Waterhouse, G., 2016. Effect of alkali treatment on interfacial bonding in abaca fiber-reinforced composites. *Composites Part A: Applied Science and Manufacturing*, 90, pp.589-597.

Cao, X., Ismail, H., Rashid, A. and Takeichi, T., 2012. Kenaf Powder Filled Recycled High Density Polyethylene/Natural Rubber Biocomposites: The Effect of Filler Content. *International Journal of Integrated Engineering*, 4(1), pp.22-25.

Cao, W., Li, J. and Leo, L., 2017. Study on the ignition behavior and kinetics of combustion of biomass. *Energy Procedia,* 142, pp. 136-141.

Carvalho, K., Mulinari, D., Voorwald, H. and Cioffi, M., 2010. Chemical Modification Effect on the Mechanical Properties of Hips/ Coconut Fiber Composites. *BioResources*, 5(2).

Catto, A., Dahlem Júnior, M., Hansen, B., Francisquetti, E. and Borsoi, C., 2019. Characterization of polypropylene composites using yerba mate fibers as reinforcing filler. *Composites Part B: Engineering*, 174, p.106935.

Celino, A., Freour, S., Jacquemin, F. and Casari, P., 2013. The hygroscopic behavior of plant fibers: A review. *Frontiers in Chemistry*, 1(43), pp. 1-12.
Chandramohan, D. and Marimuthu, K., 2011. A review on natural fibers. *International Journal of Recent Research and Applied Studies,* 8(2).

Chattopadhyay, S., Khandal, R., Uppaluri, R. and Ghoshal, A., 2009. Influence of varying fiber lengths on mechanical, thermal, and morphological properties of MA-g-PP compatibilized and chemically modified short pineapple leaf fiber reinforced polypropylene composites. *Journal of Applied Polymer Science*, 113(6), pp.3750-3756.

Chauhan, A. and Chauhan, P., 2013. Natural Fibers and Biopolymer. *Journal of Chemical Engineering & Process Technology*, s6.

Chee, S., Jawaid, M., Sultan, M., Alothman, O. and Abdullah, L., 2019. Accelerated weathering and soil burial effects on colour, biodegradability and thermal properties of bamboo/kenaf/epoxy hybrid composites. *Polymer Testing*, 79, p.106054.

Chimeni, D., Yoya, G., Stevanovic, T. and Rodrigue, D., 2017. Surface modification of cellulosic materials for polyethylene composite applications. *Polymer Composites*, 40(1), pp.E202-E213.

Chollakup, R., Tantatherdtam, R., Ujjin, S. and Sriroth, K., 2010. Pineapple leaf fiber reinforced thermoplastic composites: Effects of fiber length and fiber content on their characteristics. *Journal of Applied Polymer Science*, 119(4), pp.1952-1960.

Choudhury, B. and Choudhury, A., 2012. Luminescence characteristics of cobalt doped TiO2 nanoparticles. Journal of Luminescence, 132(1), pp.178-184
.
Clements, A., Dunn, M., Firth, V., Hubbard, L., Lazonby, J. and Waddington, D., 2010. *The Essential Chemical Industry*, 5th ed. University of York, United Kingdom.

Cordeiro, E. et al., 2014. Polymer Biocomposites and Nanobiocomposites Obtained from Mango Seeds. *Macromolecular Symposia*, 344, pp.39-54.

Craig, M., 2010. Natural fibers. In: Xanthos, M. (ed.). *Functional fillers for plastics*. 2 nd ed. Weinheim: Wiley-VCH, p.12.

Dabadi. P., Koti, B. and Katagi, T., 2011. Antiulcer activity of Mimusops elengi bark extracts against serotonin induced ulcer in rats. *International Research Journal of Pharmacy*, 2(8), pp. 173-176.

Danjaji, I., Nawang, R., Ishiaku, U., Ismail, H. and Ishak, Z., 2000. Sago starch-filled linear low-density polyethylene (LLDPE) films: Their mechanical properties and water absorption. *Journal of Applied Polymer Science*, 79(1), pp.29-37.

Dash, B., Rana, A., Mishra, H., Nayak, S. and Tripathy, S., 2000. Novel low-cost jute-polyester composites. III. Weathering and thermal behavior. *Journal of Applied Polymer Science*, 78(9), pp.1671-1679.

Daud, S., Ismail, H. and Abu Bakar, A., 2017. A Study on the Curing Characteristics, Tensile, Fatigue, and Morphological Properties of Alkali-Treated Palm Kernel Shell-Filled Natural Rubber Composites. *BioResources*, 12(1).

Daud, Z., Mohd Hatta, M., Mohd Kassim, A., Awang, H. and Mohd Aripin, A., 2014. Exploring of Agro Waste (Pineapple Leaf, Corn Stalk, and Napier Grass) by Chemical Composition and Morphological Study. *BioResources*, 9(1), pp. 872-880.

DeArmitt, C. and Rothon, R., 2017. Particulate Fillers, Selection, and Use in Polymer Composites. *Fillers for Polymer Applications*, pp.1-19.

Demir, H., Atikler, U., Balköse, D. and Tıhmınlıoğlu, F., 2006. The effect of fiber surface treatments on the tensile and water sorption properties of polypropylene–luffa fiber composites. *Composites Part A: Applied Science and Manufacturing*, 37(3), pp.447-456.

Demirbas, A., 2006. Effect of temperature on pyrolysis products from four nut shells. *Journal of Analytical and Applied Pyrolysis*, 76(1-2), pp.285-289.

Dhanola, A., Bisht, A., Kumar, A. and Kumar, A., 2018. Influence of natural fillers on physico-mechanical properties of luffa cyclindrica/polyester composites. *Materials Today: Proceeding*, 5(9), pp.17021-17029.

Diaz, G., 2015. Toxicosis by Plant Alkaloids in Humans and Animals in Colombia. *Toxins*, 7(12), pp.5408-5416.

Dittenber, D. and GangaRao, H., 2012. Critical review of recent publications on use of natural composites in infrastructure. *Composites Part A: Applied Science and Manufacturing*, 43(8), pp.1419-1429.

dos Santos, L., Thiré, R., Lima, E., Racca, L. and Silva, A., 2018. Mechanical and Thermal Properties of Environment Friendly Composite Based on Mango's Seed Shell and High-Density Polyethylene. *Macromolecular Symposia*, 381(1).

Du, B., Hou, Z. and Li, J., 2018. A Review of Polypropylene and Polypropylene/Inorganic Nanocomposites for HVDC Cable Insulation. In: Shariatinasab, R. (ed.). New Trends in High Voltage Engineering. *IntechOpen Limited*.

Elkhaoulani, A., Arrakhiz, F., Benmoussa, K., Bouhfid, R. and Qaiss, A., 2013. Mechanical and thermal properties of polymer composite based on natural fibers: Moroccan hemp fibers/polypropylene. *Materials & Design*, 49, pp.203-208.

Ercan, N., Durmus, A. and Kaşgöz, A., 2015. Comparing of melt blending and solution mixing methods on the physical properties of thermoplastic

polyurethane/organoclay nanocomposite films. *Journal of Thermoplastic Composite Materials*, 30(7), pp.950-970.

Essabir, H. et al., 2013. Mechanical and thermal properties of bio-composites based on polypropylene reinforced with Nut-shells of Argan particles. *Materials & Design*, 49, pp.442-448.

Essabir, H., Bensalah, M., Rodrigue, D., Bouhfid, R. and Qaiss, A., 2016. Structural, mechanical and thermal properties of bio-based hybrid composites from waste coir residues: Fibers and shell particles. *Mechanics of Materials*, 93, pp.134-144.

Fan, M., Dai, D. and Huang, B., 2012. *Fourier Transform Infrared Spectroscopy for Natural Fibres*. In: S. Salih, ed., Fourier Transform- Materials Analysis: InTech, pp.45-62.

Faria, H., Cordeim, N., Belgacem, M. and Dufresne, A., 2006. Dwarf Cavendish as a source of natural fibres in poly(propylene)-based composites. *Macromolecular Materials and Engineering*, 291(1), pp.16-26.

Faruk, O., Bledzki, A., Fink, H. and Sain, M., 2013. Progress Report on Natural Fiber Reinforced Composites. *Macromolecular Materials and Engineering*, 299(1), pp.9-26.

Fern, K., 2017, *Mimusops elengi - Useful Tropical Plants* [Online]. Tropical.theferns.info. Available at: http://tropical.theferns.info/viewtropical.php?id=Mimusops%20elengi [Accessed: 2 Aug. 2019].

Ferreira, D., Cruz, J. and Fangueiro, R., 2019. *Processing and characterization of green composites*. In: Koronis, G., and Silva. A. (eds.). Green composites for automotive applications. Duxford: Woodhead Publising, pp.15-19.

Ferreira, F., Pinheiro, I., de Souza, S., Mei, L. and Lona, L., 2019. Polymer Composites Reinforced with Natural Fibers and Nanocellulose in the Automotive Industry: A Short Review. *Journal of Composites Science*, 3(2), p.51.

Fiore, V., Bella, D. and Valenza, A., 2015. The effect of alkaline treatment on mechanical properties of kenaf fibers and their epoxy composites. *Composites Part B: Engineering*, 68, pp. 14-21.

Friedrich, K. and Breuer, U., 2015. *Use of special matrices/Reinforcements/Interphases*. In: Multifunctionality of polymer

composites. Oxford: Elsevier, pp.559-560.

Galván, M., Hernández, J., Baños, L., Noriega-Montes, J. and Rodríguez-García, M., 2009. Characterization of Calcium Carbonate, Calcium Oxide, and Calcium Hydroxide as Starting Point to the Improvement of Lime for Their Use in Construction. Journal of Materials in Civil Engineering, 21(11), pp.694-698.

Gami, B., Pathak, S. and Parabia, M., 2012. Ethnobotanical, phytochemical and pharmacological review of Mimusops elengi Linn. *Asian Pacific Journal of Tropical Biomedicine*, 2(9), pp.743-748.

Garside, M., 2019. *Global plastic production | Statista* [Online]. Statista. Available at: https://www.statista.com/statistics/282732/global-production-of-plastics-since-1950/ [Accessed 5 Nov. 2019].

Geyer, R., Jambeck, J. and Law, K., 2017. Production, use, and fate of all plastics ever made. *Science Advances*, 3(7).

Girones, J., Vo, L., Giuseppe, E. and Navard, P., 2017. Natural Filler-Reinforced Composites: Comparison of Reinforcing Potential among Technical Fibers, Stem Fragments and Industrial By-Products. *Cellulose Chemistry and Technology*, 51, pp. 839-855.

Gon, D., Das, K., Paul, P. and Maity, S., 2012. Jute Composites as Wood Substitute. *International Journal of Textile Science*, 1(6), pp.84-93.

Government, R. et al., 2019. Influence of Soaking Time and Sodium Hydroxide Concentration on the Chemical Composition of Treated Mango Seed Shell Flour for Composite Application. *Journal of Applied Sciences and Environmental Management*, 23(1), p.21.

Gowda, T. et al., 2018. Polymer matrix-natural fiber composites: An overview. *Cogent Engineering*, 5(1).

Grigore, M., 2017. Methods of Recycling, Properties and Applications of Recycled Thermoplastic Polymers. *Recycling*, 2(4), p.24.

Gulitah. V. and Liew. K., 2018. Effect of Plastic Content Ratio on the Mechanical Properties of Wood-Plastic Composite (WPC) Made From Three Different Recycled Plastic and Acacia Fibres. *Transactions on Science and Technology*, 5 (2), pp.184-189.

Gunning, M., Geever, L., Killion, J., Lyons, J. and Higginbotham, C., 2013. Mechanical and biodegradation performance of short natural fibre polyhydroxybutyrate composites. *Polymer Testing*, 32(8), pp.1603-1611.

Gupta, P., 2013. Mimusops elengi Linn. (Bakul) - A Potential Medicinal Plant: A Review. *International Journal of Pharmaceutical and Phytopharmacological Research*, 2(5), pp.332-339.

Han, C., 2007. *Morphology evolution in immiscible polymer blends during compounding*. In: Rheology and Processing of Polymeric Materials Volume 2 Polymer Processing. Oxford: Oxford University Press, USA, pp.134-150.

Hassen, A., Dizbay-Onat, M., Bansal, D., Bayush, T. and Vaidya, U., 2015. Utilization of Chicken Eggshell Waste as a Bio-Filler for Thermoplastic Polymers: Thermal and Mechanical Characterization of Polypropylene Filled with Naturally Derived CaCo3. *Polymers and Polymer Composites*, 23(9), pp.653-662.

Hebbar, J., 2016. *Bakula – Mimusops elengi: Benefits, Remedies, Research, Side Effects* [Online]. Easy Ayurveda: Health - Lifestyle. Available at: http://easyayurveda.com/2016/11/28/bakula-mimusops-elengi-bullet-wood-spanish-cherry/ [Accessed 8 August 2019].

Hidayat, A. and Tachibana, S., 2012. Characterization of polylactic acid (PLA)/kenaf composite degradation by immobilized mycelia of Pleurotus ostreatus. *International Biodeterioration & Biodegradation*, 71, pp.50-54.

Hogan, A. and Steinbach, A., 2019. *A Polymer Problem: How Plastic Production and Consumption is Polluting our Oceans* [Online]. Law.georgetown.edu. Available at: https://www.law.georgetown.edu/environmental-law-review/blog/a-polymer-problem-how-plastic-production-and-consumption-is-polluting-our-oceans/ [Accessed 28 December 2019].

Holbery, J. and Houston, D., 2006. Natural fiber reinforced polymer composites in automotive applications. *The Journal of The Minerals, Metals & Materials Society (TMS)*, 58, pp.80-86.

Hollaway, L., 1993. *Polymer Composites for Civil and Structural Engineering*. Dordrecht: Springer Netherlands.

Hou, X. et al., 2014. Preparation of lightweight polypropylene composites reinforced by cotton stalk fibers from combined steam flash-explosion and alkaline treatment. *Journal of Cleaner Production*, 83, pp.454-462.

Huang, C., Yang, T., Hung, K., Xu, J. and Wu, J., 2018. The effect of maleated polypropylene on the non-isothermal crystallisation kinetics of wood fiber reinforced polypropylene composites. *Polymers*, 10(4), pp.382-395.

Huda, M., Drzal, L., Ray, D., Mohanty, A. and Mishra, M., 2020. *Natural-fiber composites in the automotive sector*. In: Pickering, K. (ed.). Properties and Performance of Natural-Fibre Composites. Sawston: Woodhead Publishing, pp.221-268.

Indira, K., Parameswaranpillai, J. and Thomas, S., 2013. Mechanical Properties and Failure Topography of Banana Fiber PF Macrocomposites Fabricated by RTM and CM Techniques. *ISRN Polymer Science*, 2013, pp.1-8.

Iqbal, Z., and Goyal, A., 2010. *Carbon nanotubes/nanofibers and carbon fibers*. In: Xanthos, M. (ed.). Functional fillers for plastics. 2nd ed. Weinheim: Wiley-VCH, pp. 197-198.

Ismail, H. and Muniyadi, M., 2011. Curing Characteristics, Morphological, Tensile and Thermal Properties of Bentonite-Filled Ethylene-Propylene-Diene Monomer (EPDM) Composites. *Polymer-Plastics Technology and Engineering*, 50(14), pp.1421-1428.

Jariwala, H. and Jain, P., 2019. A review on mechanical behavior of natural fiber reinforced polymer composites and its applications. *Journal of Reinforced Plastics and Composites*, 38(10), pp.441-453.

Jelle, B. and Nilsen, T., 2011. Comparison of accelerated climate ageing methods of polymer building materials by attenuated total reflectance Fourier transform infrared radiation spectroscopy. *Construction and Building Materials*, 25(4), pp.2122-2132.

Jiang, J., Mei, C., Pan, M. and Lu, F., 2019. Effects of hybridization and interface modification on mechanical properties of wood flour/polymer composites reinforced by glass fibers. *Polymer Composites*, 40(9), pp.3601-3610.

Jlassi., K., Chehimi., M. and Thomas., S., 2017. *Clay-Polymer Nanocomposites*. Elsevier, pp.114-117.

Joel, F., 1995. *Introduction to polymer science*. In: Polymer Science & Technology: Introduction to polymer science. 3rd ed. New Jersey: Prentice Hall PTR Inc, pp.4-9.

John, M. and Thomas, S., 2008. Biofibres and biocomposites. *Carbohydrate Polymers*, 71(3), pp.343-364.
Kabir, M., Wang, H., Lau, K. and Cardona, F., 2012. Chemical treatments on plant-based natural fibre reinforced polymer composites: An overview. *Composites Part B: Engineering*, 43(7), pp.2883-2892.

Kadam, P., Yadav, K., Deoda, R., Shivatare, R. and Patil, M., 2012. Mimusops elengi: A Review on Ethnobotany, Phytochemical and Pharmacological Profile. *Journal of Pharmacognosy and Phytochemistry*, 1(3), pp.64-71.

Kaewkuk, S., Sutapun, W. and Jarukumjorn, K., 2013. Effects of interfacial modification and fiber content on physical properties of sisal fiber/polypropylene composites. *Composites Part B: Engineering*, 45(1), pp.544-549.

Kamalbabu, P. and Kumar, G., 2014. Effects of Particle Size on Tensile Properties of Marine Coral Reinforced Polymer Composites. *Procedia Materials Science*, 5, pp.802-808.

Karmarkar, A., Chauhan, S., Modak, J. and Chanda, M., 2007. Mechanical properties of wood–fiber reinforced polypropylene composites: Effect of a novel compatibilizer with isocyanate functional group. *Composites Part A: Applied Science and Manufacturing*, 38(2), pp.227-233.

Kim, S., Moon, J., Kim, G. and Ha, C., 2008. Mechanical properties of polypropylene/natural fiber composites: Comparison of wood fiber and cotton fiber. *Polymer Testing*, 27(7), pp.801-806.

Koay, S. and Husseinsyah, S., 2016. Agrowaste-based composites from cocoa pod husk and polypropylene. *Journal of Thermoplastic Composite Materials*, 29(10), pp.1332-1351.

Koay, S., Husseinsyah, S. and Osman, H., 2013. Modified Cocoa Pod Husk-Filled Polypropylene Composites by Using Methacrylic Acid. *BioResources*, 8(3).

Kocaman, S. and Ahmetli, G., 2016. Eco-Friendly Natural Filler Based Epoxy Composites. *International Journal of Chemical and Molecular Engineering*, 10(4).

Kogel, J., Trivedi, N., Barker, J. and Krokowski, S., 2006. *Market and uses. In: Industrial Minerals & Rocks: Commodities, Markets, and Uses*. 7th ed. Colorado: Society of Mining, Metallurgy, and Exploration, Inc., pp.1130-1131.

Kolawole, M., Aweda, J. and Abduikareen, S., 2017, Archachatina marginatbio-shells as reinforcement material in metal matrix composites. International *Journal of Automative and Mechanical Engineering*, 14(1), pp.4068-4079.

Komal, U., Verma, V., Ashwani, T., Verma, N. and Singh, I., 2018. Effect of Chemical Treatment on Thermal, Mechanical and Degradation Behavior of Banana Fiber Reinforced Polymer Composites. *Journal of Natural Fibers*, pp.1-13.

Koronis, G., Silva, A. and Fontul, M., 2019. Green composites: A review of adequate materials for automotive applications. *Composites Part B: Engineering*, 44(1), pp.120-127.

Krishnudu, M., Sreeramulu, D. and Reddy, P., 2019. Alkali Treatment Effect: Mechanical, Thermal, Morphological, and Spectroscopy Studies on Abutilon Indicum Fiber-Reinforced Composites. *Journal of Natural Fibers*, pp.1-10.

Ku, H., Wang, H., Pattarachaiyakoop, N. and Trada, M., 2011. A review on the tensile properties of natural fiber reinforced polymer composites. *Composites Part B: Engineering*, 42(4), pp.856-873.

Kuciel, S., Jakubowska, P. and Kuźniar, P., 2014. A study on the mechanical properties and the influence of water uptake and temperature on biocomposites based on polyethylene from renewable sources. *Composites Part B: Engineering*, 64, pp.72-77.

Kumar, N., Prabhakar, M. and Song, J., 2019. Effect if interface in hybrid reinforcement of flax/glass on mechanical properties of vinyl ester composites. Polymer Testing, 73, pp. 404-411.

Kumar, P., Ramalingaiah., Suresha, B., Rajini, N. and Satyanarayana. K., 2017. Effect of Treated Coir Fiber/Coconut Shell Powder and Aramid Fiber on Mechanical Properties of Vinyl Ester. *Polymer Composites*, 39(12), pp. 4542-4550.

Kumar, Y. and Anandh, N., 2017. Fabrication and analysis of Jute/Hemp reinforced fiber. International *Journal of Advance Research, Ideas and Innovations in Technology*, 3(6).

Kürschner, K. et al., 1933. Cellulose und Cellulosederivate. *Zeitschrift für Analytische Chemie*, 92(3-4), pp.145-154.

Lazonby, J., 2016. Poly(propene) (Polypropylene). [Online] Essentialchemicalindustry.org. Available at:

http://www.essentialchemicalindustry.org/polymers/polypropene.html [Accessed 6 Dec. 2020].

Lebreton, L. and Andrady, A., 2019. Future scenarios of global plastic waste generation and disposal. *Palgrave Communications*, 5(1).

Lee, B., Kim, H. and Yu, W., 2009. Fabrication of long and discontinuous natural fiber reinforced polypropylene biocomposites and their mechanical properties. *Fibers and Polymers*, 10(1), pp.83-90.

Li, S., Xu, S., Liu, S., Yang, C. and Lu, Q., 2004. Fast pyrolysis of biomass in free-fall reactor for hydrogen-rich gas. *Fuel Processing Technology*, 85(8-10), pp.1201-1211.

Li, X., Tabil, L. and Panigrahi, S., 2007. Chemical Treatments of Natural Fiber for Use in Natural Fiber-Reinforced Composites: A Review. *Journal of Polymers and the Environment*, 15(1), pp.25-33.

Lim, T., 2012. *Edible Medicinal And Non Medicinal Plants* Volume 2, Fruits. Dordrecht: Springer Netherlands, pp.119-128.

Lin, L., Yan, R., Liu, Y. and Jiang, W., 2010. In-depth investigation of enzymatic hydrolysis of biomass wastes based on three major components: Cellulose, hemicellulose and lignin. *Bioresource Technology*, 101(21), pp.8217-8223.

Lopez, G., Artetxe, M., Amutio, M., Bilbao, J. and Olazar, M., 2017. Thermochemical routes for the valorization of waste polyolefinic plastics to produce fuels and chemicals. A review. *Renewable and Sustainable Energy Reviews*, 73, pp.346-368.

Lu, H. et al., 2010. Effects of particle shape and size on devolatilization of biomass particle. *Fuel*, 89(5), pp.1156-1168

Lu, N. and Oza, S., 2013. Thermal stability and thermo-mechanical properties of hemp-high density polyethylene composites: Effect of two different chemical modifications. *Composites Part B: Engineering*, 44(1), pp.484-490.

Lu, X., Lv, X., Sun, Z. and Zheng, Y., 2008. Nanocomposites of poly(l-lactide) and surface-grafted TiO2 nanoparticles: Synthesis and characterization. *European Polymer Journal*, 44(8), pp.2476-2481.

Luna, I. et al., 2015. Physical and Thermal Characterization of Alkali Treated Rice Husk Reinforced Polypropylene Composites. *Advances in Materials Science and Engineering*, 2015, pp.1-7.

Luthra, P., Vimal, K., Goel, V., Singh, R. and Kapur, G., 2020. Biodegradation studies of polypropylene/natural fiber composites. *SN Applied Sciences*, 2(3).

Lyu, S. et al., 2017. Titanium as a Beneficial Element for Crop Production. *Frontiers in Plant Science*, 8.

Machmudah, S., Wahyudiono, Kanda, H. and Goto, M., 2017. *Hydrolysis of Biopolymers in Near-Critical and Subcritical Water*. In: González, H., and Muñoz, M. (eds.). Water Extraction of Bioactive Compounds From Plants to Drug Development. Amsterdam: Elsevier, pp.69-107.

Maddah, H., 2016. Polypropylene as a Promising Plastic: A Review. American *Journal of Polymer Science*, 6(1), pp.1-11.

Malkapuram, R., Kumar, V. and Negi, Y., 2008. Recent Development in Natural Fiber Reinforced Polypropylene Composites. *Journal of Reinforced Plastics and Composites*, 28(10), pp.1169-1189.

Mallick, P., 2010. *Thermoplastics and thermoplastic–matrix composites for lightweight automotive structures*. In: Materials, Design and Manufacturing for Lightweight Vehicles. Oxford: Woodhead Publishing Limited, pp.174-207.

Mamtaz, H., Fouladi, M., Al-Atabi, M. and Namasivayam, S., 2016. Acoustic Absorption of Natural Fiber Composites. *Journal of Engineering*, 2016, pp.1-11.

Manimaran, P., Saravanan, S. and Prithiviraj, M., 2019. Investigation of Physico Chemical Properties and Characterization of New Natural Cellulosic Fibers from the Bark of Ficus Racemosa. *Journal of Natural Fibers*, pp.1-11.

Mansor, A., Lim, J., Ani, F., Hashima, H. and Ho, W., 2019. Characteristics of Cellulose, Hemicellulose and Lignin of MD2 Pineapple Biomass. *Chemical Engineering Transactions*, 72, pp.79-83.

Marques, M., Melo, R., Araujo, R., Lunz, J. and Aguiar, V., 2014. Improvement of mechanical properties of natural fiber-polypropylene composites using successive alkaline treatments. *Journal of Applied Polymer Science*, 132(12), pp.1-12.

Mishra, S. et al., 2003. Studies on mechanical performance of biofibre/glass reinforced polyester hybrid composites. *Composites Science and Technology*, 63(10), pp.1377-1385.

Mittal, V., 2016. *Spherical and fibrous filler composites*. Wiley –VCH., pp.162-164.

Mohammad, Z., Sunil, K. and Gupta. M., 2018. Tensile and flexural properties of natural fiber reinforced polymer composites: A review. *Journal of reinforced Plastics and Composites*, 37(24), pp. 1435-1455.

Mohammed, L., Ansari, M., Pua, G., Jawaid, M. and Islam, M., 2015. A Review on Natural Fiber Reinforced Polymer Composite and Its Applications. *International Journal of Polymer Science*, 2015, pp.1-15.

Mohan, D., Pittman, C. and Steele, P., 2006. Pyrolysis of Wood/Biomass for Bio-oil: A Critical Review. *Energy & Fuels*, 20(3), pp.848-889.

Mohanty, A., Drzal, L. and Misra, M., 2002. Engineered natural fiber reinforced polypropylene composites: influence of surface modifications and novel powder impregnation processing. *Journal of Adhesion Science and Technology*, 16(8), pp.999-1015.

Mohanty, M., Misra, M. and Drzal, L., 2002. Sustainable Bio-Composites from Renewable Resources: Opportunities and Challenges in the Green Materials World. *Journal of Polymers and the Environment*, 10(1), pp.19-26.

Mohanty, S., Verma, S. and Nayak, S., 2006. Dynamic mechanical and thermal properties of MAPE treated jute/HDPE composites. *Composites Science and Technology*, 66(3-4), pp.538-547.

Moharir, R. and Kumar, S., 2019. Challenges associated with plastic waste disposal and allied microbial routes for its effective degradation: A comprehensive review. *Journal of Cleaner Production*, 208, pp.65-76.

Monteiro, S., Calado, V., Rodriguez, R. and Margem, F., 2012. Thermogravimetric behavior of natural fibers reinforced polymer composites-An overview. *Materials Science and Engineering: A*, 557, pp.17-28.

Morgan, T. et al., 2015. Quantitative X-ray Fluorescence Analysis of Biomass (Switchgrass, Corn Stover, Eucalyptus, Beech, and Pine Wood) with a Typical Commercial Multi-Element Method on a WD-XRF Spectrometer. *Energy & Fuels*, 29(3).

Muniyadi, M., Ng, T., Munusamy, Y. and Ooi, Z., 2018. Mimusop elengi Seed Shell Powder as a New Bio-Filler for Polypropylene-based Bio Composite. *Bioresources*, 13(1), pp.272-289.

Mylsamy, K. and Rajendran, I., 2011. Influence of alkali treatment and fibre length on mechanical properties of short Agave fibre reinforced epoxy composites. *Materials & Design*, 32(8-9), pp.4629-4640.

Naidu, A., Jagadeesh, V. and Bahubalendruni, M., 2017. A Review on Chemical and Physical Properties of Natural Fiber Reinforced Composites. *International Journal of Advanced Research in Engineering and Technology (IJARET)*, 8(1).

Nam, T., Ogihara, S., Tung, N. and Kobayashi, S., 2011. Effect of alkali treatment on interfacial and mechanical properties of coir fiber reinforced poly(butylene succinate) biodegradable composites. *Composites Part B: Engineering*, 42(6), pp.1648-1656.

Nasihatgozar, M., Daghigh, V., Lacy, T., Daghigh, H., Nikbin, K. and Simoneau, A., 2016. Mechanical characterization of novel latania natural fiber reinforced PP/EPDM composites. *Polymer Testing*, 56, pp.321-328.

Nasution, H., Tantra, A. and Arista, P., 2016. The effect of filler content and particle size on the impact strength and water absorption of epoxy/cockleshell powder (anadora granosa) composite. *ARPN Journal of Engineering and Applied Sciences*, 11(7), pp.4739-4742.

Nazarudeen, A., 2007. Nutritional composition of some lesser-known fruits used by the ethnic communities and local folks of Kerala. *Indian Journal of Tradition Knowledge*, 9(2), pp.398-402.

Ngo, T., 2017. Natural Fibers for Sustainable Bio-Composites. In: Gunay, E. (ed.). Natural and Artificial Fiber-Reinforced Composites as Renewable Sources. London: *IntechOpen Limited*, pp.107-118.

Nopparut, A. and Amornsakchai, T., 2016. Influence of pineapple leaf fiber and it's surface treatment on molecular orientation in, and mechanical properties of, injection molded nylon composites. *Polymer Testing*, 52, pp.141-149.

Nourbakhsh, A. and Karegarfard, A., 2009. Effects of Particle Size and Coupling Agent Concentration on Mechanical Properties of Particulate-filled Polymer Composites. *Journal of Thermoplastic Composite Materials*, 23(2), pp.169-174.

Nourbakhsh, A., Ashori, A. and Kazemi Tabrizi, A., 2014. Characterization and biodegradability of polypropylene composites using agricultural residues and waste fish. *Composites Part B: Engineering*, 56, pp.279-283.

Nurazzi, N. et al., 2019. Thermal properties of treated sugar palm yarn/glass fiber reinforced unsaturated polyester hybrid composites. *Journal of Materials Research and Technology*, 9(2), pp.1606-1618.

Obasi, H., Igwe, I. and Madufor, I., 2013. Effect of Soil Burial on Tensile Properties of Polypropylene/Plasticized Cassava Starch Blends. *Advance in Materials Science and Engineering*, 2013.

Ogah, A. et al., 2015. Water Absorption, Thickness Swelling and Rheological Properties of Agro Fibers/HDPE Composites. *IOSR Journal of Polymer and Textile Engineering (IOSR-JPTE)*, 2 (3), pp. 66-73.
Ong, D. and Charoenkongthum, K., 2002. Thermal Properties and Moisture Absorption of LDPE/Banana Starch Biocomposite Films. *Journal of metals, materials and minerals*, 1(10).

Onuegbu, G. and Igwe, I., 2011. The Effects of Filler Contents and Particle Sizes on the Mechanical and End-Use Properties of Snail Shell Powder Filled Polypropylene. *Materials Sciences and Applications*, 2(7), pp.810-816.

Ooi, Z., Ismail, H., Abdul Aziz, N. and Abu Bakar, A., 2011. Preparation and Properties of Biodegradable Polymer Film Based on Polyvinyl Alcohol and Tropical Fruit Waste Flour. *Polymer-Plastics Technology and Engineering*, 50(7), pp.705-711.

Osman, H. and Zakaria, M., 2012. Effects of Durian Seed Flour on Processing Torque, Tensile, Thermal and Biodegradation Properties of Polypropylene and High Density Polyethylene Composites. *Polymer-Plastics Technology and Engineering*, 51, pp. 243-250.

Ouarhim, W. et al., 2018. Production and Characterization of High Density Polyethylene Reinforced by Eucalyptus Capsule Fibers. *Journal of Bionic Engineering*, 15(3), pp.558-566.

Ouarhim, W. et al., 2018. Structural laminated hybrid composites based on raffia and glass fibers: Effect of alkali treatment, mechanical and thermal properties. *Composites Part B: Engineering*, 154 (1), pp.128-137.

Palmer, B., 2013. *Recycling of plastic lags because recovery is hard and new production is cheap* [Online]. The Washington Post. Available at: https://www.washingtonpost.com/national/health-science/recycling-of-plastic-

lags-because-recovery-is-hard-and-new-production-is-cheap/2013/02/04/78ca1b92-6953-11e2-ada3-d86a4806d5ee_story.html [Accessed 28 Oct. 2019].

Pandey, J., Ahn, S., Lee, C., Mohanty, A. and Misra, M., 2010. Recent Advances in the Application of Natural Fiber Based Composites. *Macromolecular Materials and Engineering*, 295(11), pp.975-989.

Pang, A., Ismail, H. and Abu Bakar, A., 2015. Effects of Kenaf Loading on Processability and Properties of Linear Low-Density Polyethylene/Poly (Vinyl Alcohol)/Kenaf Composites. *BioResources*, 10(4).
Pardee, W., 1937. Cellulose Analysis- A Comparison of Three Principal Method. *Industrial and Engineering Chemistry*, 9(12), pp.570-572.

Pasangulapati, V. et al., 2012. Effects of cellulose, hemicellulose and lignin on thermochemical conversion characteristics of the selected biomass. *Bioresource Technology*, 114, pp.663-669.

Paul, S., Joseph, K., Mathew, G., Pothen, L. and Thomas, S., 2010. Influence of polarity parameters on the mechanical properties of composites from polypropylene fiber and short banana fiber. *Composites Part A: Applied Science and Manufacturing*, 41(10), pp.1380-1387.

Paul, V., 2015. *Synthesis And Characterization Of A Biocomposite Derived From Banana Plants (Musa Cavendish)*. Ph.D. Durban University of Technology.

Peças, P., Carvalho, H., Salman, H. and Leite, M., 2018. Natural Fibre Composites and Their Applications: A Review. *Journal of Composites Science*, 2(4), p.66.

Pérez, J., Muñoz-Dorado, J., de la Rubia, T. and Martínez, J., 2002. Biodegradation and biological treatments of cellulose, hemicellulose and lignin: an overview. *International Microbiology*, 5(2), pp.53-63.

Pickering, K., Efendy, M. and Le, T., 2016. A review of recent developments in natural fibre composites and their mechanical performance. *Composites Part A: Applied Science and Manufacturing*, 83, pp.98-112.

Pillai, G., Manimaran, P. and Vignesh, V., 2020. Physico-chemical and Mechanical Properties of Alkali-Treated Red Banana Peduncle Fiber. *Journal of Natural Fibers*, pp.1-10.

PlasticsEurope, 2018. *Plastics-the Facts 2018* [Online]. Available at: https://www.plasticseurope.org/application/files/6315/4510/9658/Plastics_the_facts_2018_AF_web.pdf [Accessed 28 Oct. 2019].

Pongdong, W., Kummerlöwe, C., Vennemann, N., Thitithammawong, A. and Nakason, C., 2016. A comparative study of rice husk ash and siliceous earth as reinforcing fillers in epoxidized natural rubber composites. *Polymer Composites*, 39(2), pp.414-426.

Pouriman, M., Dahresobh, A., Caparanga, A., Moradipour, M. and Mehrpooya, M., 2018. Morphological and physicomechanical analysis of high-density polyethylene filled with Salago fiber. *Journal of Applied Polymer Science*, 135(28), p.46479.

Prabha, M., Ajaybhan, A., Navneet, N. and Chauhan, A., 2010. Evaluation of Antimicrobial Activity of Six Medicinal Plants Against Dental Pathogens. *Report and Opinion*, 2(6).

Premalal, H., Ismail, H. and Baharin, A., 2002. Comparison of the mechanical properties of rice husk powder filled polypropylene composites with talc filled polypropylene composites. *Polymer Testing*, 21(7), pp.833-839.

Presle, M., Trias, D. and Boileau, S., 2017. *Methodology and Physicochemical Characterization Technique Used for Failure Analysis in Laboratories*. In: Hami, A., Delaux, D. and Grzeskowiak, H. (eds). Reliability of High-Power Mechatronic Systems 2. London: Elsevier, pp. 221-240.

Rajesh, G., Prasad, A. and Gupta, A., 2015. Mechanical and degradation properties of successive alkali treated completely biodegradable sisal fiber reinforced poly lactic acid composites. *Journal of Reinforced Plastics and Composites*, 34(12), pp.951-961.

Ramli, R., Yunus, R. and Beg, M., 2011. Effects of fiber loading, fiber type, its mesh sizes, and coupling agent on the properties of oil palm biomass/polypropylene composites. *Journal of Composite Materials*, 45(21), pp.2165-2171.

Rashid, B., Leman, Z., Jawaid, M., Ghazali, M. and Ishak, M., 2016. Physicochemical and thermal properties of lignocellulosic fiber from sugar palm fibers: effect of treatment. *Cellulose*, 23(5), pp.2905-2916.

Ray, D., Sarkar, B., Basak, R. and Rana, A., 2004. Thermal behavior of vinyl ester resin matrix composites reinforced with alkali-treated jute fibers. *Journal of Applied Polymer Science*, 94(1), pp.123-129.

Razavi, N., Jafarzadeh, D., Oromiehie, A. and Langroudi, A., 2006. Mechanical properties and water absorption behaviour of chopped rice husk filled polypropylene composites. *Iranian Polymer Journal*, 15, pp.757-766.

Ren, Z. et al., (2019). Effect of Alkali Treatment on Interfacial and Mechanical Properties of Kenaf Fibre Reinforced Epoxy Unidirectional Composites. *Sains Malaysiana*, 48(1), pp.173-181.

Richardson, J., 2018. *Polyethylene versus polypropylene: Expect the unexpected – Asian Chemical Connections* [Online]. Icis.com. Available at: https://www.icis.com/asian-chemical-connections/2018/09/polyethylene-versus-polypropylene-expect-the-unexpected/ [Accessed 5 Jan. 2019].

Ritchie, H. and Roser, M., 2018. *Plastic Pollution* [Online]. Our World in Data. Available at: https://ourworldindata.org/plastic-pollution [Accessed 28 Oct. 2019].

Roqaiya, M., Begum, W. and Jahan, D., 2015. A review on pharmacological property of *Mimusops elengi* Linn. *International Journal of Herbal Medicine*, 2 (6), pp.24-30.

Saha, P. et al., 2015. A brief review on the chemical modifications of lignocellulosic fibers for durable engineering composites. *Polymer Bulletin*, 73(2), pp.587-620.

Samal, S., Mohanty, S. and Nayak, S., 2008. Polypropylene—Bamboo/Glass Fiber Hybrid Composites: Fabrication and Analysis of Mechanical, Morphological, Thermal, and Dynamic Mechanical Behavior. *Journal of Reinforced Plastics and Composites*, 28(22), pp.2729-2747.

Sanjay, M., Arpitha, G., Naik, L., Gopalakrishna, K. and Yogesha, B., 2016. Applications of Natural Fibers and Its Composites: An Overview. *Natural Resources*, 7(3), pp.108-114.

Santiagoo, R., Ismail, H. and Kamarudin, H., 2011. Mechanical properties, water absorption, and swelling behaviour of rice husk powder filled polypropylene/recycled acrylonitrile butadiene rubber (pp/nbrr/rhp) biocomposites using silane as a coupling agent. *Bioresources*, 6(4), pp.3714-3726.

Sareena, C., Ramesan, M. and Purushothaman, E., 2012. Utilization of peanut shell powder as a novel filler in natural rubber. *Journal of Applied Polymer Science*, 125(3), pp.2322-2334.

Sareena, C., Sreejith, M., Ramesan, M. and Purushothaman, E., 2013. Biodegradation behaviour of natural rubber composites reinforced with natural resource fillers – monitoring by soil burial test. *Journal of Reinforced Plastics and Composites*, 33(5), pp.412-429.

Sari, N., Wardana, I., Irawan, Y. and Siswanto, E., 2016. Physical and Acoustical Properties of Corn Husk Fiber Panels. *Advances in Acoustics and Vibration*, 2016, pp.1-8.

Sarifuddin, H., Ismail. H. and Ahmad, Z., 2013. The effect of kenaf core fibre loading on properties of low density polyethylene/thermoplastic sago starch/kenaf core fiber composites. *Journal of Physical Science*, 24 (2) 97-115.

Sastri, V., 2010. *Material used in medical devices*. In: Plastics in medical devices. 2nd ed. Norwich, N.Y: Elsevier/William Andrew, pp.21-24.

Sastri, V., 2014. *Commodity thermoplastics: polyvinyl chloride, polyolefins and polystyrene*. In: Plastics in medical devices. 2nd ed. Oxford: Elsevier, pp.95-103.

Sathishkumar, T., Navaneethakrishnan, P., Shankar, S. and Rajasekar, R., 2013. Characterization of new cellulose sansevieria ehrenbergii fibers for polymer composites. *Composite Interfaces*, 20(8), pp.575-593.

Sawpan, M., Pickering, K. and Fernyhough, A., 2011. Improvement of mechanical performance of industrial hemp fibre reinforced polylactide biocomposites. *Composites Part A: Applied Science and Manufacturing*, 42(3), pp.310-319.

Sekar, V., Fouladi, M., Namasivayam, S. and Sivanesan, S., 2019. Additive Manufacturing: A Novel Method for Developing an Acoustic Panel Made of Natural Fiber-Reinforced Composites with Enhanced Mechanical and Acoustical Properties. *Journal of Engineering*, 2019, pp.1-19.

Sen, S., Sahu, N. and Mahato, S., 1995. Pentacyclic triterpenoids from Mimusops elengi. *Phytochemistry*, 38(1), pp.205-207.

Sepe, R., Bollino, F., Boccarusso, L. and Caputo, F., 2018. Influence of chemical treatments on mechanical properties of hemp fiber reinforced composites. *Composites Part B: Engineering*, 133, pp.210-217.

Sgriccia, N., Hawley, M. and Misra, M., 2008. Characterization of natural fiber surfaces and natural fiber composites. *Composites Part A: Applied Science and Manufacturing*, 39(10), pp.1632-1637.

Shah, A., Hasan, F., Hameed, A. and Ahmed, S., 2008. Biological degradation of plastics: A comprehensive review. *Biotechnology Advances*, 26(3), pp.246-265.

Shamiri, A. et al., 2014. The Influence of Ziegler-Natta and Metallocene Catalysts on Polyolefin Structure, Properties, and Processing Ability. *Materials*, 7(7), pp.5069-5108.

Shamsuri, A., Zolkepli, M., Ariff, A., Sudari, A. and Zarin, M., 2015. A Preliminary Investigation on Processing, Mechanical and Thermal Properties of Polyethylene/Kenaf Biocomposites with Dolomite Added as Secondary Filler. *Journal of Composites*, 2015, pp.1-7.

Shanmugasundaram, N., Rajendran, l. and Ramkumar, T., 2018. Characterization of untreated and alkali treated new cellulosic fiber from an Areca palm leaf stalk as potential reinforcement in polymer composites. *Carbohydrate Polymers*, 195, pp.566-575.

Shesan, O., Stephen, A., Chioma, A., Neerish, R. and Rotimi, S., 2019. *Fiber-Matrix Relationship for Composites Preparation*. In: Pereira, P., and Fernandes, F. (eds). Renewable and Sustainable Composites. London: IntechOpen Limited.

Shi, J., Xing, D. and Lia, J., 2012. FTIR Studies of the Changes in Wood Chemistry from Wood Forming Tissue under Inclined Treatment. *Energy Procedia*, 16, pp.758-762.

Shivatare, R., Deoda, R., Kadam, P., Bhusnar, H., Narappanawar, N. and Patil, M., 2013. Pharmacognostic Standards for Mimusops elengi Linn - A Review. *Journal of Pharmacognosy and Phytochemistry*, 2(3), pp.12-18.

Shubhra, Q. et al., 2010. Characterization of plant and animal based natural fibers reinforced polypropylene composites and their comparative study. *Fibers and Polymers*, 11(5), pp.725-731.

Shubhra, Q. et al., 2010. Study on the mechanical properties, environmental effect, degradation characteristics and ionizing radiation effect on silk reinforced polypropylene/natural rubber composites. *Composites Part A: Applied Science and Manufacturing*, 41(11), pp.1587-1596.

Shubhra, Q., Alam, A. and Quaiyyum, M., 2011. Mechanical properties of polypropylene composites: A review. *Journal of Thermoplastic Composite Materials*, 26(3), pp.362-391.

Silva, C., 2008. Synthesis, Spectroscopy and Characterization of Titanium Dioxide Based Photocatalysts for the Degradative Oxidation of Organic Pollutants. Ph.D. University of Porto.

Simonassi, N. et al., 2017. Reinforcement of Polyester with Renewable Ramie Fibers. *Materials Research*.

Singh, K., Srivastava, P., Kumar, S., Singh, D. and Singh, V., 2014. Mimusops elengi Linn. (Maulsari): a potential medicinal plant. *Archives of Biomedical Sciences*, 2(1), pp.18-29.

Singh, N. and Dutta, S., 2013. Reinforcement of Polypropylene Composite system via Fillers and Compatibilizers. *Open Journal of Organic Polymer Materials*, 3(1), pp.6-11.

Sinha, E. and Rout, S., 2009. Influence of fibre-surface treatment on structural, thermal and mechanical properties of jute fibre and its composite. *Bulletin of Materials Science*, 32(1), pp.65-76.

Song, J., Murphy, R., Narayan, R. and Davies, G., 2009. Biodegradable and compostable alternatives to conventional plastics. *Philosophical Transactions of the Royal Society B: Biological Sciences*, 364(1526), pp.2127-2139.

Sozen, E., Aydemir, D. and Zor, M., 2017. The Effects of Lignocellulosic Fillers on Mechanical, Morphological and Thermal Properties of Wood Polymer Composites. *Drvna industrija*, 68(3), pp.195-204.

Stein et al., 1994. *Manufacturing: Materials and processing*. In: Polymer Science and Engineering: The Shifting Research Frontiers. Washington: National Academy Press, pp.104-108.

Stelescu, M. et al., 2017. Property correlations for composites based on ethylene propylene diene rubber reinforced with flax fibers. *Polymer Testing*, 59, pp.75-83.

Stuart, B. (2004). *Infrared spectroscopy*. Chichester, Eng.: J. Wiley

Sudha, S. and Thilagavathi, G., 2015. Effect of alkali treatment on mechanical properties of woven jute composites. *The Journal of The Textile Institute*, 107(6), pp.691-701.

Sullins, T., Pillay, S., Komus, A. and Ning, H., 2017. Hemp fiber reinforced polypropylene composites: The effects of material treatments. *Composites Part B: Engineering*, 114, pp.15-22.

Sumathi, V., 2017. Optical Characterisation of Calcium Oxide Nanoparticles. In: International Conference on Recent Trends in Engineering Science,Humanities and Management. Sattur, pp.506-510.

Suradi, S., Yunus, R. and Beg, M., 2010. Oil palm bio-fiber-reinforced polypropylene composites: effects of alkali fiber treatment and coupling agents. *Journal of Composite Materials*, 45(18), pp.1853-1861.

Suwanruji, P., Tuechart, T., Smitthipong, W. and Chollakup, R., 2016. Modification of pineapple leaf fiber surfaces with silane and isocyanate for reinforcing thermoplastic. *Journal of Thermoplastic Composite Materials*, 30(10), pp.1344-1360.

Tahir, D., Liong, S. and Bakri, F., 2014. Molecular and structural properties of polymer composites filled with activated charcoal particles. *AIP Conference Proceedings*, pp.1-4.

Tajuddin, M., Ahmad, Z. and Ismail, H., 2016. A review of natural fibers and processing operations for the production of binderless boards. *BioResources*, 11(2).

Tan, W., Mathialagan, M. and Ooi, Z., 2019. Physico-mechanical and biodegradability study of Mimusops elengi seed shell powder filled PVOH films produced through membrane casting method. *Bioresource*, 14(3), 5595-5614.

Tareq, A., 2010. *Comparative Study On Biodegradation Of Some Synthetic Polymers Blended With Some Different Naturally Occurring Polymers*. Master. University of Mosul College of Science.

Thakre, A., Baxi, R., Shelke, R. and Bhuyar, S., 2018. Composites of Polypropylene and Natural Fibers: A Review. *International Journal of Research in Engineering, IT and Social Sciences*, 8(12), pp.56-59.

Thakur, V., Thakur, M. and Gupta, R., 2014. Review: Raw Natural Fiber–Based Polymer Composites. *International Journal of Polymer Analysis and Characterization*, 19(3), pp.256-271.

Thiruchitrambalam, M. and Shanmugam, D., 2012. Influence of pre-treatments on the mechanical properties of palmyra palm leaf stalk fiber–polyester

composites. *Journal of Reinforced Plastics and Composites*, 31(20), pp.1400-1414.

Thomas, S., Paul, S., Pothan, L. and Deepa, B., 2011. *Natural Fibres: Structure, Properties and Applications*. In: Kalia, S., Kaith, B., and Kaur, l. (eds.). Cellulose Fibers: Bio- and Nano-Polymer Composites. New York: Springer Berlin, Heidelberg, pp.4-6.

Thyrel, M., 2014. *Spectroscopic Characterization of Lignocellulosic Biomass*. PhD thesis, Swedish University of Agricultural Sciences Umeå, Sweden.

Titan (1999). *Technical Data Sheet-TitanPro 6331*. Titan PP Polymers (M) Sdn. Bhd., Johor.

Todor, M., Bulei, C., Heput, T. and Kiss, I., 2018. Researches on the development of new composite materials complete / partially biodegradable using natural textile fibers of new vegetable origin and those recovered from textile waste. *IOP Conference Series: Materials Science and Engineering*, 294.

Tolinski, M., 2015. *Trends in polyolefin and additives used*. In: Additives For Polyolefins. 2nd ed. Ann Arbor: William Andrew Publishing, pp.9-21.

Torun, S., Pesman, E. and Cavdar, A., 2019. Effect of alkali treatment on composites made from recycled polyethylene and chestnut cupula. *Polymer Composites*, 40(11), pp.4442-4451.

Trilokesh, C. and Uppuluri, K., 2019. Isolation and characterization of cellulose nanocrystals from jackfruit peel. *Scientific Reports*, 9(1).

Truong, M., Zhong, W., Boyko, S. and Alcock, M., 2009. A comparative study on natural fibre density measurement. *Journal of the Textile Institute*, 100(6), pp.525-529.

Väisänen, T., Haapala, A., Lappalainen, R. and Tomppo, L., 2016. Utilization of agricultural and forest industry waste and residues in natural fiber-polymer composites: A review. *Waste Management*, 54, pp.62-73.

Vasile, C. et al., 2018. Study of the soil burial degradation of some PLA/CS biocomposites. *Composites Part B: Engineering*, 142, pp.251-262.

Venkateshwaran, N. and Elayaperumal, A., 2010. Banana Fiber Reinforced Polymer Composites - A Review. *Journal of Reinforced Plastics and Composites*, 29(15), pp.2387-2396.

Vijay, R. et al., 2019. Characterization of raw and alkali treated new natural cellulosic fibers from Tridax procumbens. *International Journal of Biological Macromolecules*, 125, pp.99-108.
Vu. N., Tran. H. and Nguyen. T., 2018. Characterization of Polypropylene Green Composites Reinforced by Cellulose Fibers Extracted from Rice Straw. *International Journal of Polymer Science*, 2018 (4), pp.1- 10.

Wambua, P., Ivens, J. and Verpoest, I., 2003. Natural fibres: can they replace glass in fibre reinforced plastics?. *Composites Science and Technology*, 63(9), pp.1259-1264.

Wang, C. and Liu, C., 1999. Transcrystallization of polypropylene composites: nucleating ability of fibres. Polymer, 40(2), pp.289-298.

Wang, C. and Ying, S., 2014. A novel strategy for the preparation of bamboo fiber reinforced polypropylene composites. *Fibers and Polymers*, 15(1), pp.117-125.

Wang, Q., Xu, H., Liu, H., Jia, C. and Bai, J., 2011. Thermogravimetric analysis of the combustion characteristics of oil shale semi-coke/biomass blends. *Oil Shale*, 28(2), pp. 284-295.

Wardhana, Y., Hasanah, A. and Primandini, P., 2014. Deformation and Adsorption Capacity of Kaolin that is Influenced by Temperature Variation on Calcination. *International Journal of Pharmacy and Pharmaceutical Sciences*, 6(3).

Wechsler, A., Molina, J., Cayumil, R., Núñez Decap, M. and Ballerini-Arroyo, A., 2019. Some properties of composite panels manufactured from peach (Prunus persica) pits and polypropylene. *Composites Part B: Engineering*, 175, pp.1-7.

Witayakran, S., Smitthipong, W., Wangpradid, R., Chollakup, R. and Clouston, P., 2017. Natural Fiber Composites: Review of Recent Automotive Trends. *Reference Module in Materials Science and Materials Engineering*, pp.166-174.

Xu, E., Wang, D. and Lin, L., 2020. Chemical Structure and Mechanical Properties of Wood Cell Walls Treated with Acid and Alkali Solution. *Forest*, 11(1), pp.87-98.

Yang, H., Yan, R., Chen, H., Zheng, C., Lee, D. and Liang, D., 2006. In-Depth Investigation of Biomass Pyrolysis Based on Three Major Components: Hemicellulose, Cellulose and Lignin. *Energy & Fuels*, 20(1), pp.388-393.

Ye, C., Ma, G., Fu, W. and Wu, H., 2015. Effect of fiber treatment on thermal properties and crystallization of sisal fiber reinforced polylactide composites. *Journal of Reinforced Plastics and Composites*, 34(9), pp.718-730.

Yeh, S., Hsieh, C., Chang, H., Yen, C. and Chang, Y., 2015. Synergistic effect of coupling agents and fiber treatments on mechanical properties and moisture absorption of polypropylene–rice husk composites and their foam. *Composites Part A: Applied Science and Manufacturing*, 68, pp.313-322.

Ying, S., Wang, C. and Lin, Q., 2013. Effects of heat treatment on the properties of bamboo fiber/polypropylene composites. *Fibers and Polymers*, 14(11), pp.1894-1898.

Yoon, Y., Ibrahim, N., Zainuddin, N., Ariffin, H., Wan Yunus, W. and Buong, W., 2014. Surface Modifications of Oil Palm Mesocarp Fiber by Superheated Steam, Alkali, and Superheated Steam-Alkali for Biocomposite Applications. *BioResources*, 9(4).

Yuan, Q., Wu, D., Gotama, J. and Bateman, S., 2008. Wood Fiber Reinforced Polyethylene and Polypropylene Composites with High Modulus and Impact Strength. *Journal of Thermoplastic Composite Materials*, 21(3), pp.195-208.

Zaaba, N. and Ismail, H., 2019. Thermoplastic/Natural Filler Composites: A Short Review. *Journal of Physical Science*, 30(1), pp.81-99.

Zaaba, N., Ismail, H. and Jaafar, M., 2016. Recycled Polypropylene/Peanut Shell Powder Composites: Pre-Treatment of Lignin Using Alkaline Peroxide. *BioResources*, 11(2).

Zainudin, E., Yan, L., Haniffah, W., Jawaid, M. and Alothman, O., 2013. Effect of coir fiber loading on mechanical and morphological properties of oil palm fibers reinforced polypropylene composites. *Polymer Composites*, 35(7), pp.1418-1425.

Zaki, M., Knözinger, H., Tesche, B. and Mekhemer, G., 2006. Influence of phosphonation and phosphation on surface acid–base and morphological properties of CaO as investigated by in situ FTIR spectroscopy and electron microscopy. Journal of Colloid and Interface Science, 303(1), pp.9-17.

Zaman, H. and Beg, M., 2013. Preparation, structure, and properties of the coir fiber/polypropylene composites. *Journal of Composite Materials*, 48(26), pp.3293-3301.

Zhang, H., Pang, H., Shi, J., Fu, T. and Liao, B., 2011. Investigation of liquefied wood residues based on cellulose, hemicellulose, and lignin. *Journal of Applied Polymer Science*, 123(2), pp.850-856.

LIST OF PUBLICATION

Tan, W., Muniyadi, M. and Ooi, Z., 2019. Characterization and feasibility of *Mimusops Elengi* seed shell powder as filler for thermoplastic materials. *AIP Conference Proceedings 2157*, pp.1-8.